



JIMMA UNIVERSITY
JIMMA INSTITUTE OF TECHNOLOGY
SCHOOL OF GRADUATE STUDIES
FACULTY OF CIVIL AND ENVIRONMENTAL ENGINEERING
GEOTECHNICAL ENGINEERING

Soil Water Characteristic Curve Predictive Model from Index Properties for Red Clay Soils, case
in Jimma, Ethiopia

The thesis submitted to School of Graduate Studies, Jimma University, Jimma Institute of
Technology, Faculty of Civil and Environmental Engineering in Partial Fulfillment of the
Requirements for the Degree Master of Science in Geotechnical Engineering Chair

By

TENAYE ZEBERGA KINATE

Feb. 2022

Jimma, Ethiopia

JIMMA UNIVERSITY
JIMMA INSTITUTE OF TECHNOLOGY
SCHOOL OF GRADUATE STUDIES
FACULTY OF CIVIL AND ENVIRONMENTAL ENGINEERING
GEOTECHNICAL ENGINEERING CHAIR

Soil Water Characteristic Curve Predictive model From Index Properties for Red Clay
Soils, case in Jimma, Ethiopia

The thesis submitted to School of Graduate Studies, Jimma University, Jimma Institute of
Technology, Faculty of Civil and Environmental Engineering in Partial Fulfillment of the
Requirements for the Degree Master of Science in Geotechnical Engineering

Chair

Advisor: Damtew Tsige, PhD

Co-Advisor: Tigist Mezmur, MSc

Feb. 2022
Jimma, Ethiopia

DECLARATION

I declare that this research entitled “Soil Water Characteristic Curve Predictive model From Index Properties for red Clay Soils, case in Jimma, Ethiopia” is my original work and has not been submitted as a requirement for the award of any master of science in Jimma University or elsewhere.

TENAYE ZEBERGA KINATE

NAME

SIGNATURE

DATE

As research Advisor, I hereby certify that I have read and evaluated this research paper prepared under my guidance, by Tenaye Zeberga entitled “Soil Water Characteristic Curve Predictive model From Index Properties for red Clay Soils, case in Jimma, Ethiopia” and recommend and would be accepted as a fulfilling requirement for the Degree Master of Science in Geotechnical engineering.

Advisor: Damtew Tsige, PhD

Name

signature

Date

Co-Advisor: Tigist Mezmur, MSc

Name

signature


Date

APPROVAL SHEET

I, the undersigned certify that the thesis entitled: “**Soil Water Characteristic Curve Predictive model From Index Properties for Red Clay Soils, case in Jimma, Ethiopia**” is the work of Tenaye Zeberga Kinate and has been accepted and submitted for examination with my approval as university advisor in partial fulfillment of the requirements for degree of Master of Science in Geotechnical Engineering.

Name	Signature	Date
1. Main Advisor: Damtew Tsige (PhD)	_____	_____
2 .Co Advisor : Tigist Mezmur (MSc)	_____	_____

As member of Board of Examiners of the MSc Thesis Open Defense Examination, We certify that we have read, evaluated the thesis prepared by Tenaye Zeberga Kinate and examined the candidate. We recommended that the thesis could be accepted as fulfilling the thesis requirement for the Degree of Master of Science in Geotechnical Engineering.

1. Dr. Indalu Tadele (PhD)	 _____	_____
[External Examiner]	[Signature]	[Date]
2. Bereket Mamo (MSc.)	_____	_____
[Internal Examiner]	[Signature]	[Date]
3. Alemineh Sorsa (PhD Candidate)	_____	_____
[Chair Person]	[Signature]	[Date]

ABSTRACT

The Soils in tropical and arid regions which found above the groundwater table is known as unsaturated soils. Ethiopia is also considered to be in this region. Jimma is found in Ethiopia with high precipitation and evaporation through the year this causes the dominancy of unsaturated soil broadly in the city. Because most of our infrastructures built on unsaturated soils, the response of unsaturated soils is the most important consideration for many geotechnical projects. The testing of unsaturated soils required significantly more money and time. In addition, laboratory equipment for determining unsaturated soil properties has established to be technically challenging and difficult to use. For the characterization of unsaturated soil property functions, indirect estimation procedures were developed. Combined with saturated soil properties, the SWCC helped a means of moving unsaturated soil mechanics into real engineering practice. Therefore the aim of this research was to predictive SWCC by developing an empirical relationship between simple tests and those requiring complicated test equipment and procedures. SWCC data point was measured by contact filter paper method, and the measured data point optimized using MATLAB® R2019a to obtain the model fitting parameters. The linear regression was conducted with the help of JMP® Pro14 statistical software to correlate the optimized model fitting parameters with index properties. Based on index properties, a general equation for the soil-water characteristic curve was developed. The accuracy of the developed model was checked through different error measurement mechanisms .In this study, red clay soils were obtained from eight field sites. Laboratory experiments including index testing and SWCC testing carried out on the soil samples. The water content measurements were in the range of 35.44 percent to 43.09 percent. From the gradation test result the content of gravel soil ranges from 0 to 0.3%, sandy soils ranges from 1.21 to 4.03%, silt soil range from 28.25 to 33.85% and clay soil range from 61.9 to 70.38%. The specific gravity of the selected soil samples were ranges 2.69-2.76. Plasticity index of the soil was ranges 35.14 to 45.41. The X-ray diffraction results show that the kaolinite was the dominant clay mineral for all test pits. Based on the index properties result the developed af was $5.558+1.032wPI$,nf equal to $0.471+0.397(1/mf)$,mf equal to $0.184+0.000351wPI^2$,and residual suction vale equal to $-2830.57+2.84wPI^2$. Furthermore the proposed model was validated with other works and it reveals that the result was in acceptable range.

Keywords: *Unsaturated Soils, Soil–Water Characteristic Curve (SWCC), Matric Suction, Water content.*

ACKNOWLEDGMENT

My first and foremost thanks go to God Almighty, the foundation of life and the fountain of all Knowledge; indeed he has been gracious to me throughout my life and I am very grateful to him.

I would also like to acknowledge to the support given by Jimma University the department of Geotechnical engineering stream.

My sincere gratitude and heartfelt appreciation also go to my advisor, Dr. Damtew Tsige, for his tireless support to mentor, supervise, and supply me with valuable reference resources. My particular thanks also go to my co-advisor, Ms. Tigist Mezmur (MSc), provided me with continual encouragement, support, and constructive feedback from the beginning until the end of this research.

My special thanks also go to my Instructors Dr.Jemal J., Dr.Kifle W., Dr.Ing Tinsae G., Prof.Anand H., Engr.Bien M. (Ass.Prof.), and all Geotechnical staffs of Jimma Institute of Technology for their effort in teaching me all the Geotechnical related courses and guiding me in all aspects during my study of the master's program. My special thanks also extend to for Mr.Esrael Samual his assistance in different software analysis.

Mr. Dakabi Ch., Mr. Haile, Mr. Hailamariam, Ms. Firdos and other JIT Soil Laboratory staffs deserve special thanks for their voluntary support during my laboratory work. Special thanks to Mr.Mulatu, Diba, and Engida, my fellow MSc classmates, for their continued support and assistance. And also I greatly acknowledged for my best friends Mr. Adane.G, Mr. Adse.G. Mr. Desalegn.T and Mr.Defar for their continuous Support by providing internet access and other supportive items

Finally, I want to express my gratitude to my parents for their love, care, and unwavering support. Most significantly, I would like to express my heartfelt gratitude to my wife Ms.Seble Berhanu her continuous encouraging me to complete my studies by providing financial and spiritual assistance.

TABLE OF CONTENT

	Page
DECLARATION	i
APPROVAL SHEET	ii
<i>ABSTRACT</i>	iii
ACKNOWLEDGMENT.....	iv
TABLE OF CONTENT	v
LIST OF FIGURE.....	viii
LIST OF TABLE	xi
ACRONOMY	xii
NOMENCLATURE	xiii
CHAPTER ONE.....	1
INTRODUCTION	1
1.1 Background the Study	1
1.2 Statement of the problem	2
1.3 Research questions	3
1.4 Objectives	4
1.4.1 General objectives	4
1.4.2 Specific objectives	4
1.5 scope of the study	4
1.6 significance of the study.....	5
1.7 organization of the study	5
CHAPTER TWO	6
LITERATURE REVIEW	6
2.1 Definition and concepts.....	6
2.1.1 Tropical Soil	6
2.1.2 Classification of the amount of soil water	7
2.2 Suction.....	8
2.2.1 Stress state variables	8
2.2.2 Techniques for Measuring Soil Suction	9

2.3 Soil water characteristics curve.....	17
2.3.1 Determination of soil-water characteristic curve.....	20
2.3.2 Previous investigation of the significance of SWCC	22
2.3.3 SWCC Curve Fitting Empirical Models.....	23
2.3.4 Pervious SWCC Predictive Models.....	25
2.4 Physical properties of clay soil.....	28
2.5 Research gap	29
CHAPTER THREE	31
MATERIALS, METHODS, AND PROCEDURES FOR LABORATORY TESTING.....	31
3.1 General	31
3.2 Site Description And Soil Sampling	31
3.2.1 Site Description	31
3.2.2 Soil Sampling	32
3.2.3 Sample preparation.....	33
3.3 laboratory Tests of Index Properties	33
3.3.1 Natural Water Content.....	33
3.3.2 Specific gravity.....	34
3.3.3 Particle Size Distribution Test.....	34
3.3.4 Liquid Limit (LL)	34
3.3.5 Plastic Limit (PL)	34
3.3.6 Soil classification.....	34
3.4 X-ray Diffraction (XRD).....	35
3.5 Filter Paper Method of Testing	35
3.5.1 Soil Matric Suction Measurements.....	36
3.6 SWCC Predictive Model Development set up, data analysis, and validation approaches..	37
3.6.1 General over view.....	37
3.6.2 primary and secondary source of data	37
3.6.3 Approaches used for model development	38
3.7 Regression Analysis	39
3.7.1 Model variable.....	39

3.7.2 Model Development and Setup	41
3.8 Statistical goodness of fit measure	43
3.8.1 Sum of Squared Error (SSE)	43
3.8.2 R-Squared (R ²).....	43
3.8.3 Root Mean Square Error (RMSE)	43
3.8.4 Akaike’s Information Criteria (AIC).....	44
3.8.5 Mean algebraic error.....	44
3.8.6 Mean absolute error	44
CHAPTER FOUR.....	46
RESULT AND DISCUSSION	46
4.1 Index properties test result	46
4.1.1 Natural moisture content	46
4.1.2 Specific gravity.....	47
4.1.3 Results of Atterberg limit test.....	47
4.1.4 Particle Size Distribution Test Result of the soil.....	49
4.1.5 Soil Classification.....	51
4.2 XRD analysis result.....	52
4.3 Results of filter paper test.....	55
4.4 output of the proposed model.....	62
4.4.1 Introduction	62
4.4.2 Relation between the model fitting parameters and the index properties.....	62
4.4.3 Statistical prediction model for the (fredlund and xing) model fitting parameters	65
4.5 Model validation or performance of the model.....	68
4.5.1 Experimental fit Versus Model fit	70
4.6 Validation with related works	75
CHAPTER FIVE	84
CONCLUSION AND RECOMMENDATION.....	84
5.1 Conclusion.....	84
5.2 Recommendation.....	85
References.....	86

Appendix A. Natural moisture content	90
Appendix B. Specific gravity	93
Appendix C: Atterburg limit test result	98
Appendix D1: Wet Sieve analysis result	106
Appendix D2: Hydrometer analysis result.....	109
Appendix E: Filter paper method of suction measurement result data.....	114
Appendix F: MATLAB [®] 2019a fmincon script for optimization of curve fitting parameters	122
Appendix G. JMP [®] Pro 14 outputs	125
Appendix G3. model development using fit model.....	134
Appendix H:.....	153

LIST OF FIGURE

Figure 2.1 Calibration curve for whatman 42 paper based on the wetting procedure (modified after ASTM D5298-10).....	13
Figure 2.2 Typical swcc for silty soil by (Delwyn G.Fredlund, Rahardjo and Fredlund,2012) ...	19
Figure 2.3 comparative desorption SWCCs for sand,silt,and clay soils adopted by (DG Fredlnd,Rahardjo and Fredlund,2012).....	20
Figure 3.1 Map of the study area	32
Figure 4.1 Liquid limit determination of test pit TP5.....	48
Figure 4.2 Grain size distribution curve	49
Figure 4.3 Plasticity chart	51
Figure 4.4 XRD pattern analyses for test pit TP3.....	53
Figure 4.5 XRD pattern analyses for test pit TP5.....	54
Figure 4.6 XRD pattern analyses for test pit TP1.....	54
Figure 4. 7 XRD pattern analyses for test pit TP7.....	55
Figure 4.8 Soil water characteristics curve for TP1.....	58
Figure 4.9 Soil water characteristics curve for TP2.....	58
Figure 4.10 Soil water characteristics curve for TP3.....	59
Figure 4.11 Soil water characteristics curve for TP4.....	59
Figure 4.12 Soil water characteristic curves for TP5.....	60
Figure 4.13 Soil water characteristic curve for TP6	60
Figure 4.14 Soil water characteristic curve for TP7	61
Figure 4.15 Soil water characteristic curves for TP8.....	61
Figure 4.16 Scatter plot of a_f with predictor variables	63
Figure 4.17 Basic linear fittings between a_f and index property: (a) wPI ; (b) fine content; (c) clay content; (d) plasticity index; (e) sand content; (f); silt content.	65
Figure 4.18 Regression plot of a_f without transformation.....	67
Figure 4.19 Actual by predicted plot of a_f	67
Figure 4.20 Residual by predicted plot of a_f	67
Figure 4.21 Prediction profile of a_f	68
Figure 4.22 Predicted vs actual value of a_f , m_f , and $R_{suction}$	70

Figure 4.23 Actual vs predicted soil water characteristics curve plot for TP1	71
Figure 4.24 Actual vs predicted soil water characteristics curve plot for TP2	71
Figure 4.25 Actual vs predicted soil water characteristics curve plot for TP3	72
Figure 4.26 Actual vs predicted soil water characteristics curve plot for TP4	72
Figure 4.27 Actual vs predicted soil water characteristics curve plot for TP5	73
Figure 4.28 Actual vs predicted soil water characteristics curve plot for TP6	73
Figure 4.29 Actual vs predicted soil water characteristics curve plot for TP7	74
Figure 4.30 Actual vs predicted soil water characteristics curve plot for TP8	74
Figur 4.31 Validation between the the proposed model with Zapata,Perera et al,andHernandez for test pit 1	76
Figure 4.32 Validation between the the proposed model with Zapata,Perera et al,andHernandez for test pit 2	77
Figure 4.33 Validation between the the proposed model with Zapata,Perera et al,andHernandez for test pit3	77
Figure 4.3 Validation between the the proposed model with Zapata,Perera et al,andHernandez for test pit4.....	78
Figure 4.35 Validation between the the proposed model with Zapata,Perera et al, and Hernandez for test pit 5	78
Figure 4.36 Validation between the the proposed model with Zapata,Perera et al, and Hernandez for test pit 6	79
Figure 4.37 Validation between the the proposed model with Zapata,Perera et al,andHernandez for test pit 7	79
Figure 4.38 Validation between the proposed model with Zapata,Perera et al,and Hernandez for test pit 8.....	80
Figure 4.39 Error analysis based on the plot of actual and predicted gravimetric water content .	81
Figure 4.40 Error analysis based on the plot of actual and predicted gravimetric water content .	82

LIST OF TABLE

Table 2.1 Table 2.1 Calibration curve equation available in the literature for whatman42 filter paper by (Bicalho, correira, 2007)	13
Table 2.2 Models to best fit SWCC data [adopted from (DG Fredlund, Rahardjio and Fredlund,2012)]	23
Table 3.1 Profile of sampling area	32
Table 4.1 Moisture content result of the study area.....	46
Table 4. 2 Specific gravity result for all test pits	47
Table 4.3 Atterberg limit result for all test pits.....	48
Table 4.4 Combined grain size distribution curve result of all samples	50
Table 4.5 Percentage of grain size distribution curve result for all test pits	51
Table 4.6 percentage of grain size distribution.....	52
Table 4.7 Determination of suction and gravimetric water content from filter paper test.....	56
Table 4.8 Optimized (Fredlund & Xing, 1994) model fitting parameters	57
Table 4.9 Summary of data used for model development	62
Table 4.10 Correlation matrix for af parameter with predictor variables	63
Table 4.11 Linear prediction model expression proposed for the (Fredlund and Xing) model fitting parameters	69
Table 4.12 Percentage difference between actual and predicted fitting parameters.....	75
Table 4.13 Analysis of Error for predicted versus actual gravimetric water content at different suction value for different models.	82

ACRONOMY

AASHTO	American Association of State Highway and Transportation Officials
AIC	Akaka's Information Criteria
ASTM	American Society for Testing and Material
AEV	Air entry value
ECS	electrical conductivity sensors
Fmincon	Function Minimum constraint
FPM	Filter paper method
GSD	Grain size distribution
GI	Group index
JMP ^R Pro14	Jump
LL	Liquid limit
MATLAB	Matrix Laboratory
USCS	Unified Soil Classification System
PL	Plastic limit
PI	Plastic index
SST	Sum of Total Square
SSE	Sum of Squared Error
SWCC	Soil water characteristic curve
RMSE	Root Mean Square Error
TP	Test pit
TCS	thermal conductivity sensors
TDR	Time domain reflectometry
wPI	Weighted Plasticity Index
W_{fp}	Filter paper water content
XRD	X-ray Diffraction

NOMENCLATURE

Symbol	Description	Unit
M_w	- Mass of water	[kg]
M_s	- Mass of solid	[kg]
U_a	- Pore-air pressure	[kPa]
U_w	- Pore-water pressure	[kPa]
S	- Degree of saturation	[%]
$^{\circ}C$	- Degree centigrade	-
w	- Moisture content	[%]
w_n	- Natural moisture content	[%]
ψ_r	- Residual suction	[kPa]
ψ	- Suction	[kPa]
θ_i	- Is the volumetric water content represented by a pore volume for which the largest size pore corresponds to the upper limit of the i^{th} particle-size range	[m^3/m^3]
a_f, n_f, m_f	- Fredlund & Xing(1994) model fitting parameters	[kPa ,-, -]

CHAPTER ONE INTRODUCTION

1.1 Background the Study

In unsaturated soils, the structure is established. However, geotechnical practitioners are following the concept of saturated soil mechanics in the construction of structures. The principle of unsaturated soil mechanics needs to be implemented in the design of structures in order to pursue a sustainable approach and to minimize costs (Hernandez, 2011). Depending on the degree of saturation S , the soil is classified into three groups as saturated soil $S=1$, dry soil $S=0$, and unsaturated soil $0<S<1$.

Delwyn G. et al. (2012) states an unsaturated soil has more than two phases and the pore-air pressure is positive relative to pore-water pressure. In classic soil mechanics (i.e. saturated soil mechanics) pore water is considered as positive. The determination of unsaturated soil parameters is required for the application of unsaturated soil mechanics in normal geotechnical engineering applications. Unfortunately, the cost of direct measurement of unsaturated soil parameters is out of most clients' budget range (Fredlund.D and Fredlund, 2020).

Many researchers noted that unsaturated soil properties can be estimated from the soil-water characteristic curve (Perera et al., 2005). Partially saturated soil engineering characteristics may now be predicted using mathematical models built for unsaturated soil mechanics; these models are widely used and recognized around the world (Dafalla et al., 2020). There have been many studies on the different laboratory testing mechanisms to formulate the SWCC. At the same time, newer techniques and testing equipment are continuously being developed. It is not possible to evaluate all the different available techniques and procedures, and, thus, this paper focused on filter paper methods.

Power and Vanapalli, (2008) states that the filter paper method, ASTM Standard D5298-03, is widely regarded as a low-cost, technically simple, and reasonably accurate method for measuring a wide range of soil suction. The precision of the calibration curve that connects filter paper water content to soil suction, on the other hand, is critical to the process. By proposing a prediction model using index properties of soil, several researchers (Ganjian et al., 2007, Chiu, Yan and Yuen, 2012, Perera and Zapata, 2005) try to put unsaturated soil mechanics into effect.

The purpose of this research is to simplify the application of unsaturated soil mechanics by developing an empirical relationship between simple tests and those requiring complicated test equipment and procedures. Different study on this area aimed to make the application of unsaturated soil mechanics easier by establishing an empirical relationship between the easily measurable index property test parameters and those that require advanced testing equipment and procedures for (Fredlund and Xing, 1994) SWCC fitting model parameters. The developed models having significant importance to predict the SWCC from index properties. For many geotechnical engineering applications measuring the unsaturated soil property directly in the laboratory become expensive due to the complexity of the instrument required and a large amount of time required. As a result, an indirect method to measure the unsaturated soil property function is necessary. In such cases, predictive models will become a sensible approach to obtain an estimate of the SWCC fitting parameters (Perera et al., 2005; Ganjian et al., 2007; Perera and Zapata, 2005; Hernandez, 2011).

As a result, for this study eight typical red clay soil samples were gathered from different field sites (test pit excavation) in Jimma city, in South Western Ethiopia. The soil samples were subjected to a comprehensive laboratory testing program, which included index property laboratory testing like determining moisture content, specific gravity, particle size, liquid limit, and plastic limit, and classification of soils, and also indirect SWCC measurement in the laboratory using filter paper measurement techniques. Filter paper techniques were used to test the matric suction vs water content of red clay soils. The mathematical properties of several physical-based SWCC prediction processes and principles were assessed, and a brand-new model for predicting the SWCC of red clay soils using SWCC fitting model parameters was established. Therefore, with these SWCC curves and measuring the conventional classical soil mechanics testing and data, one can fairly predict many unsaturated property functions. The purpose of this research was to shorten the time it took to build the SWCC curve, this is commonly accomplish by simplifying and predicting the (Fredlund and Xing, 1994) SWCC fitting empirical model parameters using basic soil index property data.

1.2 Statement of the problem

Due to soil water deficiencies caused by the tropical climate, many tropical soils are unsaturated. While certain tropical locations may have heavy rainfall, this will be counterbalanced by

increased evaporation and transpiration, which will drain water from the soil. For this scenario, the bottom groundwater level will be at deep depths (perhaps greater than 10 m) which implies that the zone of soil concerned in geotechnical engineering and construction operations will be on top of the water table and doubtlessly unsaturated (Huat and Toll, 2012).

Different researchers (Fredlund, 1994, Zapata, 1999, Perera and Zapata, 2005, Fredlund, 2006, Lu, Godt and Wu, 2010, D G Fredlund, Rahardjo and Fredlund, 2012, Chiu, Yan and Yuen, 2012, and Fredlund, 2020) said that unsaturated soil mechanics play an important role in engineering characteristics of soil, but it was difficult to go further for practical application due to its complexity for determining unsaturated soil property. One of the ways used to determine unsaturated soil property is developing soil water characteristics curve. The burning issue to plot SWCC is soil suction. To measure soil suction in laboratory takes much time, cost, and qualified laboratory experiment. And also the equipments used for measuring suctions is very expensive. To minimize such problems predicting mathematical model with those requiring simple testing procedures was the best solution. Thus, on this study the simplified model was developed for SWCC variables from index properties of soil.

As an study done by (Jemal J, 2017) in-depth Investigation into Engineering Characteristics of Jimma Soils was studied. Based on his study the soil around Jimma city was covered with black grey and red type of clay soils. He broadly investigated the basic engineering properties of saturated soil, but he didn't study about the unsaturated soil properties around this area. In this study the parameters used to know unsaturated soil properties were determined and also the mathematical model was developed.

1.3 Research questions

1. How can develop SWCC model from suction vs water content discrete data point for each test pit using FPM?
2. How can we fit the laboratory measured SWCC points using Curve fitting model and obtain the optimized curve fitting parameters?
3. What empirical equation can develop from laboratory measured SWCC and index properties of soil?

4. Can this newly built predictive SWCC model is agree with other predictive SWCC models?

1.4 Objectives

1.4.1 General objectives

The main objective of this study is to develop model to predict the Soil Water Characteristic Curve (SWCC) fitting parameters of red clay soils from index properties of soil in case of Jimma city.

1.4.2 Specific objectives

The specific objective of this research is:

- ❖ To determine suction versus water content discrete data point and develop SWCC curves for each soil in each test pit using filter paper method
- ❖ To determine laboratory measured SWCC points and obtain the optimized curve fitting parameters using Curve fitting model.
- ❖ To develop empirical equation from the laboratory measured swcc and index properties.
- ❖ Validate developed predictive SWCC model with other predictive SWCC models.

1.5 Scope of the study

This study focuses on various areas where red clay soils were prevalent in Jimma city. In this study, it is difficult to analyze the entire clay soil of the Jimma; therefore, a representative soil sample collected from eight test pits to a depth of 2 m. The key subject of this study was the wetting curve of front soil water characteristics of red clay soil. This study does not recognize the impact of hysteresis. Hysteresis is critical in cases where air is trapped in the soil or where soil structure (pores and connectivity between pores) causes the soil to behave differently under conditions of drying or wetting. The primary focus of this study was the creation of a SWCC prediction model on red clay soil only. The prediction model was used as an experiment using a filter paper method of testing procedure. Filter pater water content was recorded on each soil samples as recommended by ASTM D 5298-03 for whatman42 filter brand. Thus, the filter paper water content correlated with previously determined calibration curve equation, and the resulting matric suction was collected. The prediction model can be used for all existing red clay soils in Jimma except the number of test pits limits the model.

1.6 Significance of the study

It was well known that various types of soil show a distinctive SWCC. In the indirect determination of the unsaturated soil property, SWCC plays an important role. In Ethiopia, unsaturated soil mechanics were not practiced. Currently, several geotechnical engineering projects have been planned in Ethiopia in unsaturated soil based on the concept of classic soil mechanics (i.e. saturated soil mechanics) due to the unpracticed concept of unsaturated soil mechanics. As a result of the establishment of a prediction model to simplify SWCC on red clay soil, this research will make a significant contribution to overcoming the idea of unsaturated soil in practice in Ethiopia and to other scientific world. Due to the relation of prediction with simple and well-known engineering soil properties, the model is an important tool in the introduction of unsaturated soil mechanics into engineering practice. In addition, this research will provide future researchers with some understanding into the field of unsaturated soil mechanics.

1.7 Organization of the study

This document of the thesis consists of five chapters, each covering a specific topic of the thesis work. In the first Chapter background of the problem, objectives, research questions, scope and significance of the study were presented. Chapter two deals with a brief literature review about unsaturated soil mechanics, suction measurement techniques and previous related works relevant to the present study. Chapter three deals the description of study area, materials and methods used in the study. Chapter four presents the analysis, interpretation, discussion and comparison of laboratory test results and software results for the model development software. Chapter five consists of the conclusions and recommendations which were drawn from the research work. Finally, references and appendices were attached at the end of the thesis.

CHAPTER TWO

LITERATURE REVIEW

2.1 Definition and concepts

2.1.1 Tropical Soil

Tropical soils are residual soils because they are created predominantly by in-situ weathering processes. Many classification schemes exist for tropical soils, based on pedological, geochemical, or engineering criteria. For classification schemes to be helpful, they must take into account the impacts of weathering, mineralogy (especially the "unusual" clay mineral). At both the macro and micro scales, tropical residual soils are highly structured materials. The micro-structure is created by minerals leaching away during weathering, resulting in an open structure. Due to mineral deposition during or after weathering, tropical soils are also prone to be cemented soils. Tropical soils are difficult to work with as engineering materials due to their highly structured character and the fact that they are frequently unsaturated. They do, however, usually have good engineering features (Greene, 2012).

Because of soil water deficits caused by the tropical climate, many tropical soils live in an unsaturated state. Although high precipitation can occur in many tropical regions, this can be offset by much greater evaporation and transpiration, which removes water from the soil. The groundwater level will be at large depths (perhaps greater than 10 m) in this case, which means that the region of soil involved in engineering and construction activities would be above the water table and possibly unsaturated. This unsaturated region is known as the Vadose zone above the water table. The water process in the soil is preserved by negative pressure under unsaturated conditions (or suction). In understanding how the soil would behave in an engineering sense, the effect of suction is very important. Suction affects the shear behavior and also controls volume changes in response to wetting and drying. The fact that a soil is unsaturated also has a significant effect on the water permeability (Huat and Toll, 2012).

An unsaturated soil is commonly expressed to as a three-phase system (i.e., solids, air, and water). As a result of solutions to a number of significant difficulties or challenges; unsaturated soil mechanics has gradually become a component of geotechnical engineering practice. Numerous research investigations focusing on challenges that limit the use of unsaturated soil mechanics have yielded the solutions. The need to understand the fundamental, theoretical

behavior of an unsaturated soil, the formulation of suitable constitutive equations and testing for uniqueness of proposed constitutive relationships, the ability to formulate and solve one or more nonlinear partial differential equations using numerical methods are the primary challenges to the implementation of unsaturated soil mechanics (Delwyn G. Fredlund, Rahardjo and Fredlund, 2012 .Lu, Godt and Wu, 2010) States that classical soil mechanics is foundation of modern unsaturated soil mechanics, and is not scientifically sound; the prevailing definitions of matric suction pore water pressure, capillary effective stress, and independent stress variables fail to represent the important physical mechanism of sorption. Now a day the routine software use unsaturated soil state variables to provide some basis for frameworks aimed to solve practical problems.

2.1.2 Classification of the amount of soil water

The amount of water in the soil can be defined using more than one variable. The variables used to define the amount of water in the soil are (i) gravimetric water content w , (ii) volumetric water content θ , (iii) degree of saturation S .

$$w = M_w / M_s \quad (2.1)$$

Where, W = gravimetric water content, M_w = mass of water, and M_s = mass of soil solids.

Volumetric water content, θ , is commonly used in agriculture-related disciplines and relates the amount of water in the soil to the total volume of the soil:

$$\theta = V_w / (V_v + V_s) \quad (2.2)$$

Where, θ = volumetric water content, V_w = volume of water, V_v = volume of void, and V_s = volume of soil solids.

The degree of saturation, S , references the volume of water to the instantaneous volume of voids and therefore requires a measurement of the instantaneous total volume of the soil specimen.

$$S = V_w / V_v \quad (2.3)$$

Where, S = degree of saturation

2.2 Suction

Soil suction is made up of two components: matric suction and osmotic suction (also called solute suction). The sum is known as the total suction. Matric suction is due to the surface tension forces present in unsaturated soils (surface tension effect is also referred to as capillarity) at the interfaces (menisci) between the water and the gas (usually air) phases. Osmotic suctions are due to the presence in the pore water of dissolved salts. Total suction is defined as the negative pressure which must be applied to a pool of pure water at the same elevation and temperature in order for it to be in equilibrium with the soil water. This negative pressure is needed to balance the suction forces acting within the soil due to capillarity (matric suction) and the suction induced by different concentration of salts in the pore water in the soil and the pure water outside (osmotic suction) The pressure difference across the water/air interface ($u_a - u_w$) controls matric suction, where u_a is the pore air pressure and u_w is the pore water pressure. In general, the pore air pressure (u_a) will be at atmospheric pressure in the field ($u_a = 0$), so the negative pore water pressure ($-u_w$) will describe the suction (Huat and Toll, 2012). All theories and design approaches for unsaturated soil have focused on soil matric suction. Matrix suction was previously characterized as the difference between pore air pressure u_a and water pressure u_w , i.e., $u_a - u_w$ (Lu, 2020).

As soil-water content changes osmotic suction is not influenced when as compared to matric suction. Hence, in most geotechnical testing for unsaturated soil, it is reasonably acceptable to control only total suction and matrix suction. In defining unsaturated soil stress state matric suction has an important role. Therefore, it is necessary to control or measure matric suction in laboratory studies on unsaturated soils (Strength *et al.*, 2021).

2.2.1 Stress state variables

The first attempts to explain the engineering behavior of unsaturated soils used an equivalent effective stress approach, attempting to extend the successful use of Terzaghi's effective stress principle for saturated soils. To do this, the stress variables of total stress and suction were combined into a single effective stress (Huat and Toll, 2012).

$$\sigma' = \sigma - u_a + \chi(u_a - u_w) \quad (2.4)$$

Where σ' is effective stress

σ is total stress

u_a is pore air pressure

u_w is pore water pressure

χ is a factor related to the degree of saturation.

The χ variable was an empirical factor that varied between 0 and 1 as a function of degree of saturation, with $\chi = 1$ coinciding with full saturation. If $\chi = 1$ the equation Reduces to the effective stress equation for saturated soils, so this provided a simple Transition between saturated and unsaturated conditions.

2.2.2 Techniques for Measuring Soil Suction

In geotechnical engineering, filter paper equilibration has long been a popular approach for evaluating soil suction. Filter paper is a secondary measurement method that uses a SWCC of the filter paper to relate the measured water content of a piece of filter paper in suction equilibrium with a soil sample to soil suction. Although the filter paper technology is cost-effective, measurement errors and time commitment limit its application.

Traditionally, SWCCs have been created using axis translation methods (pressure plate extractors) by equilibrating samples at predetermined matric suctions and then oven drying to determine the water content of the equilibrated samples. However, concerns about its performance at suction pressures of less than 200 to 300 kPa (Bittelli and Flury, 2009) , as well as whether the process of water loss from soil under pressure is similar to water loss under suction point to the need for alternative suction analysis methods.

Another typical way to evaluate matric suction is with tensiometers. Most are restricted to a pressure range of 0 to 80 kPa. Although some units may reach 1500 kPa with special designs and pretreatments, they are not routinely available. Tensiometers in an evaporating soil core to continually measure both suction and gravimetric water content to construct an automated SWCC for wet soil (named the Wind/Schindler method, WSM).

Suction measurements of materials that are drier than the tensiometer or axis translation range are best done with vapor pressure methods (VPM). Because lowering the potential energy (raising suction) of water in the soil matrix (t) reduces the amount of water molecules (and hence the equilibrium vapor pressure, p) in the headspace above the sample, these measurements are possible.

Soil suctions can be found above the water table in any surface. Suction is one of the most essential characteristics for defining the moisture stress condition of unsaturated soils, and laboratory studies of suction may be highly valuable for determining sample quality, calculating in situ effective stress, and simulating unsaturated soil mechanics applications. There are two types of soil suction measurements techniques (i.e. Indirect and direct suction measurement's). The axis transition technique, tensiometer, and suction probe are the most used direct suction measurement procedures. The three types of indirect suction measuring techniques include matric suction, osmotic suction, and total suction measurement approaches. Time domain reflectometry (TDR), electrical conductivity sensors (ECS), thermal conductivity sensors (TCS), and in-contact filter paper method are examples of indirect matric suction measurement techniques (Pan, Qing and Pei-yong, 2010).

2.2.2.1 Direct Measurement of Soil Suction

Matrix suction can be determined by measuring the negative pore-water pressure directly. The difference between air pressure and pore-water pressure is matric suction, which is normally equivalent to on-site atmospheric pressure. The direct measurement of matric suction required the use of a ceramic disk or a ceramic cup to separate the water and air phases. In geotechnical engineering, soil matrix suction is becoming increasingly important. Soil suction is no longer considered to be limited to arid or semi-arid regions of the world. In temperate regions, it is regularly encountered in a wide range of geotechnical difficulties (A.M. RIDLEY et al, 2003).

Axis-translation Technique

The axis translation approach, which directly regulates matric suction by increasing air pressure while keeping pore water pressure equal to atmospheric pressure, was used for the pressure plate and Tempe cell tests (Nam et al., 2010). To prevent recording negative pore-water pressure, the operating idea of this technique is to artificially raise the atmospheric pressure sensed by a soil

sample while preserving the pore-water pressure at a positive reference pressure. As a result, the matric suction, or the pressure differential $u_a - u_w$, remains unchanged. In the low suction range, the approach was used to determine unconfined wetting and drying curves (i.e., less than 1500 kPa). The highest air pressure that can be imposed on the experiment system and the air entrance value of the ceramic disk limit the range of axis translation technique to detect or adjust matric suction. One disadvantage of the axis translation technique is that it does not produce instantaneous results when used to impose matric suction; another disadvantage is that the long equilibrium times associated with the axis translation technique make these experiments particularly susceptible to air diffusion.

Tensiometer

A tensiometer is a device that measures the negative pore-water pressure of soil directly. The way to ensure is that the water pressure contained in a high air entry material will equalize with the soil water pressure, allowing negative soil water pressures to be measured. The limitation is that air in the sensor causes inaccurate or less negative pore water pressure measurements for the following reasons: a) As the soil water pressure approaches the vapor pressure of water at atmospheric conditions, water vaporizes. b) Air in the soil can diffuse through the ceramic layer; c) as water pressures drop, air escapes the solution. For low suction range, i.e., matric suction <14,400 kPa (14.4 MPa or RH $\frac{1}{4}$ 90%), currently, tensiometer is the only reliable and time efficient technique to measure matric suction but is limited to less than 100 kPa (RH > 99.93%). Although axis translation has been widely used to control matric suction less than 1,500 kPa (RH > 98.9%), it is time consuming and is only capable of controlling capillary water (Lu, 2020).

Suction Probe

A.M. RIDLEY et al, (2003) created a suction probe for determining soil matric suction. The equilibrium between the pore-water pressure in the soil and the pore-water pressure in the water container is the basis for taking suction measurements with a suction probe. It is unique in that it can make direct readings over a wide range of soil suctions (up to 1500 kPa) and has been used widely for a number of users and on a variety of soil types in both laboratory and field settings. The key problem is that during the suction measurement, there may be cavitation and air diffusion through the ceramic head.

2.2.2.2 Indirect matric suction measurement

A common porous sensor composed of a specific substance is widely used to measure matric suction indirectly (e.g., filter paper, fiberglass, gypsum, nylon, sintered glass, clay ceramics, and metal). The measurement is made by balancing the porous sensor with the soil's matric suction. As a result, the water content of the porous sensor corresponds to the magnitude of the soil's matric suction.

In-contact filter paper technique

Filter paper technique was established for measuring soil suction by soil scientists and agronomists. In geotechnical engineering fields, many researchers have also used the technique as a routine method for suction measurement like (Bicalho, Correia and Ferreira, 2007, Power and Vanapalli, 2008, Pan, Qing and Pei-yong, Leong, He and Rahardjo, 2002, Bicalho, Correia and Ferreira, 2007, and Bulut and Leong, 2008). Soil matric suction is measured using the in-contact filter paper technique. Water in the liquid phase and solutes can freely exchange due to direct contact between the filter paper and the soil. The water content of an originally dry filter paper increases due to a flow of water in liquid form from the soil to the filter paper in the in-contact filter paper technique until both come into balance.

The capillary pressure of the soil (i.e., the pressure difference between air and water components in soil voids) is an important variable in the study of unsaturated soil hydro-mechanical behavior. As a result, even if a degree of approximation is involved, a simple and inexpensive laboratory method for measuring the capillary pressure of the soil (also known as soil matric suction, with the reference being atmospheric pressure) is of considerable importance. By measuring the gravimetric water content of the filter paper at equilibrium, which is connected to soil suction by a predefined calibration curve, the filter paper method indirectly determines soil suction. The technique has the advantages of simplicity, economy, and reasonable accuracy. It can measure suctions ranging from 10 to 30000 kPa (Bicalho, Correia and Ferreira, 2007).

The equilibrium water content of a filter paper that is either in direct contact with a soil sample or inside an airtight container with the sample but not in direct contact with it is determined using the filter paper technique. The suction in the soil is computed from a previously defined calibration curve relating the filter paper water content and suction after the final water content of the filter paper is obtained. For indirect suction estimation from Whatman Grade 42 filter

paper water content measurements, the (ASTM D5298-10) calibration curve is commonly used (Kim, Prezzi and Salgado, 2017).

Calibration equation proposed by ASTM D5298-10(2010)

$$\text{For } w_{c_{fp}} > 45.3\% : \log_{10} s = 5.336 - 0.0779 w_{c_{fp}} \quad (2.5)$$

$$\text{For } w_{c_{fp}} < 45.3\% : \log_{10} s = 2.142 - 0.032 w_{c_{fp}} \quad (2.6)$$

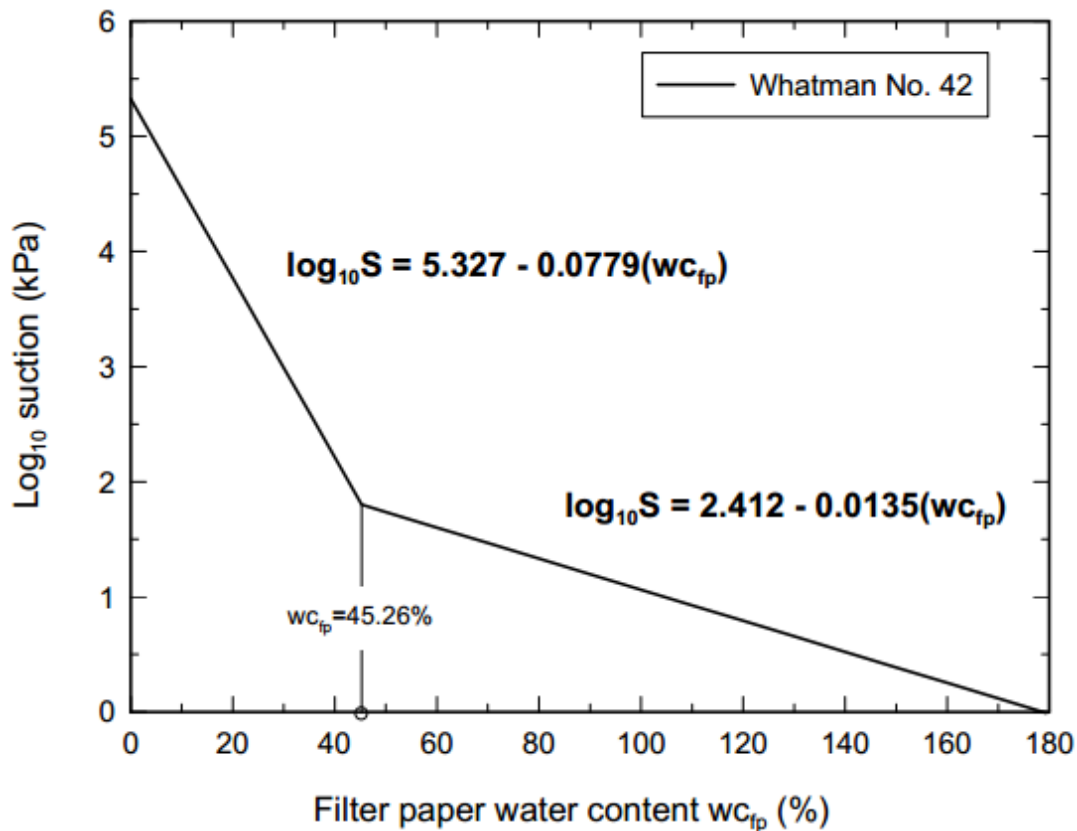


Figure 2.1 Calibration curve for whatman 42 paper based on the wetting procedure (modified after ASTM D5298-10)

Table 2.1 Calibration curve equation available in the literature for whatman42 filter paper by (Bicalho, correira, 2007)

Reference	Suction	W (%) range	Log10 (suction) (kPa)
ASTM D5298	Total and Matric	W < 45.3	5.327 - 0.0779 w

ASTM D5298	Total and Matric	W >45.3	2.412 -0.0135 w
Chandler & Gutierrez(1986)	Matric	(*)	2.85 -0.0622 w
Chandler et al. (1992)	Matric	W < 47	4.842-0.0622 w
Chandler et al. (1992)	Matric	W > 47	6.050-2.48 Log w
Oliveira & Marinho (2006)	Matric and Total	W < 33	4.83 – 0.0839w
Oliveira & Marinho (2006)	Matric and Total	W > 33	2.57 – 0.0154w

Note: w = Gravimetric water content (*) suction range (80-6000 kPa)

The filter paper method is used to measure soil suctions in an indirect manner. The method's benefits include its ease of use, low cost, and capacity to measure a wide range of suctions. In the field, the filter paper method has been used to measure soil suctions. However, the filter paper method's simplicity has resulted in a lack of understanding and, as a result, incorrect application. Recent research suggests the necessity for greater caution when using the filter paper method to assess suction (Leong, He and Rahardjo, 2002).

To test the reliability of the filter paper approach, soil suction measurements were done on an unsaturated soil using the filter paper method and a high capacity tensiometer. The results suggest that employing a previously wetted filter paper as an alternate strategy to measuring suction can be beneficial if an adequate calibration curve is utilized. This method was compared to the traditional filter paper method, in which the paper is dry at first, and good agreement was discovered between the two approaches, with the “wet” method being slightly faster in terms of suction equilibration (Pereira, Delage and Cui, 2010).

Hydraulic routes were initiated from the natural water content of the loess (14.2 percent) and followed by either drying or wetting phases for both suction measurement methods. Allowing evaporation of the soil specimen under laboratory settings for intervals of time ranging from 1 to 4 hours was used to dry it. Wetting was attained by adding small quantities of water to the soil sample. To ensure uniform wetting, a sheet of filter paper was placed on top of the sample and

water drops were uniformly spread over the surface using a syringe. A new suction measurement was conducted once the target water content was determined (Pereira, Delage and Cui, 2010). Unsaturated soils are commonly found in many parts of the World, especially at shallow depths from the surface and in arid and semi-arid areas where the natural ground water table typically is at a greater depth (George, 2020).

The filter paper method has been frequently used to analyze soil suction because to its simple testing setup, methods, and data processing. A filter paper is used to achieve vapor equilibrium with the soil in the filter paper method. One filter paper is usually in contact with the soil sample, while the other is put a short distance above it. Water migrates from the soil sample to the filter paper. The Whatman No. 42 filter paper, as well as the Schleicher and Schuell No. 589 papers, are the most commonly used filter papers, both of which have ASTM calibration curves (ASTM D 5298, 2003). To reach balance, you'll need to have at least seven days. One of the key limitations of the filter paper approach is that one test is required to generate one data point in the SWCC, implying that constructing the full SWCC takes a significant amount of time and work. Furthermore, when a soil sample is dry and the suction value is normally greater than 500 kPa, it is very difficult to establish excellent contact between the soil and the filter paper, resulting in erroneous results (Nam et al., 2010).

Unsaturated soil mechanics ideas have gained widespread acceptance, resulting in a progressive shift in geotechnical engineering practice. As soil suction becomes a fundamental component of engineering practice in many instances involving unsaturated soils, there is a greater demand than ever for dependable soil suction measuring methodologies. Soil suction is caused by capillary action, the surface energy characteristics of soil particles, and the pore water's ionic concentration. When both processes are working, total suction is achieved. When just capillary action and surface energy qualities are active, matric suction occurs. The filter paper technique is the only method that can infer both total and matric suction from all known suction measurement methods. The soil specimen and filter paper are brought to moisture equilibrium using the filter paper method, either in direct touch (matric suction) or not in direct contact (total suction) in a constant temperature environment. Direct contact between the filter paper and the soil allows liquid water and solutes to easily interchange, whereas a vapor barrier separates the filter paper

and the soil, limiting water exchange to the vapor phase alone and preventing solute movement (Bulut and Leong, 2008).

The relationship between matric suction and water content (such as gravity water content, volumetric water content, and degree of saturation) of unsaturated soil is commonly described by the soil water characteristic curve (SWCC). Because the SWCC is so important in forecasting the mechanical characteristics, permeability parameters, and shear strength of unsaturated soil, it's interesting to look into measuring suction. The pressure plate method, vapor equilibrium method, tensiometer method, dewpoint potentiometer method, osmotic method, and filter paper method, among others, are all well-known suction measurement procedures in the laboratory. Many researchers have examined various suction measurement procedures in order to establish SWCC. Because of its simplicity, low cost, and wide range of suction measurement, the filter paper method is preferred. However, without a thorough comprehension of its principles and safeguards, an unfavorable outcome will be achieved (V.Bund, 2013).

Because the majority of geotechnical engineering projects take place in unsaturated soil zones, unsaturated soil mechanics is extremely important. The unsaturated soil behavior is controlled by soil suction, particularly matric suction. However, geotechnical engineers and researchers are still concerned about the accuracy, practicality, cost, and reliability of measurements for determinations of soil suction. The SWCC is required to determine the strength, stiffness, conductivity, serviceability, and other characteristics of unsaturated or partially saturated soil. The SWCC is measured by taking the matric suction of soil to the water content or degree of saturation. The filter paper method is employed in this study as a secondary indirect measurement approach since it can determine both total and matric suction. The matric suction, which is defined as the pressure that tends to equalize the moisture content in a soil block and equal to the difference between pore air (u_a) and (negative) water (u_w) pressures, is of more importance in geotechnical engineering than total suction (Al-hashemi, 2018).

Extensive laboratory procedures are required to measure soil properties for unsaturated soil constitutive models. For the majority of practical situations, estimated soil properties have been proven to be sufficient for analysis. As a result, empirical approaches for assessing unsaturated soil properties would be beneficial. Because of its practical importance, unsaturated soil

mechanics has gotten a lot of attention in the geotechnical community. The behavior of unsaturated soils must be investigated by determining the specific behavior parameters in these soils. Over the last three decades, a theoretical foundation for unsaturated soil mechanics has been constructed. In geotechnical engineering, the constitutive equations for volume change, shear strength, and flow across unsaturated soil have been widely recognized. The basic premise of this theory is that the behavior of unsaturated soils cannot be characterized just by a single stress state variable. In other words, the constitutive models often require both the net normal stress, $(\sigma - u_a)$, where σ is the total stress and u_a is the pore-air pressure, and the matric suction, $(u_a - u_w)$, where u_w is the pore-water pressure. As a result, evaluation of suction is most important to study the unsaturated soil behavior (Ganjan *et al.*, 2007).

Ganjan *et al.*, (2007) mentioned that at a given level of saturation, the equilibrium soil suction should be proportional to the soil's specific surface area. The PI is a good predictor of surface area, and it can be used on its own. A soil with a limited amount of very active clay, on the other hand, would have a high PI but a low specific surface area. As a result, the weighted PI (W.PI) was found to be a more accurate indicator of soil particle surface area for predicting the Soil–Water Characteristic Curve.

2.3 Soil water characteristics curve

As a soil dries out, or wets up, the suction within the soil will change. The relationship between water content and suction is known as the Soil Water Retention Curve (SWRC). This relationship has also been called the Soil Water Characteristic Curve (Huat and Toll, 2012). The design of SWCC in unsaturated soil mechanics is to define the amount of water in a soil corresponding to soil suction. The amount of water contained in the soil pores defined by the water content. It is well known that the Soil water characteristic curve used to predict the unsaturated soil property. Hence, the characterization of the Soil water characteristic curve should be reasonably accurate (Chiu, Yan and Yuen, 2012) and (Fredlund and Xing, 1994). It has been argued that that the relationship between volumetric water content which is the ratio of the volume of water in the void to total volume, and matrix suction represented by the term Soil water characteristic curve. In SWCC the suction is plotted in a logarithmic scale because the low suction range needs to be expanded and the high-suction range needs to be compressed and the

water content measure is plotted arithmetically (Delwyn G. Fredlund, Rahardjo and Fredlund, 2012). SWCC yield a meaning only for the condition $0 \leq S \leq 1$. Experimental data have previously shown that the matric suction of soil reaches a maximum value of approximately 1×10^6 kPa at zero water content (Fredlund and Xing, 1994).

Soil water retention curves are often expressed in terms of volumetric water content, θ , or degree of saturation, S_r versus suction. However, in geotechnical practice, measurements are usually made of gravimetric water content (by weight). These readings are often converted to volumetric water content or degree of saturation based on the initial dry density or void ratio. This makes no allowance for changes in volume due to drying and wetting and can result in errors for soils that shrink or swell by significant amounts. Therefore, it is essential that volumetric measurements are made throughout the test (Huat and Toll, 2012).

The SWCC shows the relationship between the mass (and/or volume) of water in a soil and the water phase's energy state. The SWCC has proven to be an interpretive model that employs the basic capillary model to provide insight into water distribution in voids. The influences of soil texture, gradation, and void ratio have all been taken into account when interpreting laboratory SWCC results. The SWCCs have a critical role in determining the properties of unsaturated soils. The approaches for studying unsaturated soil properties that have been proposed are approximate, but they are often enough for analyzing unsaturated soil mechanics problems. Within the geotechnical engineering profession, there has been widespread agreement on the processes for measuring and interpreting SWCC data obtained in the laboratory (D G Fredlund, Rahardjo and Fredlund, 2012).

The assessment of the soil-water characteristic curve forms the basis for all other unsaturated soil property functions. This paper explains some of the factors that must be taken into consideration in order to obtain the most reliable possible solution for unsaturated soils problems. There is a linkage between the soil-water characteristic curves and the unsaturated soil property functions and this linkage must always be maintained in order to obtain reasonably accurate results from numerical analysis (Fredlund, 2006).

Figure 2.2 shows a typical SWCC for a silt soil along with identification of some of its main characteristics. The air-entry value of the soil is the matric suction where air starts to displace

water in the largest pores in the soil. The residual water content is the water content where a larger suction change is required to remove additional water from the soil. In other words, there is a change in the rate at which water can be extracted from the soil (D G Fredlund, Rahardjo and Fredlund, 2012).

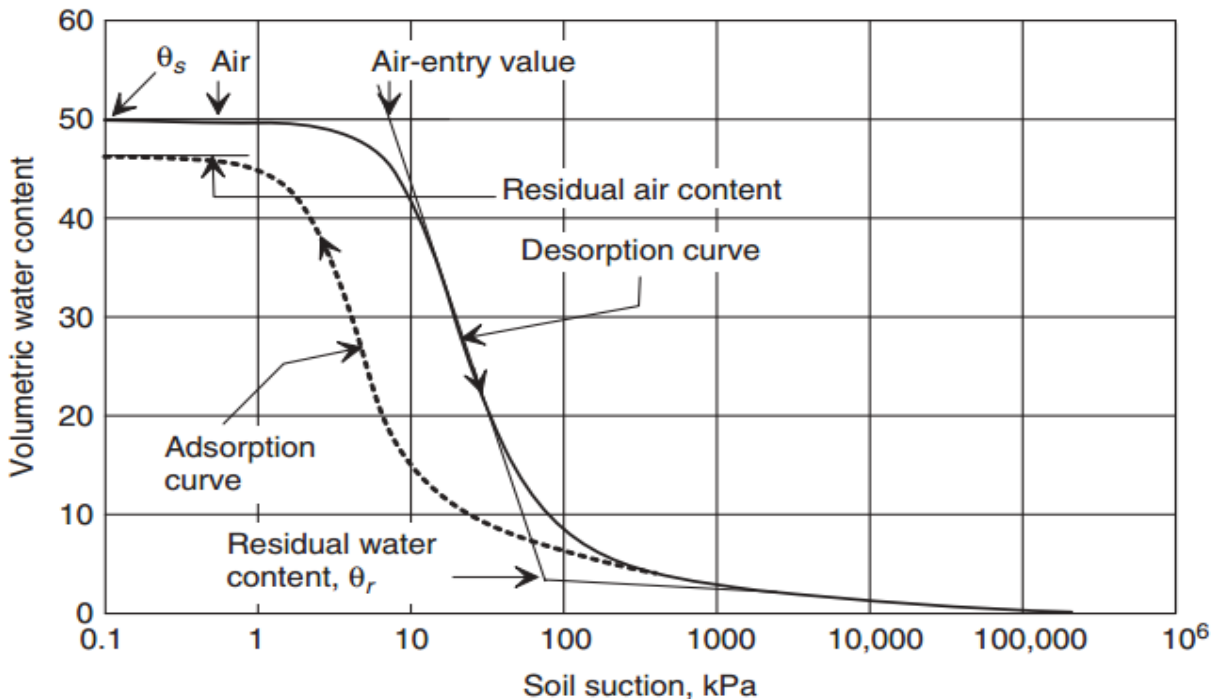


Figure 2.2 typical swcc for silty soil by (Delwyn G.Fredlund, Rahardjo and Fredlund,2012)

The main curve shown in Fig. 2.2 is a desorption curve. The adsorption curve differs from the desorption curve as a result of hysteresis related to wetting and drying. The end point of the adsorption curve may differ from the starting point of the desorption curve because of air entrapment in the soil. The drying and wetting SWCCs have similar forms (i.e., are essentially congruent).

Typical SWCCs (i.e., desorption curves) for soils ranging from sands to clays are shown in Fig. 2.3. The saturated water content and the air-entry value (or bubbling pressure), $(u_a - u_w)_b$, generally increase with the plasticity of the soil. Other factors such as stress history and secondary soil structure also affect the shape of the SWCCs.

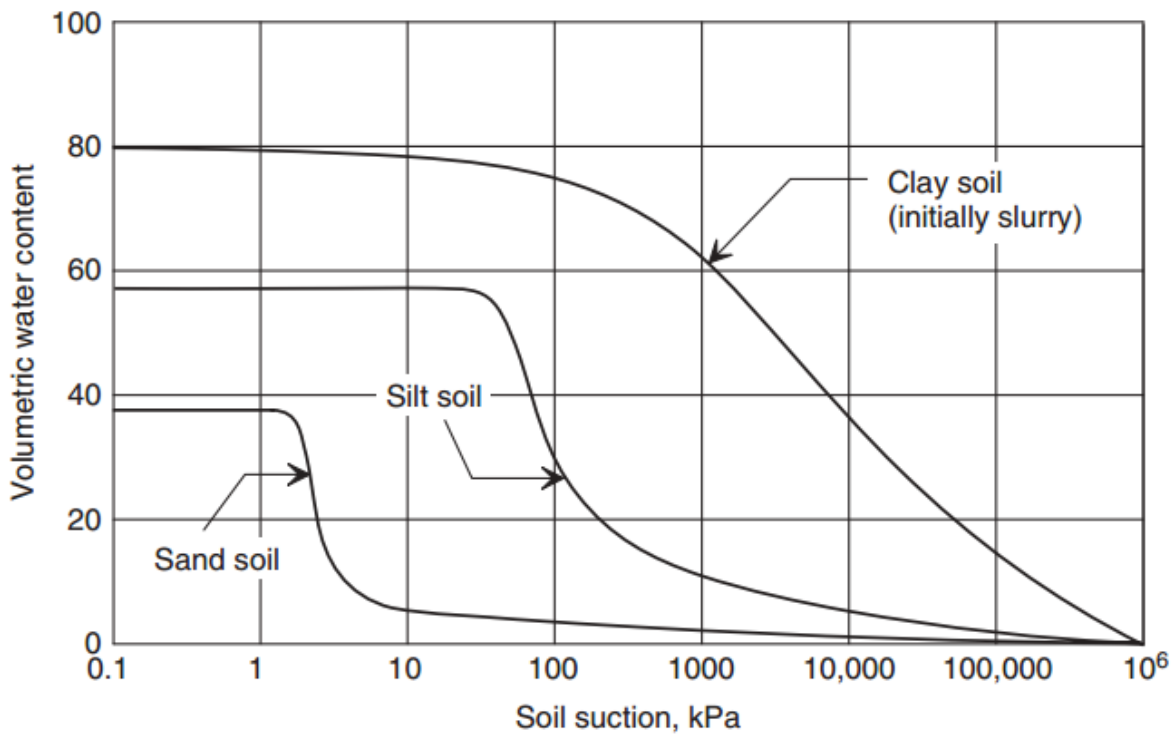


Figure 2.3 comparative desorption SWCCs for sand,silt,and clay soils adopted by (DG Fredlund,Rahardjo and Fredlund,2012)

2.3.1 Determination of soil-water characteristic curve

The methods to determine the SWCC can be generally classified into two: Experimental methods and prediction methods.

2.3.1.1 Experimental Methods

These methods are based on fitting a curve through several points obtained doing some tests to measure the suction in the soil on the different water content conditions. The development of a SWCC for a particular soil can require several tests and can take some time to obtain all the necessary information. To facilitate this problem several mathematical models have been developed to describe the SWCC for a particular soil from just a few points. Most of the equations are empirical and are based on the shape of SWCC. The process of fitting experimental suction data to one of the proposed equations requires a minimum number of experimentally obtained suction measurements, depending on the number of unknown parameters in the chosen function (D G Fredlund, Rahardjo and Fredlund, 2012).

Based on experimental observations most of the models define the shape of the SWCC as a sigmoidal or an S-shaped curve. Several studies have shown that the sigmoidal curve is the best shape for the soil-water characteristic curve among the other models. A study conducted by Zapata 1999 showed that the Fredlund and Xing (1994) model fits very well with several different soils. According to Zapata 1999 the best-fitting model for sandy and clay soil is proposed by Fredlund and Xing (1994). The Fredlund and Xing (1994), the soil-water characteristic curve can also be written in terms of the degree of saturation.

In summary, the implementation of unsaturated soil mechanics under this method requires testing to find directly the unsaturated soil property functions. Being these tests highly expensive, this level should be considered mainly for projects of great importance.

2.3.1.2 Prediction Methods

In the progress of unsaturated soil mechanics techniques, the soil-water characteristic curve is a specialized test that involves laboratory equipment which is quite complex to operate. This situation has created the need to estimate procedures, approaches, or use correlations to characterize unsaturated soils. This methodology is fundamental in the implementation of unsaturated soil mechanics into geotechnical engineering practice. These methods can be divided into three main categories (Perera and Zapata, 2005).

a. The first of these approaches are based upon the statistical estimation of water contents at selected matric suction values. These water contents, at each suction value, are correlated to soil properties. This process requires a regression analysis followed by a curve-fitting procedure.

b. The second approach includes those methods that correlate, by regression analysis, soil properties with the fitting parameters of an analytical equation of SWCC. This statistical approach has been followed by many researchers such as(Zapata, 1999) proposed relations to predict the constants of the fitting equations for SWCC based on soil index properties. The proposed option of this paper classified in this category

c. The third approach includes the methods that estimate the SWCC using a physics-based conceptual model. It involves physical models based upon the conversion of the GSD (textural information) into a pore-size distribution, which in turn is related to the distribution of water

contents and associated pore pressures. This approach was followed by Fredlund et al. (1997). The prediction of the SWCC following this approach seems to be reasonable for non-plastic soils.

In this section, only the second approach proposed above is discussed in detail. The others are beyond the scope of this thesis. In this approach, correlations are based on regressions analysis. The water content can be computed by statistical correlations of soil properties with the fitting parameters of the SWCC.

2.3.2 Previous investigation of the significance of SWCC

Different researchers (Zhang *et al.*, 2019, Ganjian *et al.*, 2007, Al-hashemi, 2018, Perera and Zapata, 2005, Nam *et al.*, 2010), Choudhury and Tadikonda, 2015, and Matlan, Mukhlisin and Taha, 2014) were develop a model to determine the unsaturated soil properties and simplifying the application of unsaturated soil mechanics into practice . Researchers also attempts to estimate SWCC with methylene blue value. Regression equations for determining the (Fredlund, D.G., and Xing, A, 1994) four fitting parameters in a previously developed SWCC equation by using the measured methylene blue value were utilized to generate the SWCC (Zhang *et al.*, 2018). To determine the SWCC parameters such as air entry value, residual water content, and residual suction graphically consume a time. To solve this difficulty (Zhai and Rahardjo, 2013) develop an equation for determining SWCC parameters by considering the relationships between SWCC parameters and fitting parameters.

For SWCC numerous curve-fitting equations previously proposed. In geotechnical engineering, these equations have been important values. However, for a soil that changes volume when suction is changed the equations are not able to adequately fit gravimetric SWCC data over the entire suction range. (Fredlund, Sheng and Zhao, 2011) Propose an equation to define gravimetric water content versus soil suction relationships for a soil exhibiting volume change and Soil-water characteristic curves (SWCCs) are routinely used for the estimation of unsaturated soil property functions (e.g., permeability functions, water storage functions, shear strength functions, and thermal property functions). (Fredlund, Sheng and Zhao, 2011) try to examines the possibility of using the SWCC for the estimation of in situ soil suction. The paper

focuses on the limitations of estimating soil suctions from the SWCC and also suggests a context under which soil suction estimations should be used.

2.3.3 SWCC Curve Fitting Empirical Models

(Fredlund, and Xing 1994) Propose a general equation for the soil-water characteristic curve. They determine the best fit parameter using a nonlinear, least-squares computer program for experimental data presented in the literature. The equation developed by (Fredlund, D.G., and Xing, A, 1994) for the entire suction range from 0 to 10^6 kPa gives a good fit for clay, silt, and sand soils. Many empirical equations have been proposed to curve fit the SWCC. (Chiu, Yan and Yuen, 2012) found that different model classes give essentially the same normalized SWCC. Several equations have been introduced by researchers to best fit laboratory data for SWCCs. The introduced equation divided into two namely, two-parameter SWCC equations, and three-parameter SWCC equations. Some equations are continuous while others are discontinuous. To fit the laboratory data more accurately the SWCC fitting parameter should be higher. A least-squares regression analysis was used to predict the best fit laboratory data of the introduced equation (D G Fredlund, Rahardjo and Fredlund, 2012).

The saturated water content value is influenced by the porous nature of the mixture, as well as the clay's retention ability and sand percentage. A higher degree of saturation is expected when the clay and particles in the mixture are dominating. Water retention in liners and wastewater barriers formed of sand reinforced by clay is significantly connected to volume increase and shrinkage (Dafalla *et al.*, 2020).

Table 12.2 Models to best fit SWCC data [adopted from (DG Fredlund, Rahardjo and Fredlund, 2012)]

Model	Equation	Curve fitting parameter
Gardner (1958b)	$\Theta_{dv} = \frac{1}{1 + a_g \psi^{n_g}}$	<p>a_g = fitting parameter which is a function of the air-entry value of the Soil</p> <p>n_g = fitting parameter which is a function of the rate of water extraction from the soil once the air-entry value of soil has been exceeded</p>

Brutsaert (1967)	$\Theta_n = \frac{1}{1 + \left[\frac{\psi}{a_b} \right]^{n_b}}$	<p>a_b = fitting parameter which is a function of air-entry value of soil</p> <p>n_b = fitting parameter which is a function of the rate of water extraction from the soil once air-entry value has been exceeded</p>
van Genuchten (1980)	$\Theta_n = \frac{1}{\left[1 + (a_{vg} \psi)^{n_{vg}} \right]^{m_{vg}}}$	<p>a_{vg} = fitting parameters primarily related to the inverse of the air-entry value</p> <p>n_{vg} = fitting parameters primarily related to the rate of water extraction from the soil once air-entry value has been exceeded</p> <p>m_{vg} = fitting parameters that are primarily related to residual water content conditions</p>
Fredlund and Xing (1994)	$\theta(\psi) = C(\psi) \frac{\theta_s}{\left\{ \ln \left[e + \left(\frac{\psi}{a_f} \right)^{n_f} \right] \right\}^{m_f}}$	<p>a_f = fitting parameter which is primarily a function of the air-entry value of soil</p> <p>n_f = fitting parameter which is primarily a function of the rate of water extraction from soil once air-entry value has been exceeded</p> <p>m_f = fitting parameter which is primarily a function of residual water content</p> <p>$C(\psi)$ = correction factor which is primarily a function of suction corresponding to residual water content.</p>

Where

$$C(\psi) = 1 - \frac{\ln \left(1 + \frac{\psi}{\psi_r} \right)}{\ln \left[1 + \left(\frac{10^6}{\psi_r} \right) \right]}$$

(Fredlund, andXing 1994)Propose an equation having three-parameters. The one fitting parameter is primarily a function of AEV of soil. The second fitting parameter is to express the rate of water extraction from the soil when the AEV has been exceeded. While the third fitting parameter is a function of residual water content. D G Fredlund, Rahardjo and Fredlund, (2012) argued that the best fit analysis using three-parameters for the SWCC gives greater flexibility.

The proposed equation can be the best fit for both drying (desorption) branch, and wetting (adsorption) branch. SWCC is plotted using the proposed empirical equation; as a result, from the SWCC plot, we can extract two drawbacks. The first drawback is found in the low suction range of SWCC, and the second drawback is found in higher suction range (i.e. beyond residual condition). The two drawback of the empirical equation is that the results become asymptotic to a horizontal line as the soil suction approaches to infinity for higher suction range, and the results become asymptotic to a horizontal line up to the AEV for lower suction range. The equation proposed by Fredlund & Xing (1994) solves the drawback for higher suction range by introducing a correction factor in their equation. SWCC is generally sigmoid in shape. In the region below AEV, and above residual condition a sigmoidal function does not perform well. A sigmoidal curve is a continuous function that can fit the SWCC plot.

2.3 4 Pervious SWCC Predictive Models

SWCC describes the volume of the voids that remain filled with water as the soil drains. To develop Soil-water characteristic curve directly by laboratory measurement is difficult due to expensive equipment setup. Hence, SWCC predictive models are an excellent option to develop SWCC. The accuracy of any modeling requires proper determination of the soil-water characteristic curve (SWCC). While the SWCC can be directly measured, several predictive models have been developed over the past two decades and are employed in practice because of their simplicity, and the lower cost, and time needed to obtain their input parameters. The predictive models are commonly developed through multiple regression analysis over a large number of measured SWCCs to establish an empirical correlation between the SWCC model parameters and soil index properties such as grain size distribution and Atterberg limits.

(Zapata, 1999) used a database of 190 soils consisting of 70 plastic and 120 non-plastic soils to generate the SWCC using weighted PI (wPI) for plastic soils, where w is the percent passing the #200 sieve, and PI is the plastic index, and using D₆₀ for non-plastic soils. The product of the percentage passing the #200 sieve (used as a decimal value) multiplied by the plasticity index is called a weighted PI value (i.e., wPI) for soils with a plasticity index greater than zero. The correlations and algorithms developed from her study provide a smooth transition across the spectrum of soils using multiple regressions and (Fredlund, D.G., and Xing, A, 1994) equation.

For non-plastic soils (Zapata, 1999) used the (Fredlund, D.G., and Xing,A, 1994) equation having four fitting parameters for each soil: a_f , m_f , n_f and ψ_r . The four parameters were correlated with the particle diameters corresponding to 60% passing. The correlations for non-plastic soils were represented by the following equations:

$$a_f = 0.8627(D_{60})^{-0.751} \quad (2.7)$$

$$m_f = 0.1772[\ln(D_{60})] + 0.7734 \quad (2.8)$$

$$n_f = 7.5$$

$$\psi_r = a_f \left(\frac{1}{D_{60} + 9.7e^{-4}} \right)^{-0.751} \quad (2.9)$$

Where: a_f is fitting parameter related to the inflection point on the SWCC, m_f is fitting parameter influencing the curvature of the SWCC at low and high suctions, n_f is fitting parameter equal to the slope at the inflection point of the SWCC, ψ_r is fitting parameter which is primarily a function of the suction at which residual water content occurs, D_{60} is grain-size diameter corresponding to 60% passing by mass, and ℓ is constant equal to 2.71828.

For Plastic soils (Zapata, 1999) found that the four fitting parameters of the Fredlund and Xing (1994) equation were well correlated to the weighted plastic index (wPI). The following expression where suggested by (Zapata, 1999) to compute the four fitting parameters of the(Fredlund, and Xing 1994) equation:

$$a_f = 0.00364(wPI)^{3.35} + 4(wPI) + 11 \quad (2.10)$$

$$m_f = 0.0514(wPI)^{0.465} + 0.5 \quad (2.11)$$

$$n_f = m_f \left(-2.313(wPI)^{0.14} + 5 \right) \quad (2.12)$$

$$\psi_r = a_f \left(32.44e^{0.0186(wPI)} \right) \quad (2.13)$$

(Perera *et al.*, 2005) extend the work of Zapata and used multiple regressions and the (Fredlund, D.G., and Xing, A., 1994) equation with a database of 154 non-plastic and 63 plastic soils to derive equations for the SWCC based on the grain-size distribution for coarse-grained soils, and the plasticity index for fine-grained or plastic soils.

Correlation equations for non-plastic soils:

$$a_f = 1.14a - 0.5 \quad (2.14)$$

$$m_f = 0.936b - 3.8$$

(2.16)

$$n_f = 0.26e^{0.78c} + 1.4D_{10} \quad (2.15)$$

$$\psi_r = 100 \quad (2.16)$$

Where:

$$a = -2.79 - 14.1 \log(D_{20}) - 1.9 \times 10^{-6} p_{200}^{4.34} + 7 \log(D_{30}) + 0.055 D_{100}$$

$$D_{100} = 10^{\left[\frac{40}{m_1} + \log(D_{60}) \right]}, \quad m_1 = \frac{30}{\left[\log(D_{90}) - \log(D_{60}) \right]}$$

$$b = \left\{ 5.39 - 0.29 \ln \left[p_{200} \left(\frac{D_{90}}{D_{10}} \right) \right] + D_0^{0.57} + 0.021 p_{200}^{1.19} \right\} m_1^{0.1}$$

$$D_0 = 10^{\left[\frac{-30}{m_2} + \log(D_{30}) \right]}, \quad m_2 = \frac{30}{\left[\log(D_{30}) - \log(D_{10}) \right]}, \quad c = \log(m_2^{1.15}) - \left(1 - \frac{1}{m_f} \right)$$

Note that if the value of a_f in equation (2.15) is zero; the value of a_f should be limited to one.

Where: a_f is fitting parameter related to the inflection point on the SWCC, m_f is fitting parameter influencing the curvature of the SWCC at low and high suctions, n_f is fitting parameter equal to the slope at the inflection point of the SWCC.

Correlation equations for plastic soils

$$a_f = 32.835 \{ \ln(wPI) \} + 32.438 \quad (2.17)$$

$$m_f = 1.421(wPI)^{-0.3185} \quad (2.18)$$

$$n_f = -0.2154 \{ \ln(wPI) \} + 0.7145 \quad (2.19)$$

$$\psi_r = 500 \quad (2.20)$$

Hernandez (2011) propose an SWCC predictive model based on group index (GI). Fernandez, 2011 proposed the following models for fine grained soil for each fitting parameters:

$$a_f = 10 \left(\frac{0.69 - \frac{2.7}{1 + e^{4 - 0.14GI}}}{1} \right) \quad (2.21)$$

$$n_f = 10 \left(\frac{0.78}{1 + e^{6.75 - 0.19GI}} \right) \quad (2.22)$$

$$m_f = 0.03 + 0.62e \left(-0.82 \left(\log(a_f) - 0.57 \right)^2 \right) \quad (2.23)$$

$$\psi_r = 494 + \frac{660}{1 + e^{4 - 0.19GI}} \quad (2.24)$$

$$GI = (F_{200} - 35) [0.2 + 0.005(LL - 40)] + 0.01(F_{200} - 15)(PI - 10) \quad (2.26)$$

Where: GI : Group index, F_{200} : Percent passing number 200 sieve expressed in percentage, LL : Liquid limit expressed in percentage, and PI : Plasticity index expressed in percentage.

2.4 Physical properties of clay soil

The term clay is applied to the fraction of grains whose equivalent diameter is less than 0.002mm. The individual grains are fragments of a single mineral i.e. a solid compound with a definite chemical composition and unique crystalline structure. The minerals of clays are formed by the weathering of rocks. Most clay minerals of interest to geotechnical engineers are composed of oxygen and silicon- two of the most abundant elements on earth. Silicates are a group of minerals with a structural unit called the silica tetrahedron. A central silica cation is

surrounded by four oxygen anions, one at each corner of the tetrahedron .(Clay, In and Dar, 2003).

Clay mineral particles are commonly too small for measuring precise optical properties. Specific gravity of most clay minerals are within the range from 2 to 3.3. Their hardness generally falls below 2.5. Refractive indices of clay minerals generally fall within a relatively narrow range from 1.47 to 1.68. Generally the size and shape, the two properties, are determined by electron micrographs. Mainly there are three common clay minerals these includes Kaolinite, Montmorillonite, and Illite that play important role in the properties of clay soil. It is important to note that physical properties depend on various other factors controlling the behavioral pattern of the material. Clay sedimentation properties depend on porosity, water content and minerals content of different specific gravity(Mukherjee, 2013).

Clay soils are the dominant soils in and around Jimma town. It is well known that clay soils are found mostly in humid temperate and tropical regions. Clay minerals influence the soil properties due to their high exchange capacities, small particles size, and high specific surface areas. This influence depends on the nature and the content of clay minerals species in soils. From visual observations and field tests, the soils of the Jimma area are categorized as clay soil with high plasticity. Based on Textural Classification System the soils studied are classified as silty-clay to clay. And from indices classification criteria these soils can be classified as clay with high plastic and firm consistency. According to the Unified Soil Classification System (USCS) and AASHTO the soils are classified as CH (clay with high plasticity) and G-7-5(clayey soils) respectively(Jemal J, 2017).

2.5 Research gap

A different researcher clarifies the importance of applying unsaturated soil mechanics principles in the field of geotechnical engineering. To apply this discipline the detailed investigations about unsaturated soil properties must be done in different areas that locate unsaturated soil dominantly. Mainly the behavior of unsaturated soil focused on the soil water characteristics curve. Therefore, SWCC serves as a tool to solve problems related to unsaturated soil properties. Ethiopia is located around tropical regions and most of soil above ground water table in these regions exists in unsaturated state. Jimma is also categorized under tropical region of Ethiopia. Many infrastructures constructed around Jimma town in the principle of saturated soil mechanics

due lack of practiced manual of unsaturated soil properties. Researchers around Jimma city deeply investigated about the saturated soil properties but still now no one is there that done about the unsaturated soil properties. The big problem behind this is lack of expert laboratory equipment to measure unsaturated soil properties due to high cost and complexity of test procedures. Thus, to solve this condition developing a mathematical model was the mandatory issue for best practice of unsaturated soil mechanics in the field construction industry.

CHAPTER THREE

MATERIALS, METHODS, AND PROCEDURES FOR LABORATORY TESTING

3.1 General

This chapter introduces the materials, methods, and procedures needed to conduct this research. This section initially describes in detail the location of the test pit and a description of the survey area. Then, the results and discussion of all laboratory tests including Suction measurements conducted at Jimma University Geotechnical engineering laboratory. The laboratory tests conducted in this thesis include under index properties category were natural moisture content, specific gravity, Atterberg limits, and particle size distribution. As the investigation according to (Jemal J, 2017) and (Town et al., 2020) Jimma soils were predominantly covered by soft clay soils with dominated clay with red, grey and black color . Filter paper method was performed to obtain soil moisture versus suction values/points based on the indirect method of a testing category to develop the soil-water characteristics curve data points. All of the laboratory tests were carried out following the ASTM standard procedures for soil testing. The remaining parts of this study will be conducted and presented in the model development and setup part in the next chapter.

3. 2 Site Description And Soil Sampling

3.2.1 Site Description

The study carried out in the city of Jimma in Southwestern Ethiopia located at latitude and longitude of $7^{\circ}40'N$ and $36^{\circ}50'E$ respectively in Oromiya National Regional State. It is 350km from Addis Ababa. The town has a rolling terrain with an elevation ranging from 1670m to 1770m above mean sea level. Lower elevation and unfavorable drainage condition and clay soils were dominant at this region (Jemal J, 2017). The detailed locations of the test pits are shown in (Table 3.1 & Figure 3.1)

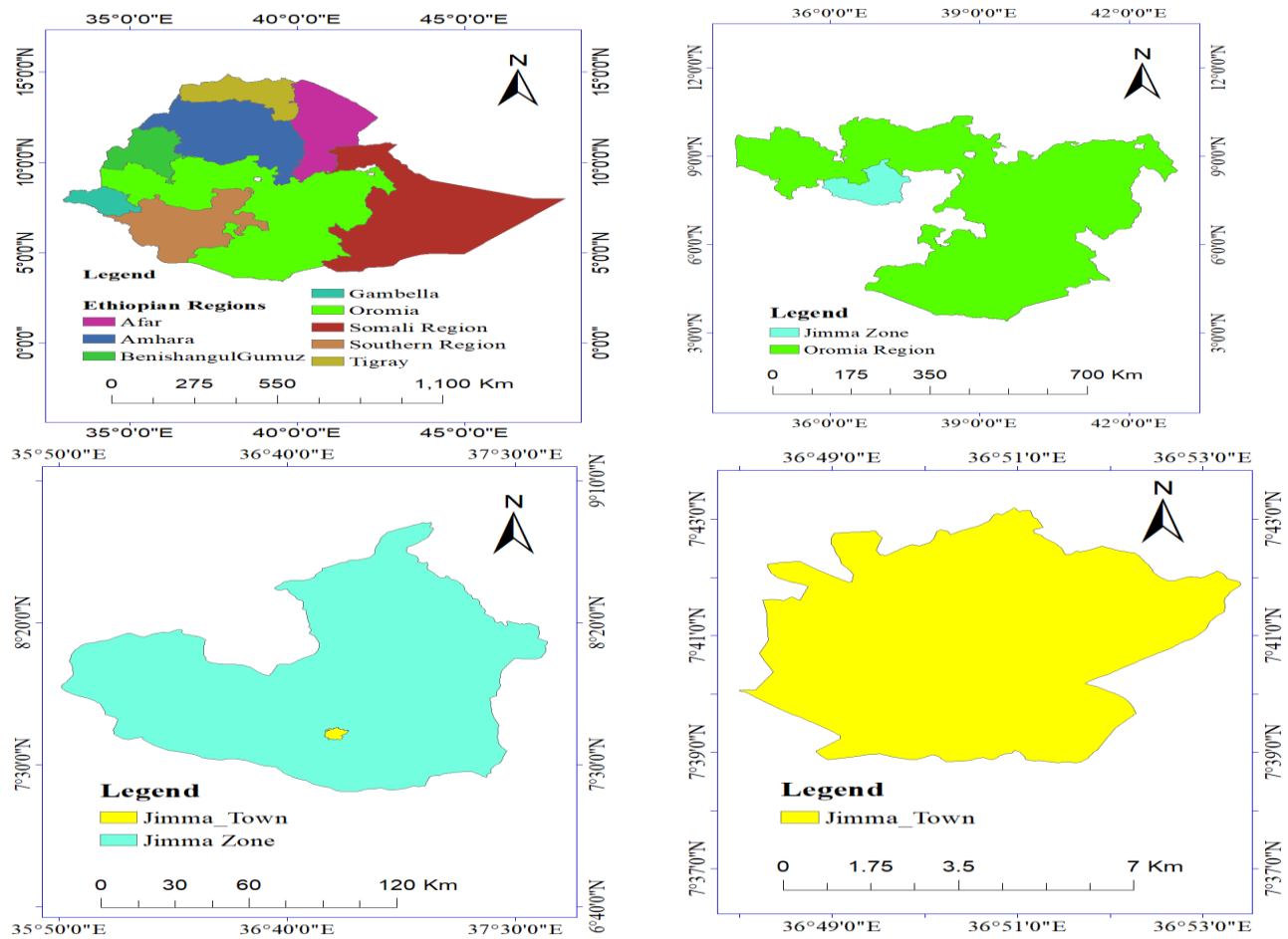


Figure 3.1 Map of the study area

Table 3.1 Profile of sampling area

no	Location	Test pit Designation	Latitude	Longitude	Sample depth	Color Type
1	kito	TP1	7° 41' 19.10" N	36° 49' 0.83" E	2m	Red
2		TP2	7° 41' 16.59" N	36° 49' 8.65" E	2m	Red
3	Awetu	TP3	7° 40' 32.76" N	36° 50' 10.46" E	2m	Red
4		TP4	7° 40' 31.97" N	36° 50' 11.21" E	2m	Red
5	Banchcho Bore	TP5	7° 38' 56.15" N	36° 50' 37.26" E	2m	Red
6		TP6	7° 38' 55.68" N	36° 50' 43.99" E	2m	Red
7	Main Campus	TP7	7° 41' 13.40" N	36° 51' 30.78" E	2m	Red
8		TP8	7° 41' 13.81" N	36° 51' 37.16" E	2m	Red

3.2.2 Soil Sampling

In this investigation, eight red clay soil samples taken from eight test pits from various field locations in Jimma city, in south western Ethiopia. First random locations selected based on the

area coverage of red clay soil in Jimma. Eight test pits excavated at different location of Jimma city to cover as much as possible. To select the location of the eight test pits, first random soil samples collected from different sites and transported to the Jimma geotechnical engineering laboratory to classify the soil based on the USCS system. Disturbed soil samples were taken from all test pits at a depth of 2 m for the soil index property tests and undisturbed samples for filter paper technique. The eight experimental pits for this study were dug by hand using a pick and shovel. The test holes were 1 m by 1 m. In each test pit at 2m, disturbed soil samples were collected for all index properties except the filter paper test and the natural moisture content. Undisturbed soil samples were taken from the eight test pits at a depth of 2 m for the sole purpose of determining discrete SWCC data points with the filter paper method. Because the soil samples were collected at dry season the water table was not exist until 2m depth, so reasonable the soil is considered to be unsaturated.

3.2.3 Sample preparation

Disturbed representative samples were used to determine index characteristics of soils, such as Atterberg limit (LL, PL), specific gravity, and particle size distribution. For each test that can be performed, prepare a sample of the appropriate quantity and size. In the laboratory to achieve the required size, use the recommended sieve size for testing procedure.

3.3 laboratory Tests of Index Properties

After the samples transferred to the laboratory, a complete characterization of the index properties was carried out. All basic index tests were carried out according to the ASTM standard. The tests included were the natural moisture content, the specific gravity (ASTM D 854), the grain size distribution (i.e. Specifically Hydrometer analysis) ASTM D 7928, and the Atterberg limit tests ASTM D 4318. The material classifications were carried out based on the Unified Classification of Soils System. The details of the test procedures used to obtain the test results were described below. Two sets of laboratory tests were performed; one for index properties and the other for SWCC determination by filter paper method of testing.

3.3.1 Natural Water Content

The natural Moisture Content of all the prepared samples was performed by using ASTM D 2216 laboratory testing procedure.

3.3.2 Specific gravity

In this research, the measurement of the specific gravity of solid soil was performed according to the ASTM D 854 standard which is the standard test method for the specific gravity of soils.

3.3.3 Particle Size Distribution Test

Particle size distribution tests carried out in two stages, the first stage being wet sieving and soil hydrometer analysis being carried out on those that passed through the # 200 sieve size. To avoid the loss of fine particles, the soil sample was washed through the #200 sieve. Since fine grain soils, wet sieving is the applicable method. Dry sieving was only suitable for soils with negligible amounts of silt and clay ASTM D 422. For hydrometer analysis, the methods and procedures of (ASTM D 7928) were used. This test carried out for fine-grained soils or a soil passing a sieve size of 0.075 mm (No. 200). In this research (ASTM 152H) type of hydrometer analysis was used.

3.3.4 Liquid Limit (LL)

The procedure according to the test Method A (ASTM D 4318) used to determine the liquid limit of the red clay soil in this study. The liquid limit (LL) of the soil was the water content at the boundary between the liquid and plastic state. The water content in this limit is arbitrarily defined as the water content at which two halves of a soil layer placed in a brass cup, cut with a standard slit and dropped from a height of 1 cm, are exposed to a focal plane shutter of approximately 1.3 cm when the cup is dropped 25 times at a rate of 2 drops per second. The graph was plotted as line count versus moisture content and interpolates moisture content at 25 lines from this graph to determine the liquid limit.

3.3.5 Plastic Limit (PL)

The plastic limit value (PL) of the prepared soil sample was conducted. The water content in this limit is arbitrarily defined as the water content at which the soil begins to crumble when wound into strands of a certain size of 3.2 mm. (ASTM D 4318).

3.3.6 Soil classification

In this study the Soils classified according to the USCS Soil Classification System. The data required for this classification procedure were particle size distribution and Atterberg limits.

3.4 X-ray Diffraction (XRD)

Under this study XRD test was performed to determine the dominant clay mineral of red clay soil. A powdered sample less than 63 micro sieve number was put in front of a camera, and a thin layer is covered around the inner wall to operate as an X-ray detector and recorder. According to Bragg's Law, the interaction of incident rays with the sample creates a large number of diffracted rays, which is described by the equation $n\lambda = 2d\sin\theta$, where n is an integer, w is the wavelength of the rays, and θ is the angle between the diffracted and incident X-ray beam planes. By converting the diffraction peaks to d-spacing and comparing it to conventional patterns for known materials, the spacing d between the lines on the recording was utilized to identify the material. The most frequent target material for single-crystal diffraction is copper, which has a spacing of 1.54 Å with Cu K α radiation and was used in this investigation (Town et al., 2020). As expressed by (Clay, In and Dar, 2003) Kaolinite and halloysite are the predominant clay minerals of red soils in Ethiopia.

3.5 Filter Paper Method of Testing

In this research the filter paper water content was measured in laboratory by ASTM D 5298 testing procedure then by using previously determined calibration curve of whatman 42 filter paper brand the matric suction was determined. whatman NO 42 filter paper was the filter paper recommended by ASTM for measurement of soil suction. As expressed in the literature indirect method of suction measurement by using filter paper performed under two ways the first one by direct contact between the soil and filter paper matric suction was measured. Second by indirect contact total suction was measured. But in this paper only direct contact principle was adopted. Basically, the filter paper comes to equilibrium with the soil either through vapor (total suction measurement) or liquid (matric suction measurement) flow (Bicalho, Cupertino and Bertolde, 2011). At equilibrium, the suction value of the filter paper and the soil is equal. After equilibrium is established between the filter paper and the soil, the water content of the filter paper disc is measured. Then, by using filter paper water content versus suction calibration curve, the corresponding suction value determined from the curve. This is the basic approach suggested by ASTM Standard Test Method for Measurement of Soil Potential (Suction) Using Filter Paper (ASTM D 5298). In other words, ASTM D 5298 employs a single calibration curve that has been used to infer both total and matric suction measurements.

The ASTM D 5298 calibration curve is a combination of both wetting and drying curves. However, this paper demonstrates that the “wetting suction calibration curves. The current investigation used ASTM standard D5298 testing protocols and calibration curves for the Whatman No. 42 filter paper. The Researcher measured the length of the matric suction of the undisturbed soil samples.

3.5.1 Soil Matric Suction Measurements

Under this study 7.6cm internal diameter of shellby tube was prepared and commercially available 5.5cm diameter what man filter paper and 12.5 cm product quality index qualitative filter paper as protective layer was used. 76 mm diameter and 2 inch height of samples needed for each data point measurement. The prepared sample divided into two parts by using cutter device. For one data point one test conducted. Glass jars that are between 250 to 500 ml volume sizes were readily available in the market and can be easily adopted for suction measurements. Plastic jars, especially, with diameter can contain the 7.6 cm diameter Shelby tube samples prepared very nicely. A testing procedure for matric suction measurements using filter papers can be outlined as follows:

- At least 75 percent by volume of a plastic jar is filled with the soil; the smaller the empty space remaining in the plastic jar, the smaller the time period that the filter paper and the soil system requires to come to equilibrium.
- A filter paper was sandwiched between two larger size protective filter papers. The filter papers used in suction measurements was 5.5 cm in diameter bigger diameter (bigger than 5.5 cm) filter papers was used as protective.
- Then, these sandwiched filter papers were inserted into the soil sample in a very good contact manner. A good contact between the filter paper and the soil was mandatory.
- After that, the soil sample with embedded filter papers is put into the plastic jar container. The plastic jar container is sealed up very tightly with plastic tape. The prepared containers were put into humidity controller machine in a controlled temperature room for 7 day equilibrium.

Researchers suggest a minimum equilibrating period of one week (ASTM D5298-16, 2016, Bulut, 2001, Bicalho, Cupertino and Bertolde, 2011). After the equilibration time, the procedure for the filter paper water content measurements can be as follows:

- Before removing the plastic jar containers from the temperature room, all the cleaned aluminum cans that were used for moisture content measurements were weighed to the nearest 0.0001 g. accuracy and recorded.
- After that, all measurements were carried out by two persons. While one person is opening the sealed glass jar, the other is putting the filter paper into the aluminum can very quickly (i.e., in a few seconds) using tweezers.
- Then, the weights of each can with wet filter paper inside were taken very quickly.
- Then, all cans were put into the oven with the lids half-open to allow evaporation. All filter papers are kept at 105 °C temperature inside the oven for 24 hours.
- Before taking measurements on the dried filter papers, the cans were closed with their lids and allowed to equilibrate for about 5 minutes. Then, a can is removed from the oven and put on an aluminum block (i.e., heat sinker) for about 20 seconds to cool down; the aluminum block functions as a heat sink and expedites the cooling of the can. After that, the can with the dry filter paper inside is weighed very quickly. The dry filter paper is taken from the can and the cooled can is weighed again in a few seconds.

After obtaining all of the filter paper water contents, an appropriate calibration curve of ASTM D5298 for whatman 42 filter paper, was employed to get the corresponding matric suction values of the soil samples.

3.6 SWCC Predictive Model Development set up, data analysis, and validation approaches.

3.6.1 General over view

Under this section, the way how to select the best predictor among a variety of index properties for the Fredlund & Xing, (1994) model fitting parameters and the way how to develop the simplified prediction model were clearly identified. Moreover, this section illustrates the validation technique for the proposed model using statistical analysis.

3.6.2 primary and secondary source of data

Primary data for both tests analyzed for 8 samples. All the laboratory tests of the fine-grained soils performed according to the ASTM testing standard. The laboratory test results used for regression analysis and validation of the developed model. All the required laboratory tests of

eight soil samples excavated from the study site were first carried out. These tests include water content, Specific Gravity, the Atterberg limits, Particle size distribution, SWCC tests, and XRD test. The stepwise subset selection multiple regression routines of JMP-14 statistical software developed by SAS Institute Inc. in 2016 was used to undertake all the required multiple regression statistical analysis. The stepwise regression control panel is used to limit regressor effect probabilities, determine the method of selecting effects, begin or stop the selection process, and run a model. However, before the predictive model development using JMP-14 statistical software, some statistical pre-analysis and model setup is required in this part of the thesis.

3.6.3 Approaches used for model development

Multiple regression analysis is a statistical technique which can be used to model and establish correlations between two or more variables in the field of engineering and science. The investigation uses JMP-14 statistical software's multiple regressions with subset selection and interaction analysis methods. The method of subset selection multiple regression analysis is used to develop the line or curve which provides the best fit through a set of data points. Multiple Regression Models means a Regression Model that contains more than one predictor. The multiple regression equations can take two forms: these are model with intercept and model without intercept. Under this research model with intercepts was adopted for model development. Stepwise regression is part of the Fit Model platform in JMP software. The Stepwise feature computes estimates in the same way as other least-squares platforms, but it makes it easier to search and select from a large number of models. Complex model tests can be efficiently specified using the Fit Model platform. Fit Model is a tool that allows us to fit a wide range of models and effect structures. Simple and multiple linear regressions, analysis of variance and covariance, and response screening are examples of these methods for studying a large number of responses. The Fit Model platform gives an efficient way to specify models that have complex effect structures. These effect structures are linear in the predictor variables. Once the model is specified, one can select the appropriate fitting technique from several fitting personalities. Once you choose the option, the Fit Model window provides choices that are relevant for the chosen model. Fit Model can be used to specify a wide variety of models that can be fit using various methods. Standard Model Types lists some typical models that can be

defined using the Fit Model. Eqn. (3.1) are model with intercept and model without intercept in Eqn. (3.2):

$$y = b_0 + b_1x_1 + b_2x_2 + \dots + b_nx_n + c \quad (3.1)$$

$$y = b_1x_1 + b_2x_2 + \dots + b_nx_n + c \quad (3.2)$$

Where the 'b's are the regression coefficients, representing the amount the dependent variable changes when the independent changes 1 unit. The variable c is a constant, where the regression line intercepts the y axis; representing the amount the dependent y.

Because of its simplicity, a linear relationship is commonly used to solve various engineering problems; however, the reality for soils is somewhat different. Two groups of variables were used to build the model. All other factors from index property test results categorized as independent variables, whereas compression index test results produced from the related test procedures considered as a dependent variable. These dependent and independent variables have to be checked first for the normality of the corresponding data before the regression analysis is carried out to consider as a variable in the model. Therefore, first, the geotechnical parameter/data obtained from each test sample need to be checked for its normality by using JMP-14 software with the help of scatter plot and correlation matrix. Regression would be approved if the test data for the related tests have a normal distribution or if the residuals of the fit model obtained have a normal distribution. If the fit model's residuals are not normally distributed, data transformation is used to make the relevant data regularly distributed. The data analysis and model development section will go over the specifics of checking the data for normality.

3.7 Regression Analysis

3.7.1 Model variable

3.7.1.1 Independent variable

The goal of this study is to create a SWCC statistical predictive model using index property test data from Jimma fine-grained (clay) soils. Water content, specific gravity, the Atterberg limits, and particle size distribution were all included as independent variables in this study.

3.7.1.2 Dependent variable

The dependent variables are a_f , n_f , and m_f these are curve fitting parameters and ψ_r is the residual suction. These values are obtained from the fit of the (Fredlund & Xing 1994) model was used to fit the measured SWCC data point obtained from the filter paper test.

3.7.1.3 Fredlund and Xing SWCC model

To fit the collected data points to the soil-water characteristics curve, many SWCC fitting models have been developed.. These SWCC fitting models are almost derived from a generic formula and are empirical. Due to the discrete character of the collected data, curve fitting was used to define the full/continuous SWCC (Fredlund & Xing, 1994). The Fredlund & Xing (1994) model was used to fit the measured SWCC data point obtained from the filter paper, mainly due to the flexibility of the model for all matrix suction. Fredlund and Xing (1994) developed introduced a correction factor so that there is a linear drop to zero water content at the suction of 1 GPa after the residual water content using the following empirical equation (Fredlund & Xing, 1994).

$$\theta(\psi) = C(\psi) \frac{\theta_s}{\left\{ \ln \left[e + \left(\frac{\psi}{a_f} \right)^{n_f} \right] \right\}^{m_f}} \quad (3.3)$$

$$C(\psi) = 1 - \frac{\ln \left(1 + \frac{\psi}{\psi_r} \right)}{\ln \left[1 + \left(\frac{10^6}{\psi_r} \right) \right]} \quad (3.4)$$

Where: θ_w is the volumetric water content, θ_s the saturation volumetric water content, e is the natural number 2.71828, ψ is suction, a_f , n_f , and m_f are curve fitting parameters and ψ_r the suction at the residual water content (θ_r). The purpose of the correction factor is to direct the model towards zero water content at oven-dry conditions corresponding to a suction. This provides one means of improving the accuracy of the soil-water characteristic model in the dry range.

3.7.2 Model Development and Setup

3.7.2.1 Assumptions used during modeling

In practice, multiple linear regression is based on the following assumptions: The dependent and independent variables have a linear correlation; the independent variables are not significantly related; and the residual variance is constant. Independence of observations (the model implies that the observations are independent to one another). To test for this assumption, use Multivariate analysis. and Other statistical goodness of fit measures needs to be with the required range, such as RMSE, R^2 , Adj R^2 , Coefficient of Variation, Mean Square Error, and AIC. The predictor variable needs to be free from multicollinearity. The normality of the data used in the model development and the normality of the residual obtained from. Furthermore, these predictor variable included in the model need to be easily measurable index properties. In a most practical situation, the variance of the random error will be unknown and must be estimated from the sample data.

A plot of residuals versus fitting values, if the model is correct and if the assumptions are satisfied, the residuals should be structureless; in particular, they should be unrelated to any other variable including the predicted response. A simple check is to plot the residuals versus the fitted values. Plots of residuals versus other variables: if data have been collected on any other variables that might affect the response, the residuals should be plotted against these variables. Patterns in such residual plots imply that the variable affects the response. This suggests that the variable should be either controlled more carefully in future experiments or included in the analysis.

3.7.2.2 Optimization of curve fitting parameters

The optimization curve fitting parameters of Fredlund and Xing(1994) was optimized by using the latest version of matlab 2019a with a function of Fmincon routine. Fmincon stands for function minimum constrain. Several optimization techniques are available to estimate the (Fredlund & Xing, 1994) model fitting parameters by minimizing the error between the experimental data point and theoretical computed data point.

As mentioned by(Choudhury and Tadikonda, 2015) Gradient-based techniques are prevalent in the prediction of model parameters from experimental data, and they are the most common

optimization strategies. The “fmincon” MATLAB®R2019 program is used to discover the optimal SWCC model parameters that offered the best-fit to the observed retention data. It features a restricted optimization of a multivariable function using the interior-point technique. (chouhury & Tadikonda, 2014) point out that The interior-point technique outperforms the trust-region-reflective or any other gradient-based strategy in terms of convergence. In gradient-based methods, the unknown parameter vector in the search space is searched iteratively. At each iterative step, the objective function is approximated using a quadratic form and formulated as a normal equation. The following objective function, root mean square (RMSE), is used for finding the appropriateness of the model to the observed data. The main objective of constrained optimization is to convert the complex nonlinear problem into a simpler equivalent problem that can be solved and utilized for an iterative procedure. The fmincon subroutine finds a constrained minimum of a multivariate scalar function at an initial guess. To ensure the convergence of the optimized retention data to the measured data, it may be required to define a set of lower and upper bounds for the fitting parameters during the optimization to ensure that the solution is always in the range. The multivariate scalar function, or the objective function, was defined as the root mean square error (RMSE) of the fitted and measured water content values. The fmincon function starts with an initial guess of scalar variable (fitting parameters) within the defined bounds and attempts to minimize the RMSE at that particular guess.

The fmincon function continues to evaluate the RMSE using different scalar variable values within the defined bounds until the RMSE value is minimized. Consequently, the optimized fitting parameter is the value of the scalar variable at which the lowest RMSE is achieved. The optimized fitting parameters were then used in their respective retention functions to generate the corresponding SWCC. The equation for RMSE is given as. The optimization process was intended to seek the global minimum for RMSE within the given lower and upper limits of (Fredlund & Xing, 1994) model fitting parameters. Gradient-based algorithms are the classical method used to optimize the (Fredlund & Xing, 1994) model fitting parameters. Fmincon uses an interior-point or active-set algorithm which is a powerful gradient-based algorithm to optimize model parameters. However, several difficulties were encountered during the optimization process. It was found that the initial range of the parameters highly influences the final predicted model parameters by the algorithm. Hence, the ranges of the parameters were varied to verify

any discrepancy in several runs. It has also been found that the final values of the fitting parameters are depended on the initial gauss solutions.

3.8 Statistical goodness of fit measure

3.8.1 Sum of Squared Error (SSE)

A preliminary statistical calculation that leads to additional data values is the sum of squared error (SSE). It's useful to be able to determine how closely two or more variables are related.

$$SSE = \sum_{i=1}^n (w_{ip} - w_{ia})^2 \quad (3.5)$$

Where: w_{ip} is the predicted gravimetric water content, w_{ia} is the actual value of the gravimetric water content, and n is the number of data points or observations.

3.8.2 R-Squared (R2)

R-squared is a statistical measurement techniques that tells how much of a dependent variable's variance is explained by an independent variable. The R-squared value indicates how much the variation of one variable explains the variance of the other. With an R-squared near unity, the observed and fitted data sets are linearly positioned around the line of perfect agreement, or the fitted curve has a similar shape to the observed curve..

$$R^2 = 1 - \frac{SSE}{SST} \quad (3.6)$$

Where: SST is the sum of a total square and \bar{w}_{ia} is the mean of the actual or measured gravimetric water content.

$$SST = \sum_{i=1}^n (w_{ia} - \bar{w}_{ia})^2 \quad (3.7)$$

3.8.3 Root Mean Square Error (RMSE)

The Root Mean Square Error (RMSE) is a statistical term that describes how well a model predicts quantitative data. RMSE is a good tool for numerical prediction. The root mean square error (RMSE) is a strong indicator of accuracy. Furthermore, the root mean square error (RMSE) is only used to compare the prediction errors of different models.

$$RMSE = \sqrt{\sum_{i=1}^n \frac{(w_{ip} - w_{ia})^2}{n}} = \sqrt{\frac{SSE}{n}} \quad (3.8)$$

3.8.4 Akaike's Information Criteria (AIC)

The quality of a group of statistical models is compared using Akaike's information criterion (AIC). The AIC is a measure of how well a model fits the data it is supposed to describe.. Moreover, AIC is most often used to compare the relative goodness-of-fit among different models under consideration and to then choose the model that best fits the data. A low value of AIC indicates a best model. In estimating the amount of information lost by a model, AIC deals with the trade-off between the goodness of fit of the model and the simplicity of the model. In other words, AIC deals with both the risk of over fitting and the risk of under fitting.

$$AIC = n \left[\ln \left(\frac{SSE}{n} \right) \right] + 2k \quad (3.9)$$

Where: n is the number of data points (observation) and k is the number of fitting parameters. k Must be increased by 1 to reflect the variance estimate as an extra model parameter.

3.8.5 Mean algebraic error

Mean algebraic error e_{alg} indicates how well the curve fit is centered on the data. A low value of e_{alg} indicates a prediction well centered and with a very little bias. The sign of this factor describes the direction of the bias.

$$e_{alg} = \frac{\sum_{i=1}^n 100 \frac{(w_{ia} - w_{ip})}{w_{ia}}}{n} \quad (3.10)$$

3.8.6 Mean absolute error

Mean absolute error e_{abs} indicates how the predicted value are dispersed the best fitting curve.

$$e_{abs} = \frac{\left| \sum_{i=1}^n 100 \frac{(w_{ia} - w_{ip})}{w_{ia}} \right|}{n} \quad (3.11)$$

CHAPTER FOUR

RESULT AND DISCUSSION

4.1 Index properties test result

The first task to achieve the objectives of this study was determining the index properties of red clay soil around Jimma city. Under this section the index properties of Jimma city red clay soils were briefly discussed. The index property is one of the most basic soil qualities that aids in identifying soil characteristics. The terms "soil grain" and "soil aggregate property" refer to two different types of soil properties. Individual soil grain properties were determined by their size, shape, and mineralogical characteristics. Soil aggregate property, on the other hand, is based on the properties of the entire soil mass; examples include the Atterberg limit test, specific gravity, and particle size (sieve and hydrometer). This section discussed the engineering features, identification, and categorization of the red clay natural soil around Jimma city.

4.1.1 Natural moisture content

The moisture content of the soil samples was determined in the laboratory using the oven drying method at a temperature of 105 degrees Fahrenheit in accordance with ASTM D2216 (see Appendix A and table 4.1). For the purpose of determining the moisture content of a single test pit, three test specimens were constructed. The water content measurements in the laboratory were in the range of 35.44 percent to 43.09 percent. According to Das (2002), clay soils have a natural moisture content of 30-50 percent, which is consistent with this study. Table 4.1 illustrates the overall water content result of Jimma city red clay soil under eight representative samples that taken from eight test pits.as shown on table 4.1 the water content variation of the representative samples were significantly related. This can properly represent the water content of Jimma town red clay soil.

Table 4.1 Moisture content result of the study area

no	Location	Test pit Designation	Sample depth	Color Type	Moisture content (%)
1	Kito	TP1	2m	Red	40.5
2		TP2	2m	Red	38.33
3	Awetu	TP3	2m	Red	36.04
4		TP4	2m	Red	39.56

5	Bancho Bore	TP5	2m	Red	35.44
6		TP6	2m	Red	39.43
7	Main Campus	TP7	2m	Red	43.09
8		TP8	2m	Red	41.79

4.1.2 Specific gravity

The specific gravity of soil solids, G_s , is an essential and crucial parameter in geotechnical engineering. The protocol for the test was ASTM D854, Standard Test for Specific Gravity of Soil Solids by Water Pycnometer. A specific gravity bottle pycnometer used to test the specific gravity of solid soil. The complete result of specific gravity of soil solid for Jimma's red clay soil is shown in (Appendix B). For a single test pit, three trials were used, and the average value was taken as the value of the specific gravity. as shown in Table 4.2 the specific gravity of the selected soil samples were ranges 2.69-2.76 this result was fairly match with different researches that performed around this area on clay soil.

Table 4. 2 Specific gravity result for all test pits

no	Location	Test pit Designation	Sample depth	Specific gravity(G_s)
1	kito	TP1	2m	2.76
2		TP2	2m	2.69
3	Awetu	TP3	2m	2.73
4		TP4	2m	2.75
5	Bancho Bore	TP5	2m	2.74
6		TP6	2m	2.76
7	Main Campus	TP7	2m	2.7
8		TP8	2m	2.71

4.1.3 Results of Atterberg limit test

The ASTM D4318 standard has been used consistently throughout the whole testing procedure. The complete statistics for the liquid limit and the plastic limit were seen in (Appendix C1 & Appendix C2). For the plastic limit, the average of the three trials was utilized to calculate the limit. For the liquid limit result, four trials were employed, with the water content corresponding

to the 25 number of blows being used as the liquid limit (see figure 4.1).(Table 4.3) summarize the variation of liquid limit and the plastic limit result of all test pits. The maximum liquid limit was found in test pit 5 with a value of 81.41 in percentage. While in test pit TP3 the minimum liquid limit was obtained as 65.69 in percentage. Like the liquid limit, the maximum plastic limit was obtained at TP5 while the minimum plastic limit was obtained at TP3 and TP1. From the result of the liquid limit and plastic limit, it can be seen that the plasticity of Jimma soils is high. The result of Atterberg limits shows that the clay soil exhibited high plasticity as indicated by liquid limit range from 65.69 to 81.41%, plastic limit range from 28 to 36 %. And, the plasticity index range from 35.14% to 45.41% this show that the soil is high plastic.

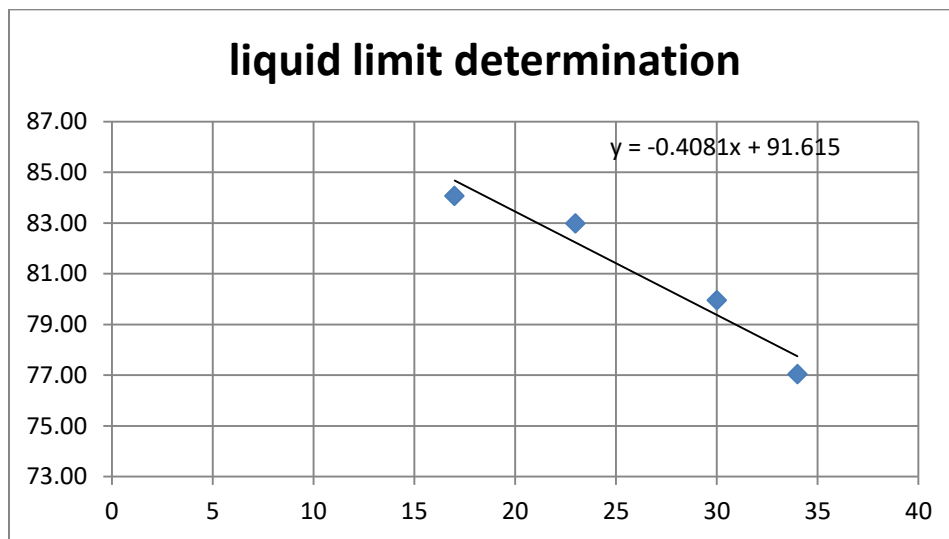


Figure 4.1 Liquid limit determination of test pit TP5

Table 4.3 Atterberg limit result for all test pits

test pit no	LL	PL	PI
TP1	66.54	30	36.54
TP2	68.14	33	35.14
TP3	65.69	28	37.69
TP4	77.02	35	42.02
TP5	81.41	36	45.41
TP6	79.37	34	45.37
TP7	72.42	31	41.42

TP8	73.66	33	40.66
-----	-------	----	-------

4.1.4 Particle Size Distribution Test Result of the soil

The percentage of different-sized grains in a given soil is an important soil feature. Two particle size analysis methods (i.e., combined curve characteristics) were conducted the first one is wet sieving, and the second one is hydrometer analysis for soil passes sieve number 200. The hydrometer analysis was carried out in accordance with ASTM D7928. During the test pit excavation, the soil was found to be fine and red in all of them. Wet sieving was implemented to prevent fine particle loss during mechanical sieve shaking. (Appendix D1 & Appendix D2) presents the detailed result of wet sieving, and hydrometer analysis. (Figure 4.2) illustrates the overall plot for all test samples.

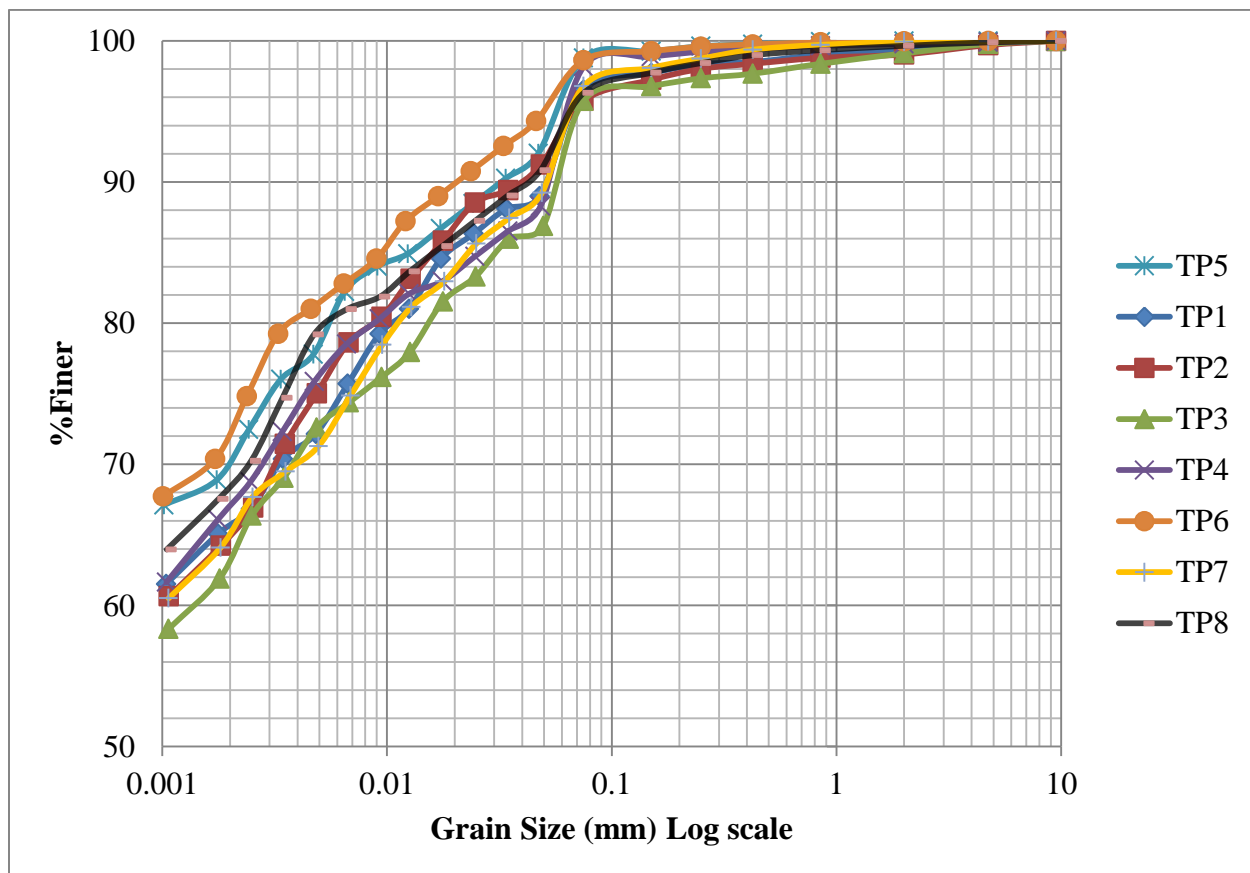


Figure 4.2 Grain size distribution curve

The grain size distribution test results expressed in % gravel, % sand, % silt, and % clay contents of each test pits. The soil contained about range from 0 to 0.3% of gravelly soil, from 1.21 to 4.03% of sand soil, range from 28.25 to 33.85% of silty soil, range from 61.9 to 70.38 % of clay soil and the remaining 95.76 to 98.79% were fine-grained soils. This indicated that the soil was dominated by clay soil (i.e. see from table 4.4 and figure 4.2). By referring to (Table 4.4 & Table 4.5.) the maximum value of soil passing sieve number 200 was obtained in test pit TP5 as 98.79 in percentage. While the minimum value was 95.51 in percentage which is found in the test pit TP1

Table 4.4 Combined grain size distribution curve result of all samples

Grain size(mm)	Percent of finer (%)							
	T1	T2	T3	T4	T5	T6	T7	T8
9.500	100.00	100.00	100.00	100.00	100.00	100.00	100.00	100.00
4.750	99.91	99.70	99.78	99.90	100.00	100.00	99.97	99.90
2.000	99.37	99.04	99.12	99.78	99.98	99.98	99.94	99.65
0.850	99.01	98.80	98.38	99.65	99.94	99.90	99.72	99.34
0.425	98.51	98.38	97.68	99.41	99.77	99.75	99.38	98.99
0.250	98.35	98.02	97.35	99.23	99.62	99.59	98.75	98.42
0.150	97.71	97.24	96.79	98.88	99.26	99.27	98.09	97.74
0.075	96.51	95.76	95.76	98.18	98.79	98.63	96.80	96.31
0.0489	89.00	91.23	86.88	88.29	92.04	94.32	89.24	90.84
0.0350	88.11	89.43	85.99	86.52	90.26	92.54	87.44	89.04
0.0250	86.34	88.53	83.31	84.74	88.48	90.77	85.65	87.25
0.0180	84.57	85.83	81.53	82.96	86.70	89.00	82.95	85.46
0.0128	81.02	83.14	77.96	82.08	84.92	87.22	81.16	83.67
0.0095	79.25	80.44	76.18	80.30	84.03	84.57	78.46	81.88
0.0069	75.70	78.64	74.39	78.52	82.25	82.79	74.87	80.98
0.0050	72.16	75.04	72.61	75.86	77.80	81.02	71.28	79.19
0.0035	70.38	71.44	69.04	72.30	76.02	79.25	69.49	74.71
0.0025	66.84	66.94	66.36	68.75	72.46	74.81	67.69	70.23
0.0020	65.06	64.24	61.90	66.09	68.90	70.38	64.10	67.54
0.0011	61.52	60.64	58.34	61.65	67.12	67.72	60.51	63.96

Table 4.5 Percentage of grain size distribution curve result for all test pits

Test Pit No	Gravel(%)	sand(%)	finer(%)	silt(%)	clay(%)
1	0.092	3.4	96.51	31.45	65.06
2	0.3	3.94	95.76	31.52	64.24
3	0.22	4.03	95.76	33.85	61.9
4	0.095	1.73	98.18	32.09	66.09
5	0	1.21	98.79	29.9	68.9
6	0	1.37	98.63	28.25	70.38
7	0.034	3.17	96.8	32.7	64.1
8	0.105	3.58	96.31	28.77	67.54

4.1.5 Soil Classification

The USCS classification system is based on the plasticity index, the liquid limit, and the particle size properties of the soil. The soil was identified using the ASTM D2487 standard for the USCS method in this study. The soil was classified based on the results of the grain size study and the Atterberg limits.

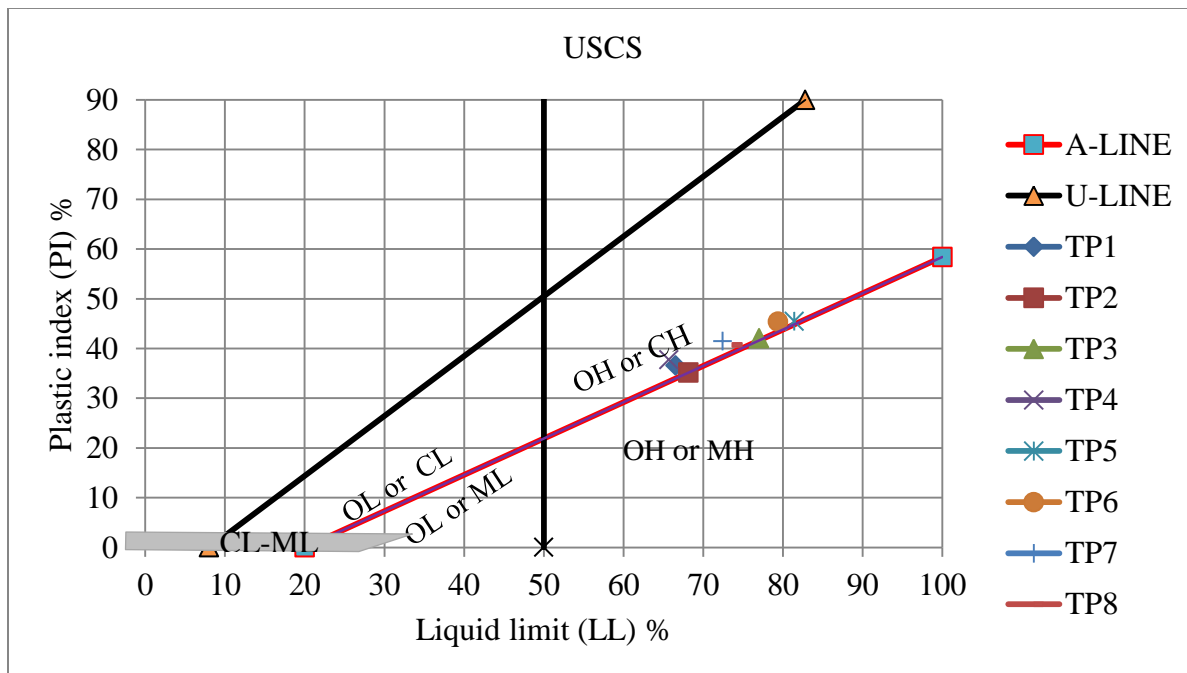


Figure 4.3 Plasticity chart

To classify the soil plasticity chart, the liquid limit value and plastic limit result for all test pits were used (Figure 4.3). Table 4.6 shows that most of the soils classified as CH. From the particle size distribution curve, it can be seen that Jimma's soil is clay dominant. Hence, the soil was classified as CH. but as indicated by figure 4.2 most of the soils were fall on the A-line. Plasticity chart is a plot of plasticity index versus liquid limit. This results shows in a high plasticity index. According to AASHTO the soil was categorized under A-7-5 and suggests that the soils were clay.

Table 4.6 percentage of grain size distribution

Tp No	Gravel(%)	sand(%)	finer(%)	silt(%)	clay(%)	USCS	AASHTO
1	0.092	3.4	96.51	31.45	65.06	CH	A-7-5
2	0.3	3.94	95.76	31.52	64.24	CH	A-7-5
3	0.22	4.03	95.76	33.85	61.9	CH	A-7-5
4	0.095	1.73	98.18	32.09	66.09	CH	A-7-5
5	0	1.21	98.79	29.9	68.9	CH	A-7-5
6	0	1.37	98.63	28.25	70.38	CH	A-7-5
7	0.034	3.17	96.8	32.7	64.1	CH	A-7-5
8	0.105	3.58	96.31	28.77	67.54	CH	A-7-5

4.2 XRD analysis result

XRD analysis was conducted on the study to investigate the mineralogical composition of the red clay soil. The data was analyzed by using match software ranging a 2theta value of 10 to 80 degree and intensity range of 0 to 1000. It can see in figure 4.4 to figure 4.7 the XRD data pattern shows the soil sample on this study area has kaolinite dominate and small amount of halloysite. The test performed for only four test pit due to equipment constraint. On the four test pits kaolinite were the governing clay minerals. By converting the diffraction peaks to d-spacing and comparing it to conventional patterns for known materials, the spacing d between the lines on the recording was utilized to identify the material. The most frequent target material for single-crystal diffraction is copper, which has a spacing of 1.54 Å with Cu K α radiation and was used in this investigation. Total of four samples were subjected to

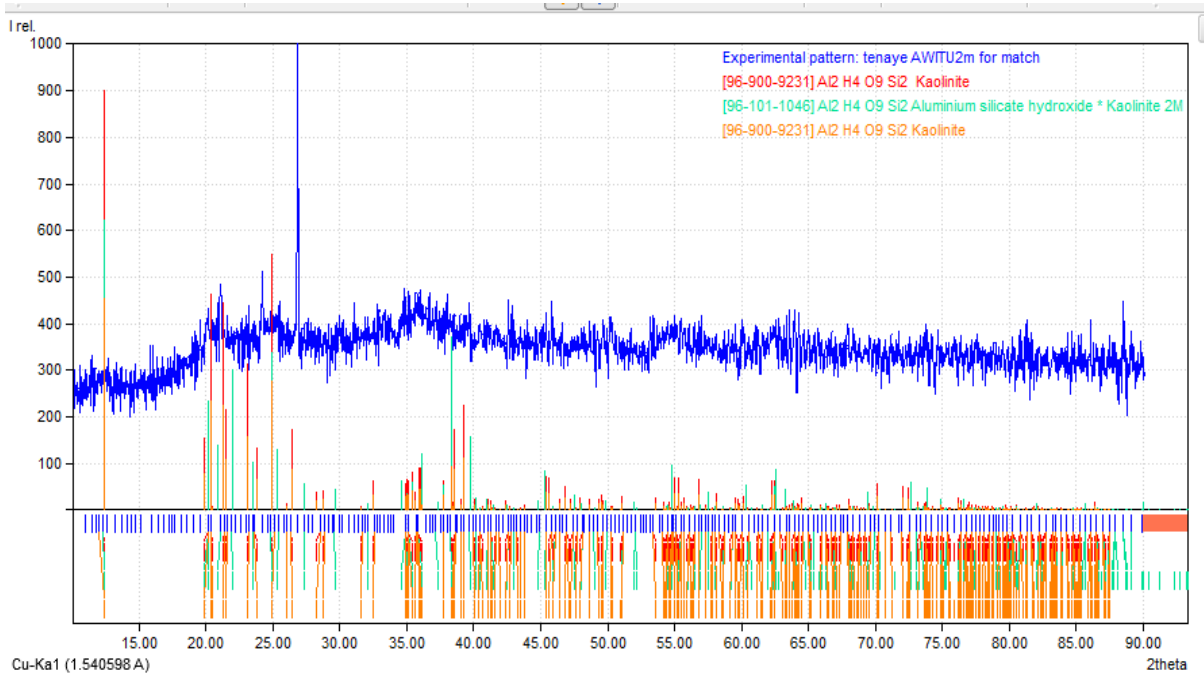


Figure 4.4 XRD pattern analyses for test pit TP3

XRD analysis with similar elemental analysis but these samples output have similar pattern with slightly different percentage of kaolinite .As indicated in the figure 4.4 the xrd pattern shows that 54.7% of kaolinite ,45.3% of Aluminum silicate hydroxide * Kaolinite 2M,and 9.5% of Unidentified peak area. Similarly figure 4.5 to 4.7 shows that the percentage of kaolinite were dominated with different percentage value.

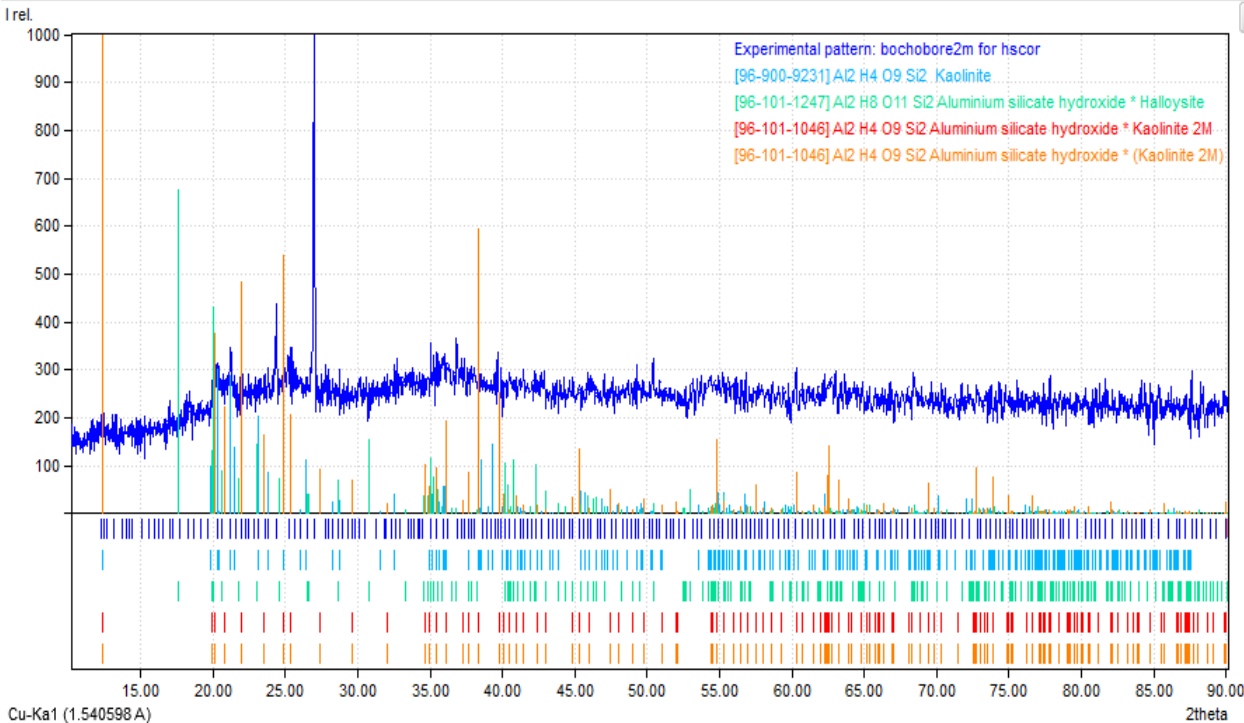


Figure 4.5 XRD pattern analyses for test pit TP5

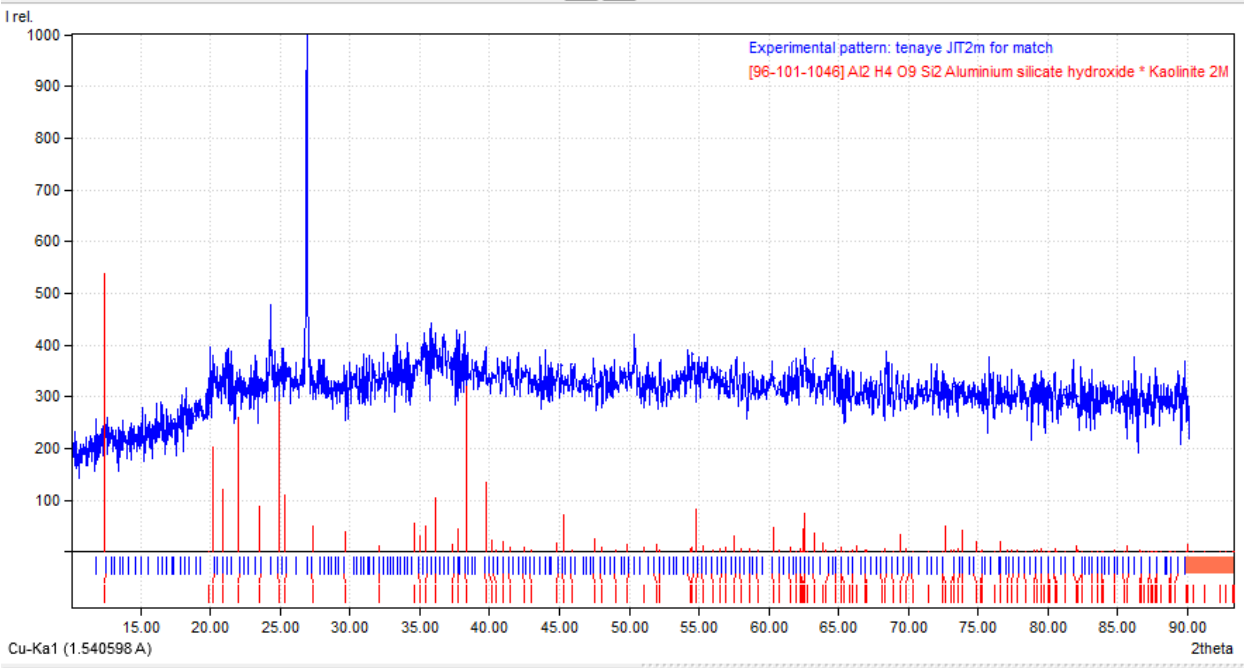


Figure 4.6 XRD pattern analyses for test pit TP1

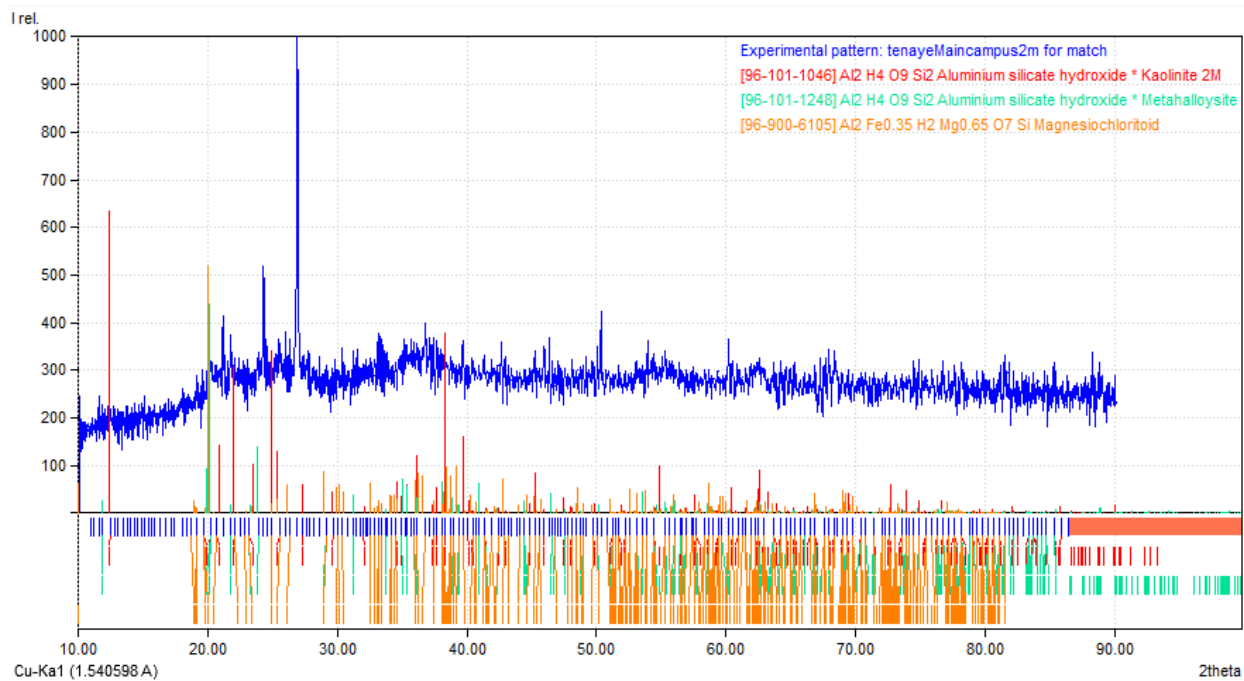


Figure 4. 7 XRD pattern analyses for test pit TP7

4.3 Results of filter paper test

In this study, a filter paper test conducted to determine the SWCC data point as a function of matric suction versus gravimetric water content. The filter paper test conducted following ASTM D5298 standard. To vary the moisture content, the soil sample was saturated by different amount of water and air dried by varying the lengthy of time .In the first trial 2% of water added to the sample, second trial 4% of water was added to the sample, and in the third trial 8% of water added to the sample the remaining samples were air dried. The gravimetric water content corresponding to matric suction were presented in (Table 4.7) for the entire test pits. Table 4.8 illustrates the soil-water characteristics curve optimized parameters for the (FREDLUND & XING) model fitting parameters using a fantastic MATLAB[®] R2019a routine called “*fmincon*”. The MATLAB[®] script of *fmincon* is available in (Appendix E). Table 4.8 presents the optimized (FREDLUND \$ XING model fitting parameters with their corresponding statistical goodness of fit. As mentioned by (D G Fredlund, Rahardjo and Fredlund, 2012) When the volume change of the soil is small, any of the three measures for the amount of water in the soil (i.e., gravimetric water content, volumetric water content, and degree of saturation) yield a similar interpretation. According the information collected in each test pit a red clay soil around Jimma city was low

volume change gives similar expressions to this. Thus, gravimetric water content was used to plot the SWCC (Fredlund, 2020) . In this study mainly focused on plots of the SWCC. The shrinkage curve was not done due to the insignificance volume change of the soil. The detailed result for the filter paper of all test pits was found in (Appendix).

The filter paper test was conducted in six samples of data point by varying the range of soil water content starting from 21.17 % (i.e., at air dried condition) to a maximum of 48.82 %. As shown in table 4.8 the (Fredlund & Xing, 1994) model fitting parameter a_f For Jimma’s red clay soil ranges from 39.86 to 52.04kpa. Similarly the vales of other fitting parameters were neatly written on table4.8. The percentage of fine particles is not the only indicator of air-entry value and (Oluyemi-ayibiowu, Akinleye and Fadugba, 2020) concluded that air-entry value is also affected by the arrangement of compacted soil. The pore size distribution in this investigation is undetermined because the filter paper test was conducted in an undisturbed soil sample. As a result, the value of the a_f parameter is acceptable. Table 4.7 shows the suction and gravimetric water content of the collected soil samples as evaluated in the laboratory. As the suction increases, the gravimetric water content decreases. Table 4.7 show that Gravimetric water content with corresponding matric suctions of filter paper test result.

Table 4.7 Determination of suction and gravimetric water content from filter paper test

TP1	Gw%	44.21	35.51	30.63	25.91	24.35	23.45
	Suction(kpa)	37.88	148.44	333.12	918.62	1307.15	1714.61
TP2	Gw%	42.56	33.85	28.25	25.62	23.62	22.43
	Suction(kpa)	43.32	170.74	559.15	990.12	1628.68	2189
TP3	Gw%	48.01	38.44	28.06	25.07	23.68	22.12
	Suction(kpa)	31.34	140.22	665.383	1172.27	1628.68	2129.36
TP4	Gw%	44.17	34.25	27.67	24.72	23.19	22.05
	Suction(kpa)	37.81	182.5	605.71	1140.42	1611.66	2048.36
TP5	Gw%	48.18	40.56	27.81	24.13	22.46	21.17
	Suction(kpa)	29.14	104.31	629.68	1285.33	1720.78	2249.42
TP6	Gw%	48.82	38.97	28.02	24.22	22.02	21.54

	Suction(kpa)	30.78	131.63	605.71	1239.09	1917.85	2189.22
TP7	Gw%	46.01	35.59	28.71	25.73	23.49	23.01
	Suction(kpa)	35.79	166.41	537.44	1025.78	1631.44	1982.49
TP8	Gw%	42.03	36.18	29.53	25.56	23.44	22.57
	Suction(kpa)	42.12	125.39	423.12	989.24	1520.29	1929.67

Table 4.8 Optimized (Fredlund & Xing, 1994) model fitting parameters

TP	w_{sat}	a_f	n_f	m_f	ψ_r	RMSE	R ²	AIC
TP1	45.76	41.94	1.59	0.28	667.86	0.09634	0.99991	-6.0005
TP2	45.95	39.86	2.42	0.21	529.31	0.09723	0.9999	-5.9521
TP3	51.86	49.08	1.35	0.44	1874.53	0.1261	0.99991	-4.5985
TP4	47.45	43.54	1.81	0.29	729.65	0.04493	0.99998	-9.9746
TP5	53.02	52.04	1.1	0.57	3280.49	0.1611	0.99987	-3.3211
TP6	52.82	51.31	1.34	0.49	2543.24	0.1066	0.99994	-5.4694
TP7	49.25	46.14	1.75	0.34	1672.84	0.17617	0.99977	-2.8549
TP8	47.889	46.08	1.95	0.31	1658.13	0.18913	0.99973	-3.054

The SWCCs for eight cohesive soils measured by the contact filter paper method of suction measurement was presented in Figure below. For each selected samples the four fredlund and Xing curve fitting parameters were evaluated as seen in the figure below .The slope of the SWCC in the middle stage represented the suction loss ratio with increasing moisture content in this figure. As expressed by (Zhang et al., 2018) the steeper suction slopes represent that soil sample is more moisture susceptible. “Moisture susceptibility” describes the rate of loss of subgrade strength, stiffness, and resistance to permanent deformation with increasing moisture. The slope parameter, n_f , in the SWCC equations was found to be associated with the moisture susceptibility of cohesive soils. A higher n_f value indicates that the material is more moisture susceptible. Therefore, the slope of the SWCCs can also be used to evaluate the moisture susceptibility of subgrade soils. Table 4.8 clearly describe all the Fredlund and Xing curve fitting parameters obtained in optimization techniques with their stastical goodness.

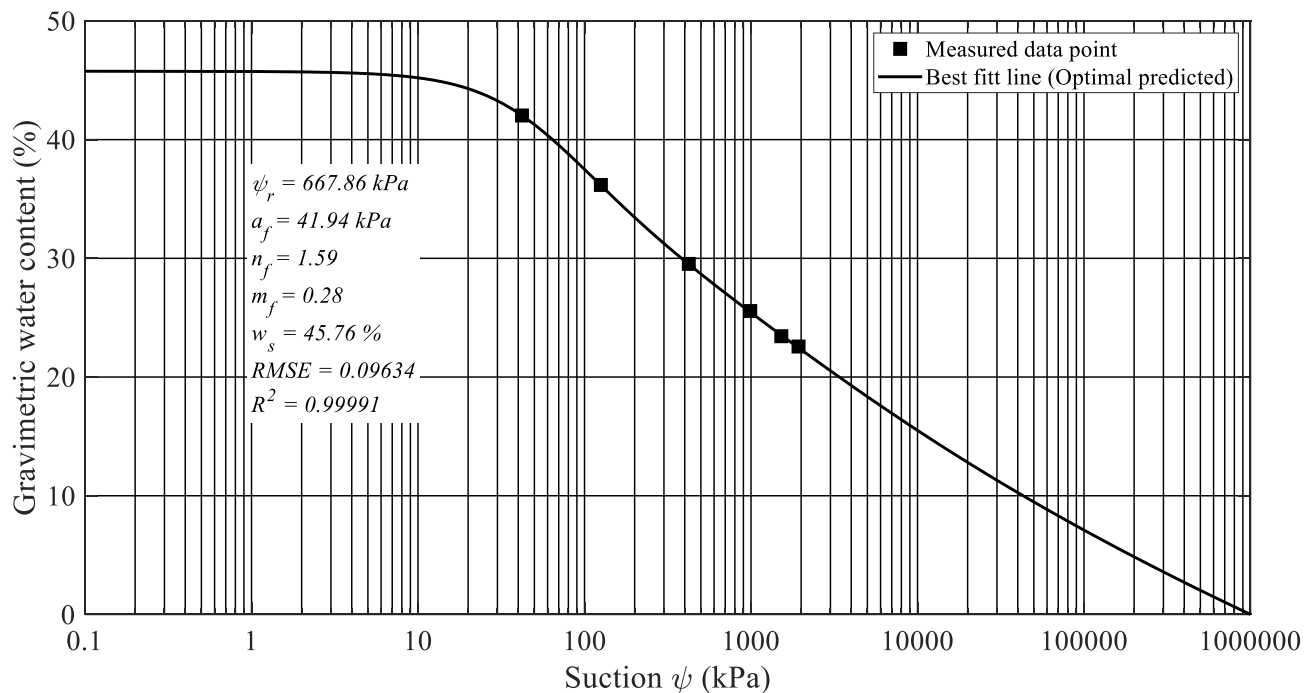


Figure 4.8 Soil water characteristics curve for TP1

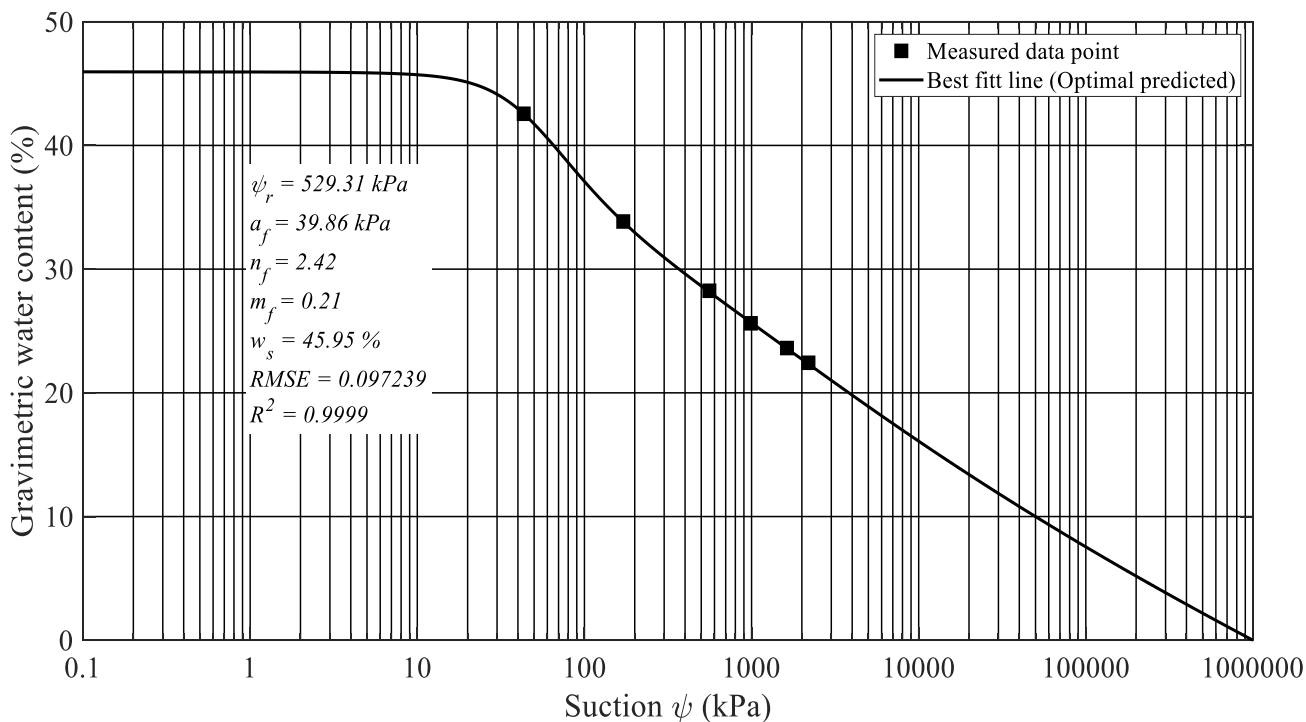


Figure 4.9 Soil water characteristics curve for TP2

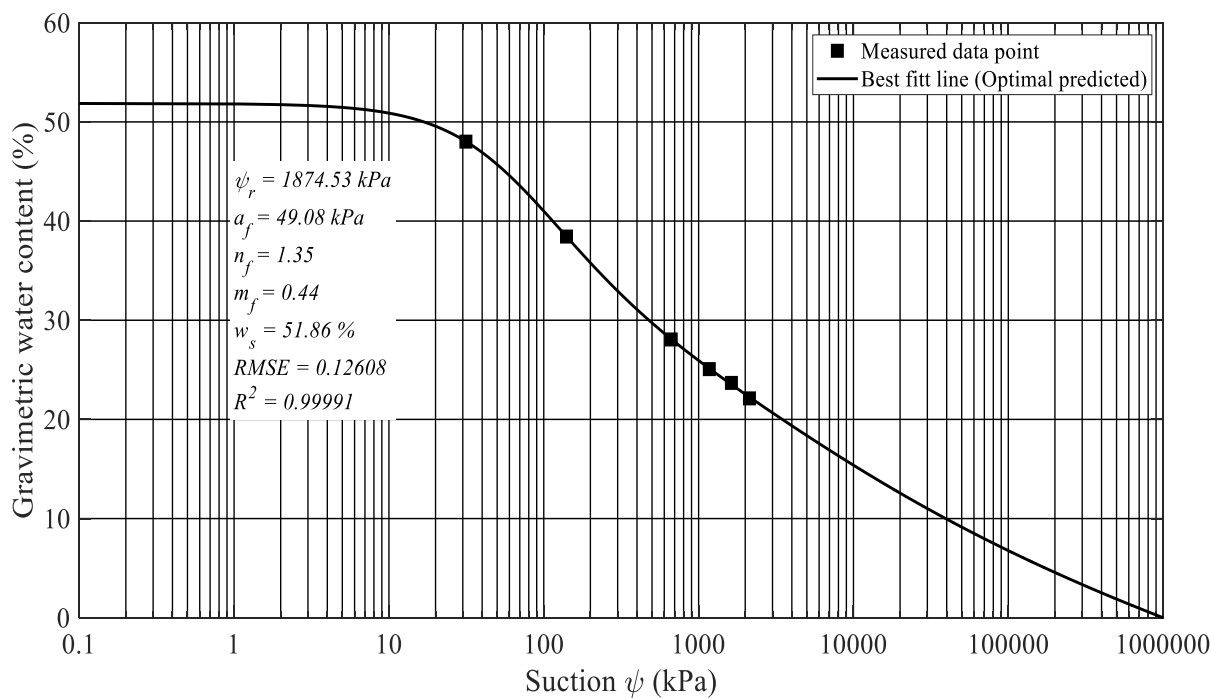


Figure 4.10 Soil water characteristics curve for TP3

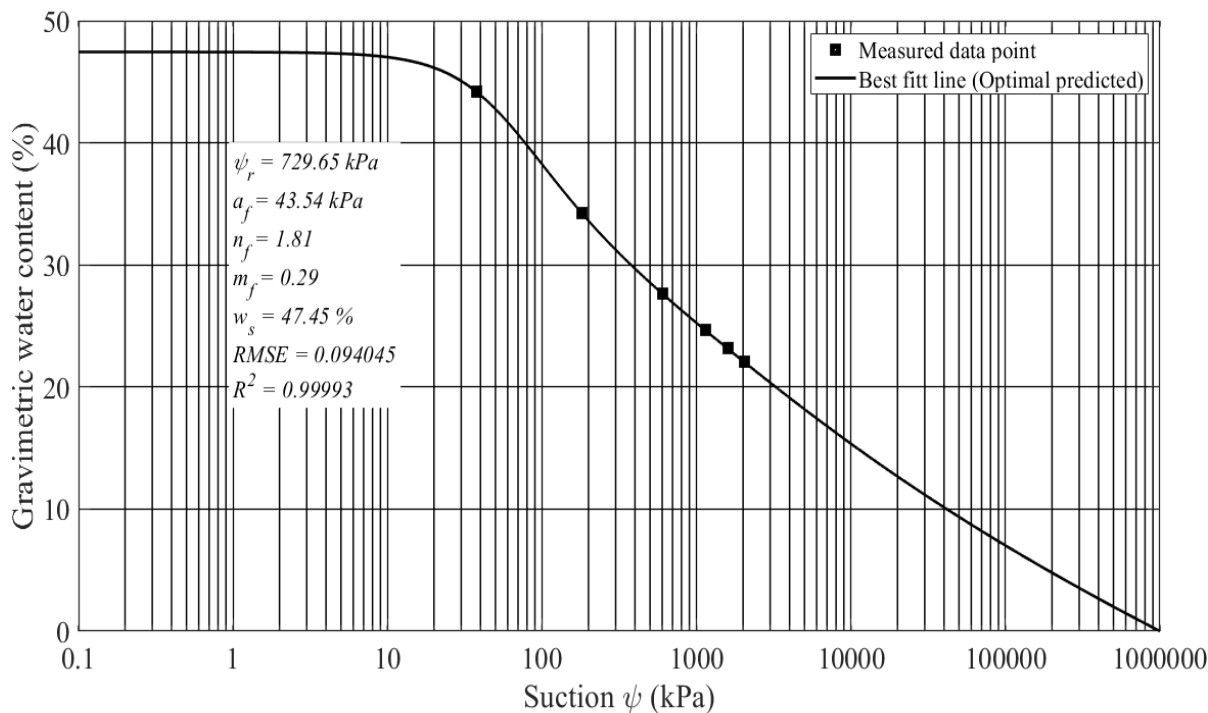


Figure 4.11 Soil water characteristics curve for TP4

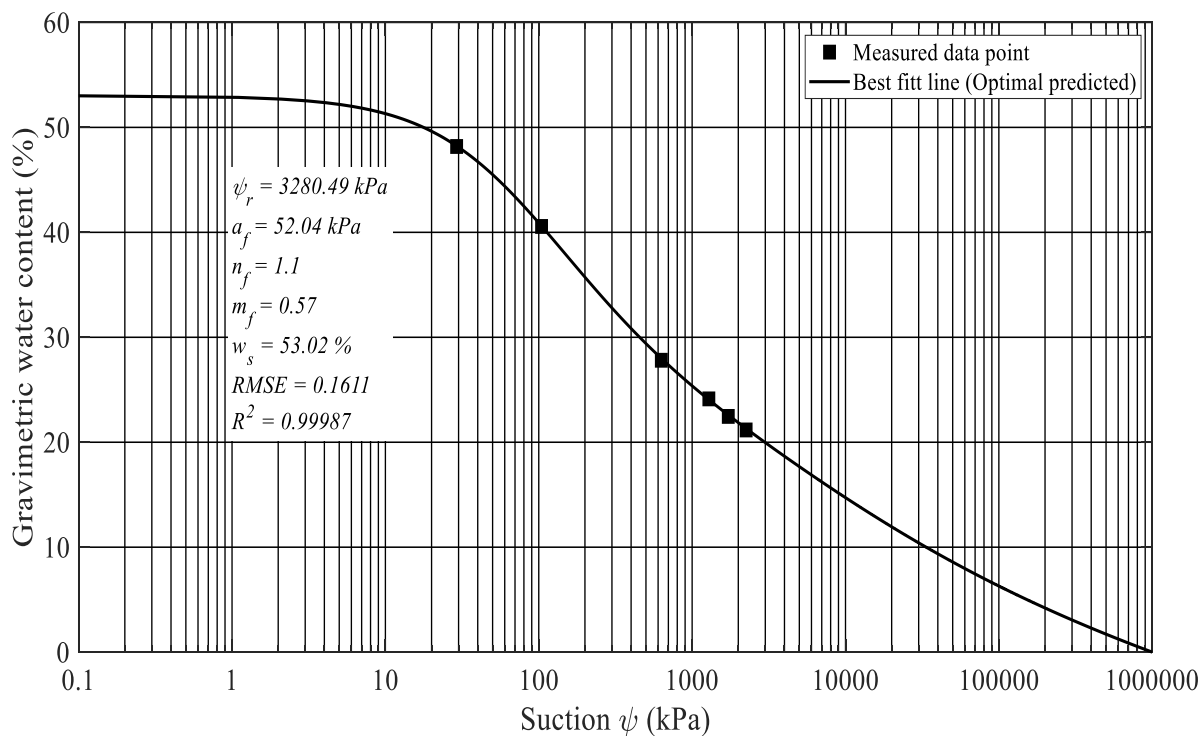


Figure 4.12 soil water characteristic curves for TP5

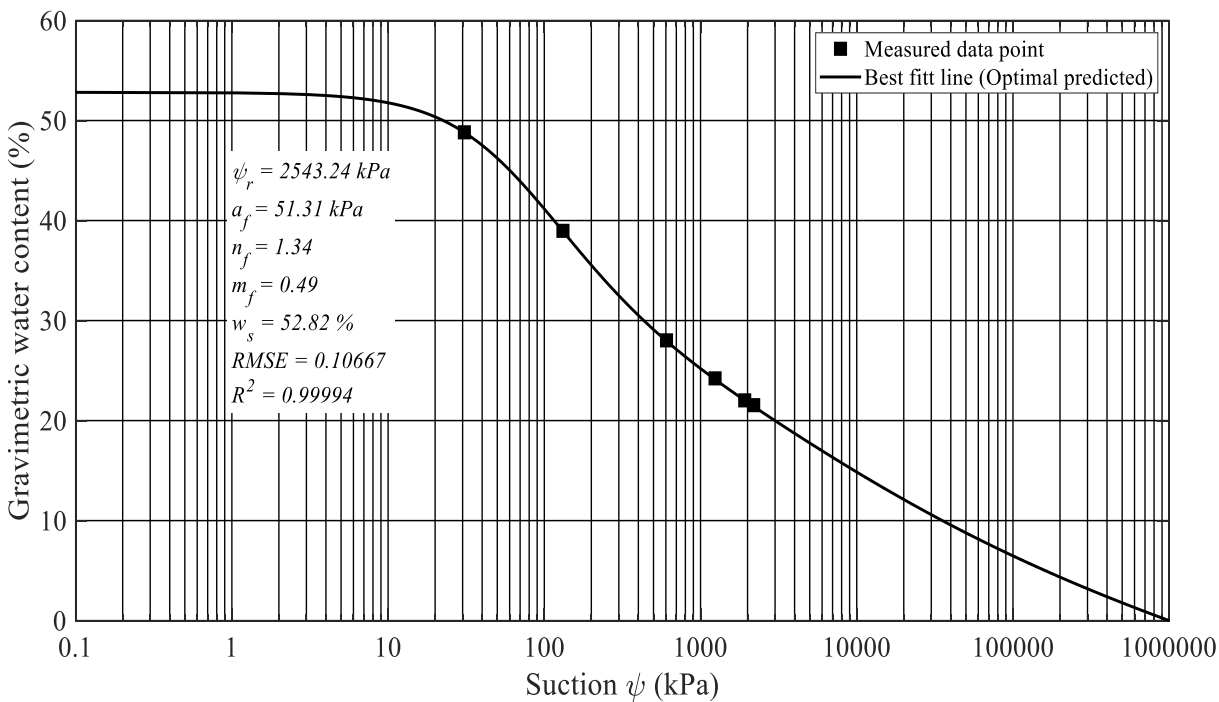


Figure 4.13 Soil water characteristic curve for TP6

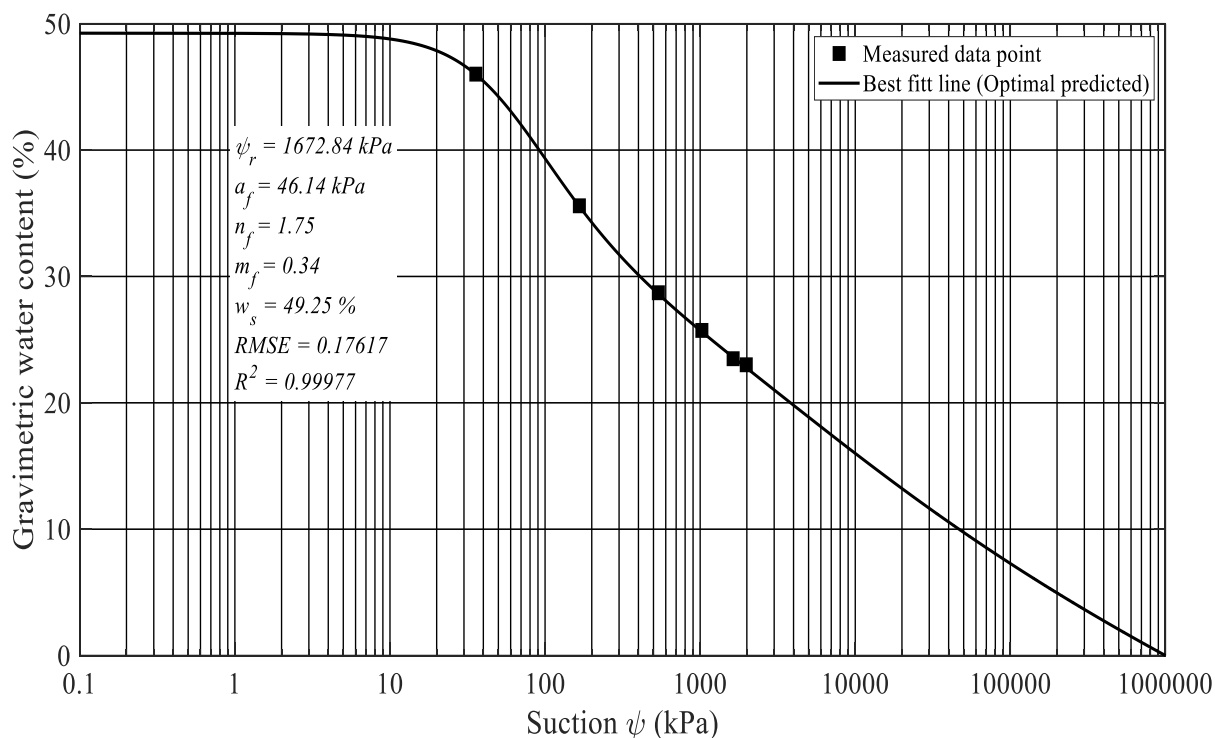


Figure 4.14 Soil water characteristic curve for TP7

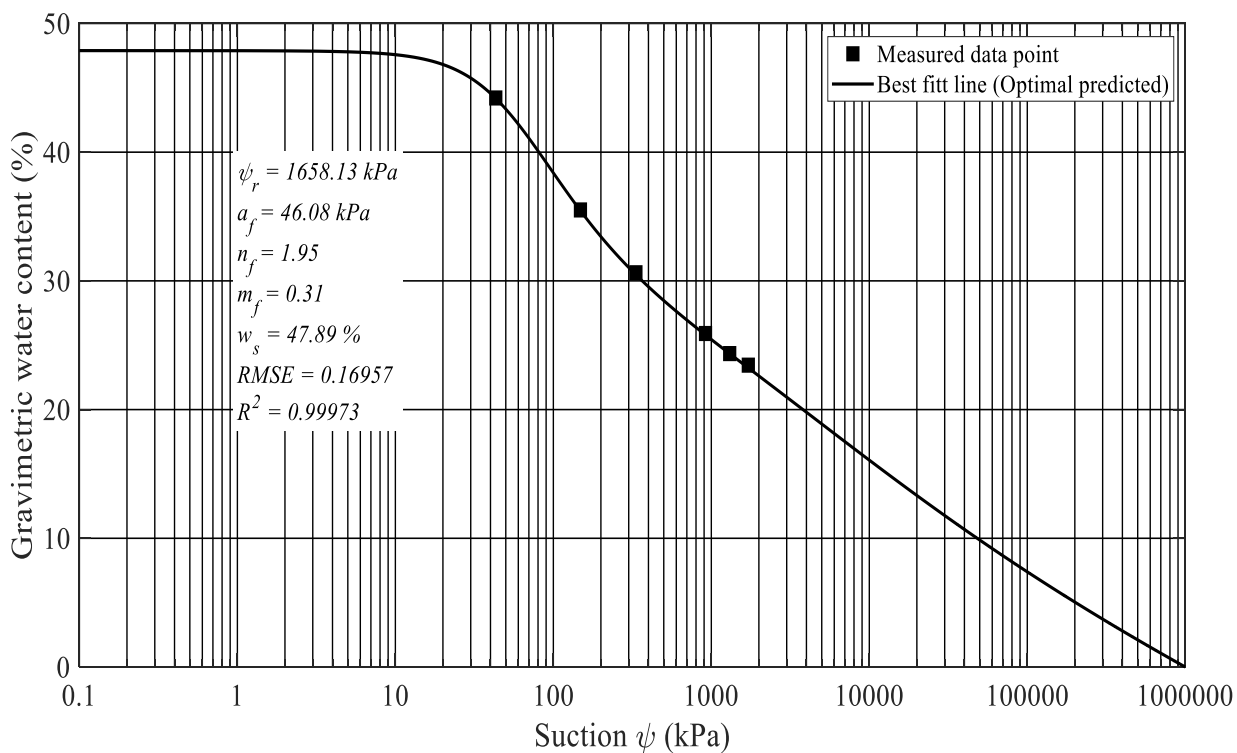


Figure 4.15 Soil water characteristic curves for TP8

Figure 4.8 to 4.15 showed that the swcc of each test pit with respected samples that plotted between measured gravimetric water content and corresponding matric suction. The matlab2019 routine function fmincon was used to optimize the curve fitting parameters of Fredlund and Xing equations. As expressed in chapter three initially the starting point of fitting parameters were guessed. Thus, by using math lab function through different iteration process the fredlund and Xing curve fitting parameters of swcc of the eight soil samples were determined as shown on the above figure.as seen that on the figure 4.8 to 4.15 all the four curve fittings parameters determined through iteration of matlab 2019 program, and the maximum and minimum value of each parameters were shown on table 4.8.

Table 4.9 Summary of data used for model development

TP no	wsatu	LL	PL	PI	sand	FINE	SILT	CLAY	GI	WPI	Rsuction	af	nf	mf
Tp1	45.79	66.54	30	36.54	3.4	96.51	31.45	65.06	21.63	35.26	667.83	41.94	1.59	0.28
Tp2	45.95	68.14	33	35.14	3.94	95.76	31.52	64.24	20.30	33.65	529.42	39.86	2.42	0.21
Tp3	51.86	77.02	35	42.02	1.73	98.18	32.09	66.09	26.63	41.26	1874.54	49.08	1.35	0.44
Tp4	47.45	65.69	28	37.69	4.03	95.76	33.85	61.19	22.36	36.09	729.64	43.54	1.81	0.29
Tp5	53.02	81.41	36	45.41	1.21	98.79	29.9	68.9	29.67	44.86	3280.58	52.04	1.1	0.57
Tp6	52.82	79.37	34	45.37	1.37	98.63	28.25	70.38	29.58	44.75	2543.25	51.31	1.34	0.49
Tp7	49.25	72.42	31	41.42	3.17	96.8	32.7	64.1	25.70	40.09	1672.87	46.14	1.75	0.34
Tp8	48.89	73.66	33	40.66	3.58	96.31	28.77	67.54	24.93	39.16	1658.14	46.08	1.95	0.31

4.4 output of the proposed model

4.4.1 Introduction

Under this section brief description about the developed model of Fredlund and Xing model fitting parameters was emphasized. Furthermore, utilizing statistical analyses to check the accuracy of the developed model and also this section illustrates the validation technique for the proposed model. Finally, the proposed prediction model's strengths and weaknesses were discussed.

4.4.2 Relation between the model fitting parameters and the index properties

The investigation was performed by using JMP-14 statistical software's multiple regressions with subset selection and interaction analysis methods. The method of subset selection multiple

regression analysis is used to develop the line or curve which provides the best fit through a set of data points. The normality

Table 4.10 Correlation matrix for af parameter with predictor variables

	af	LL	PL	PI	sand	FINE	SILT	CLAY	GI	WPI
af	1.0000	0.9381	0.6670	0.9866	-0.9206	0.9297	-0.4918	0.7425	0.9903	0.9906
LL	0.9381	1.0000	0.8715	0.9400	-0.9201	0.9216	-0.6333	0.8542	0.9483	0.9490
PL	0.6670	0.8715	1.0000	0.6519	-0.7752	0.7584	-0.6224	0.7931	0.6724	0.6742
PI	0.9866	0.9400	0.6519	1.0000	-0.8835	0.8974	-0.5464	0.7692	0.9986	0.9983
sand	-0.9206	-0.9201	-0.7752	-0.8835	1.0000	-0.9985	0.4874	-0.7841	-0.9068	-0.9089
FINE	0.9297	0.9216	0.7584	0.8974	-0.9985	1.0000	-0.4936	0.7894	0.9191	0.9211
SILT	-0.4918	-0.6333	-0.6224	-0.5464	0.4874	-0.4936	1.0000	-0.9202	-0.5480	-0.5475
CLAY	0.7425	0.8542	0.7931	0.7692	-0.7841	0.7894	-0.9202	1.0000	0.7810	0.7816
GI	0.9903	0.9483	0.6724	0.9986	-0.9068	0.9191	-0.5480	0.7810	1.0000	1.0000
WPI	0.9906	0.9490	0.6742	0.9983	-0.9089	0.9211	-0.5475	0.7816	1.0000	1.0000

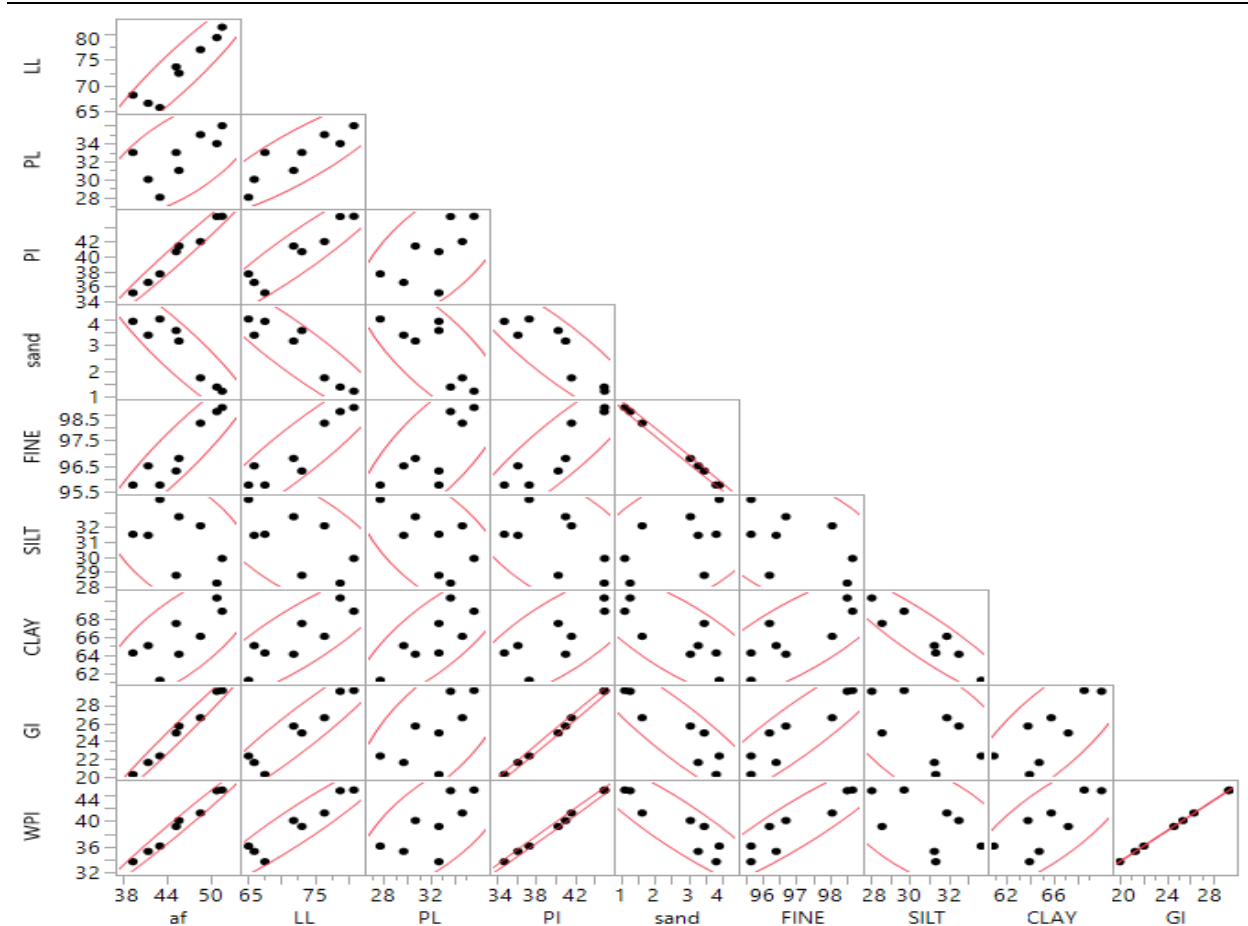
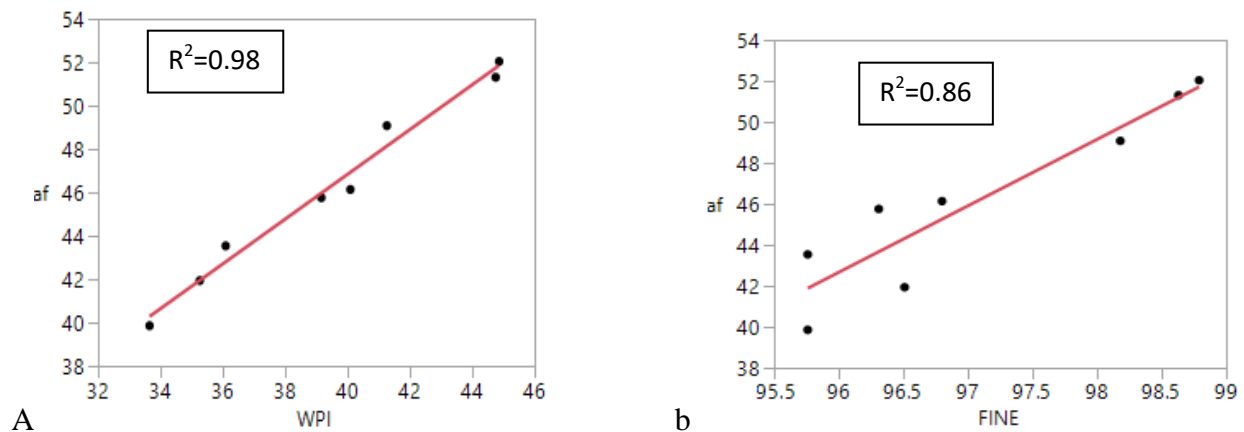


Figure 4.16 Scatter plot of af with predictor variables

of the corresponding data before the regression analysis was carried out to consider as a variable in the model. Therefore, first, the geotechnical parameter/data obtained from each test sample need to be checked for its normality by using JMP-14 software with the help of scatter plot and correlation matrix (see table4.10 and figure4.16). Regression would be approved if the test data for the related tests have a normal distribution or if the residuals of the fit model obtained have a normal distribution. If the fit model's residuals are not normally distributed, data transformation is used to make the relevant data regularly distributed. Table 4.10 and figure 4.16 clearly expressed the correlation matrix and the scatter plot of the curve fitting parameter af respectively. Appendix G1 expressed all the multivariate analysis result of all fitting parameters as shown on table 4.10 and figure4.16 the parameter af has best correlation chance to the WPI with R square value of 0.99 compared to the other independent variables.

On this part of discussion the relationship between the model fitting parameter (Fredlund & Xing, 1994) a_f and index properties such as WPI, fine percentage, clay percentage, sand percentage, silt percentage, and plasticity index was illustrated. As indicated on the figure 4.17 WPI, plasticity index and fine percentage, have strongly positive correlations with fitting parameter with statistical measurement tools of R square value of 0.98, 0.97.and 0.86 respectively. And it has a negative relationship with the percentage of sand and very poor correlation with silt content.



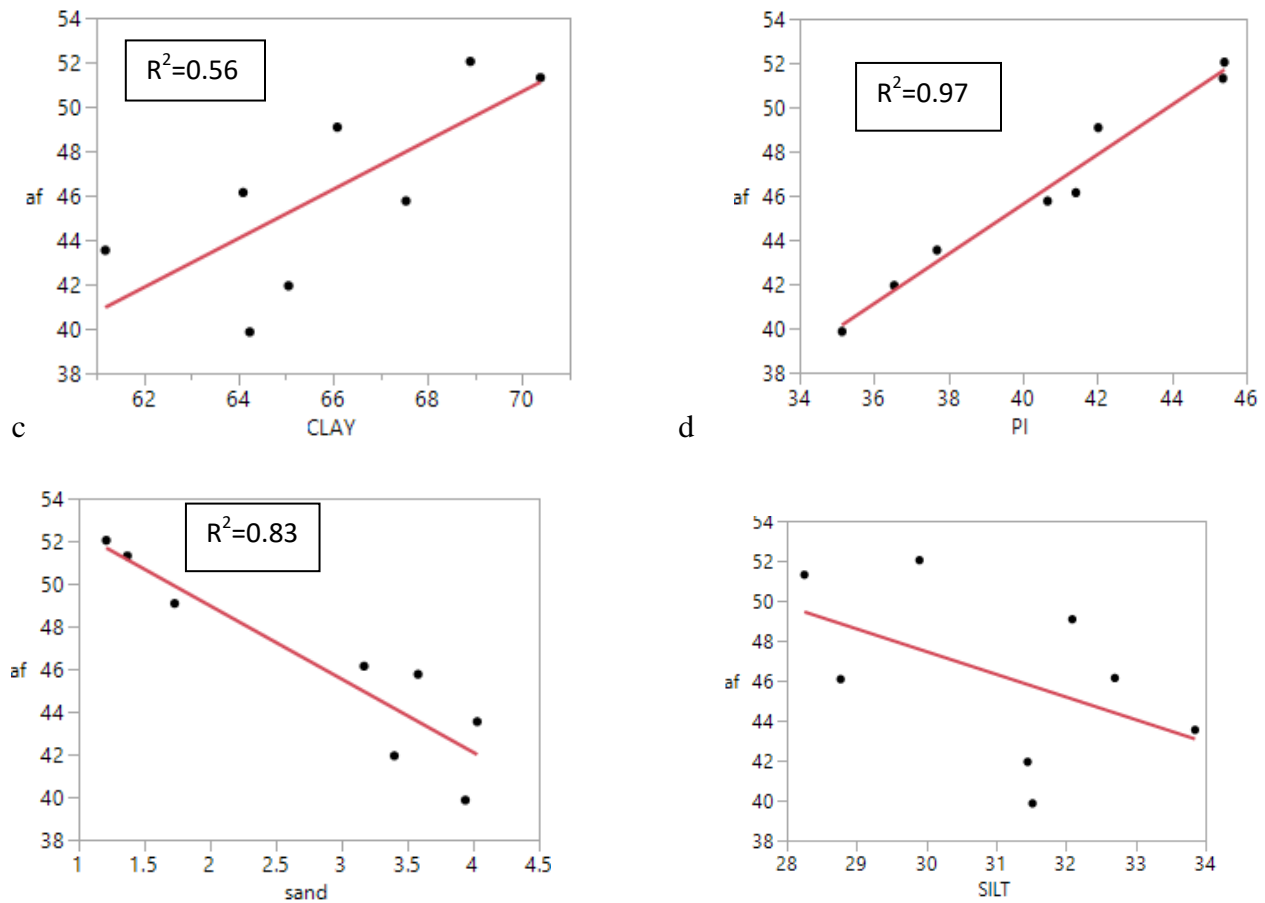


Figure 4.17 Basic linear fittings between a_f and index property: (a) wPI ; (b) fine content; (c) clay content; (d) plasticity index; (e) sand content; (f); silt content.

4.4.3 Statistical prediction model for the (fredlund and xing) model fitting parameters

To develop the prediction model of the model fitting parameters total of eight samples from eight test pits used. The distribution of index properties and the (Fredlund & Xing, 1994) model fitting parameters were analyzed through JMP[®] Pro 14. As expressed in the previous section the index properties of the selected samples were more related sample to sample means there was no huge variation between the samples. Hence, for this study, eight observations are reasonably enough data to develop a prediction model.

To develop SWCC theoretically using a filter paper method can be time taker and worry task while an empirical model provides a rapid solution to develop SWCC. Due to the clear limitations in developing SWCC indirectly through filter paper techniques; an empirical

prediction model has been developed based on index properties measurement and through statistical analysis.

To further examine the relationship between the (Fredlund & Xing, 1994) model fitting parameters and the weighted plasticity index, statistical approaches were used through JMP® Pro 14 to develop the empirical prediction model. Simple linear regression was the first empirical technique used. For the linear regression, the second option was to use a transformation technique. For the linear regression, several transformations were evaluated (Refer to AppendixG3). and the simple linear regression without transformation was found to be a good prediction model for a_f (see Table4.11). Using linear regression one set of model was developed for each fitting parameters, then after the performance was checked through validation techniques. A total of four prediction models were proposed and the performance of the proposed model checked with the help of statically analysis tool. The detailed information about the prediction model development was found in (AppendixG30 to G34).

The regression plot (Figure 4.17) shows a basic linear fitting between the dependent variable a_f and the independent variable w^{PI} . But model development procedure for all fitting parameters were discussed briefly on (AppendixG30 to G34). By entering the predictor variable into the proposed prediction model, the Actual by Predicted plot displays the plot of the actual measured dependent variable and the predicted dependent variable (Figure 4.19). The residual by predicted plot can show heteroscedasticity (i.e., close data point) and homoscedasticity (i.e., far data point) from the reference line. Homoscedasticity and heteroscedasticity is both undesirable. There was neither heteroscedasticity nor homoscedasticity in the residual by predicted plot. The data points were evenly distributed (Figure 4.20). The predictor profiler essentially tells you whether or not the proposed prediction model expressions are correct. It can be observed from the prediction profiler (Figure 4.21) that the proposed prediction model is physical (i.e., as WPI increases a_f).

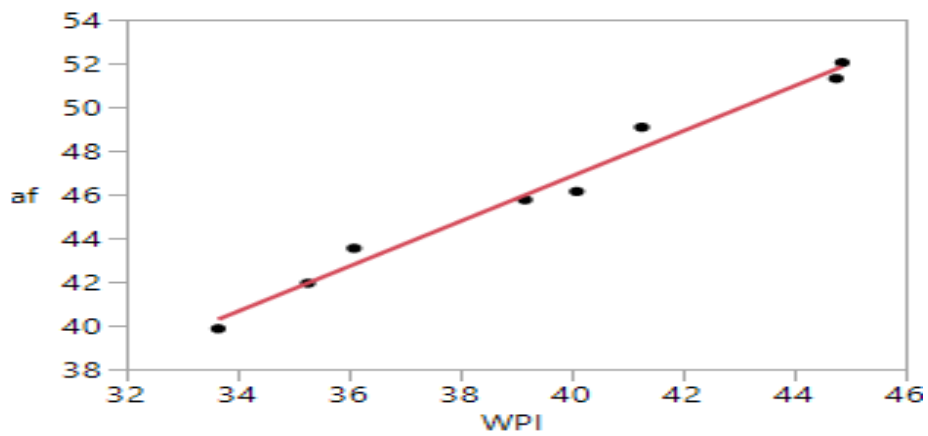


Figure 4.18 Regression plot of af without transformation

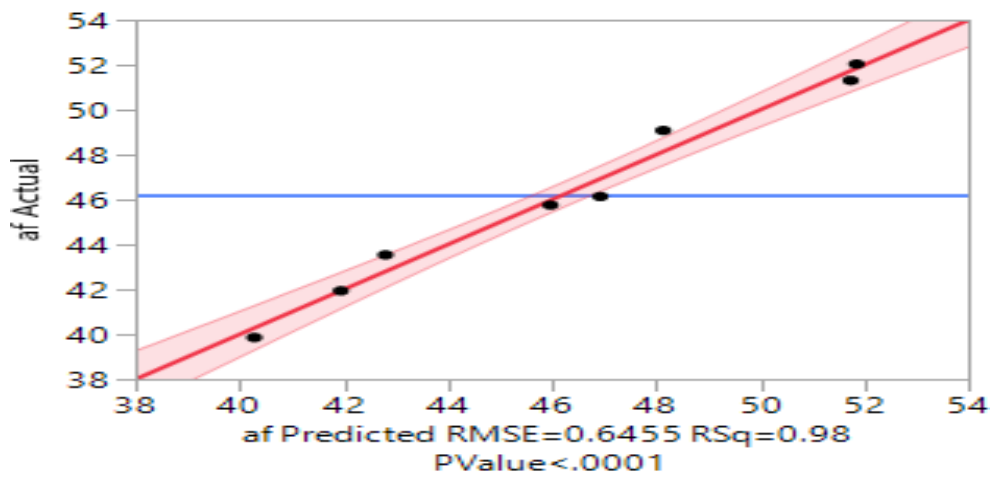


Figure 4.19 Actual by predicted plot of af

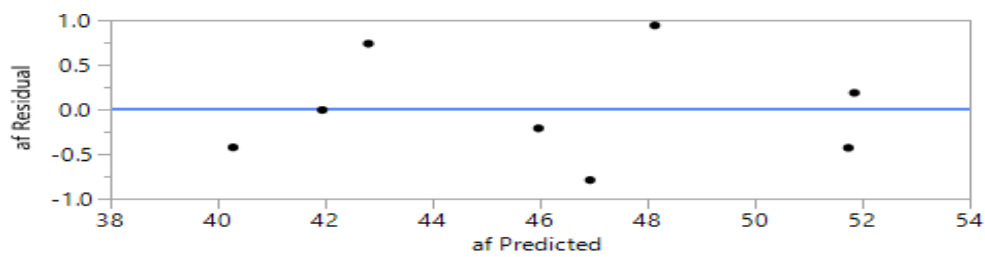


Figure 4.20 Residual by predicted plot of af

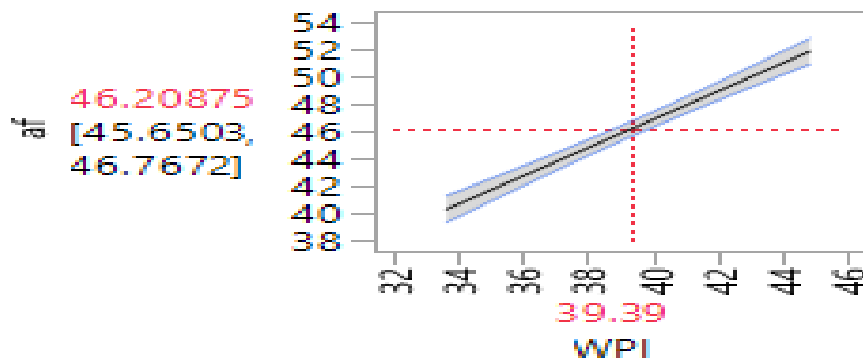


Figure 4.21 Prediction profile of af

The JMP® Pro 14 model comparison platform was used to select best prediction model from a set of transformations for basic linear regression.

From (Table 4.11) it can be seen that the linear model without transformation was found to be a good prediction model for a_f . While the square transform was found to be better in predicting ψ_r and m_f .but for n_f model prediction with WPI shows weak performance on each transform mechanisms. To solve this difficulty a solution similar to that done by Zapata 1999 was adopted. Thus, in this study the n_f parameter was correlated with the reciprocal of m_f value as seen in table 4.11. The following equation illustrates the prediction model for the model fitting parameters. The proposed prediction models were validated under model performance. The unit of a_f and ψ_r is in kPa . In the proposed prediction model wPI shall be placed in percentage.

$$a_f = 5.558 + 1.032WPI \quad (4.4)$$

$$n_f = 0.471 + 0.397(1/m_f) \quad (4.5)$$

$$m_f = 0.184 + 0.000351WPI^2 \quad (4.6)$$

$$\psi_r = -2830.57 + 2.84WPI^2 \quad (4.7)$$

4.5 Model validation or performance of the model

The overall predictive accuracy of the models was evaluated with the R^2 and RMSE statistics. From the statistical analyses, the proposed prediction model was found perfect. Table 4.11 emphasized the predicted model with corresponding statistical fitness by using different transformation techniques of JMP software.

Table 4.11 Linear prediction model expression proposed for the (Fredlund and Xing) model fitting parameters

FM	NO Transform	Square transform	Reciprocal Transform	Log transform	Exponential transform	Reference
a_f	$5.58+1.032WPI$	$25.8+0.013WPI^2$	$86.63-1576.36(1/WPI)$	$-102.42+40.52\log(WPI)$	$44.31+2.584e^{-19\text{Exp}(WPI)}$	Appendix G31
R^2	0.98	0.977	0.978	0.98	0.61	
n_f	$4.829-0.081WPI$	$3.253-0.001 WPI^2$	$-1.486+122.84(1/WPI)$	$13.24-3.16\log(WPI)$	$1.82-2.12e^{-20\text{Exp}(WPI)}$	G32
R^2	0.659	0.658	0.659	0.66	0.45	
m_f	$-0.722+0.028WPI$	$-0.184+0.0004WPI^2$	$1.43-41.62(1/WPI)$	$-3.59+1.08\log(WPI)$	$0.31+7.79e^{-21\text{Exp}(WPI)}$	G3
R^2	0.909	0.919	0.88	0.89	0.72	
ψ_r	$-7198.664+223.87WPI$	$-2830.57+2.84WPI^2$	$10296.84-338393.1(1/WPI)$	$-30457.13+8743.78\text{Log}(WPI)$	$1167.35+6.155e^{-17\text{Exp}(WPI)}$	G34
R^2	0.943	0.949	0.92	0.92	0.71	
n_f	$2.791-3.077m_f$	$2.214-3.74m_f^2$	$0.471+0.397(1/m_f)$	$0.439-1.164\log(m_f)$	$4.627-2.041\exp(m_f)$	
R^2	0.81	0.76	0.87	0.86	0.79	

To increase the confidence on the accuracy of the new predicted model the plot of actual vs predicted value of each Fredlund and xing curve fitting parameters was done .The figure shown below indicated that the plot of predicted vs actual values of the fitting parameters a_f , m_f ,and R suction with R square value of 0.98, 0.92, 0.95 respectively.

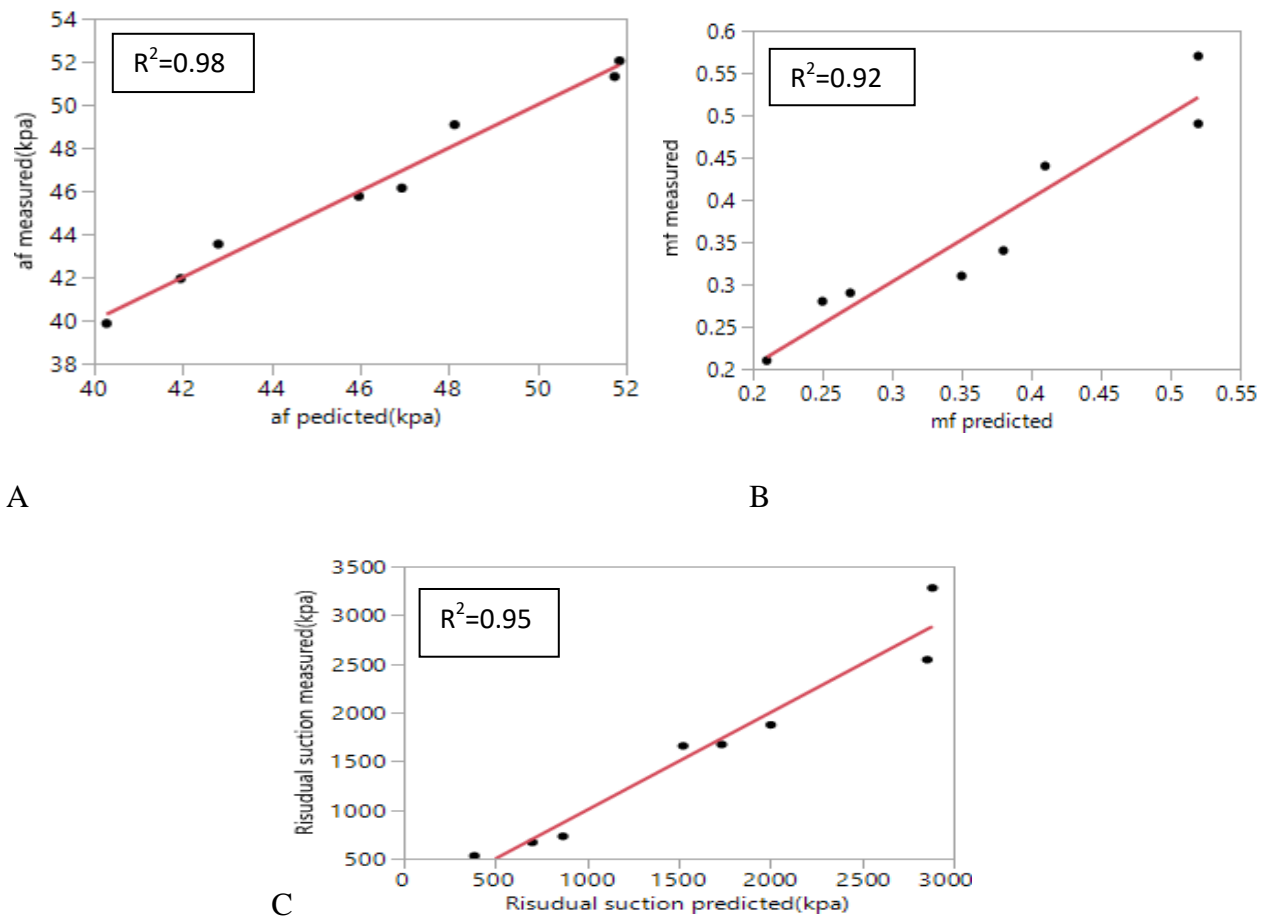


Figure 4.22 Predicted vs actual value of a_f , m_f , and Rsuction

4.5.1 Experimental fit Versus Model fit

To cross check the accuracy of the proposed prediction model, the actual soil-water characteristics curve data point in the laboratory was fitted to the experimental line and the proposed prediction model. From (Figure 4.21 through Figure 4.29) it can be seen that the experimental fitted line close to the model fitted line which suggests that the validity of the proposed prediction model. But there was a small difference between the measured and predicted value this is due to the factor during filter paper measurement in laboratory test and also the accuracy of the calibration curve recommended by (ASTM D5298).

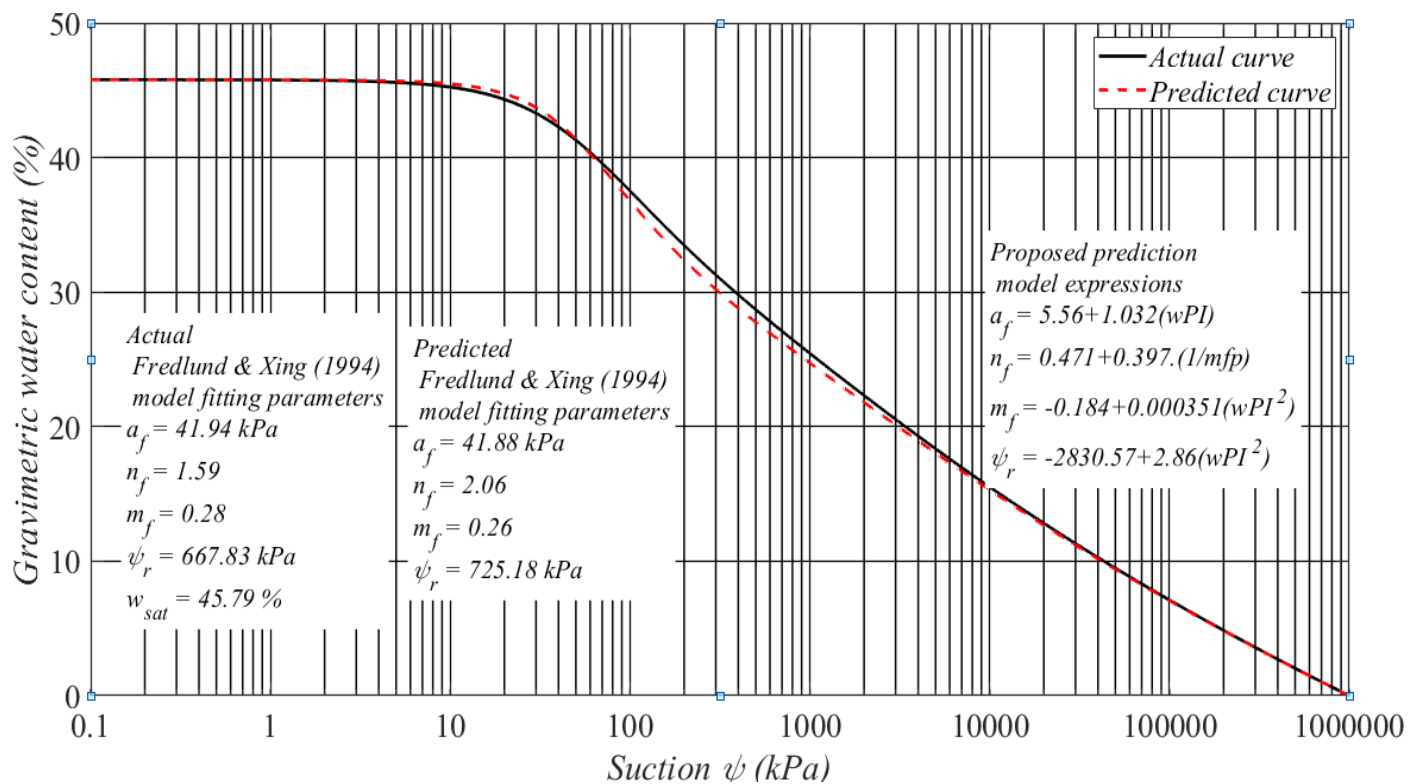


Figure 4.23 Actual vs predicted soil water characteristics curve plot for TP1

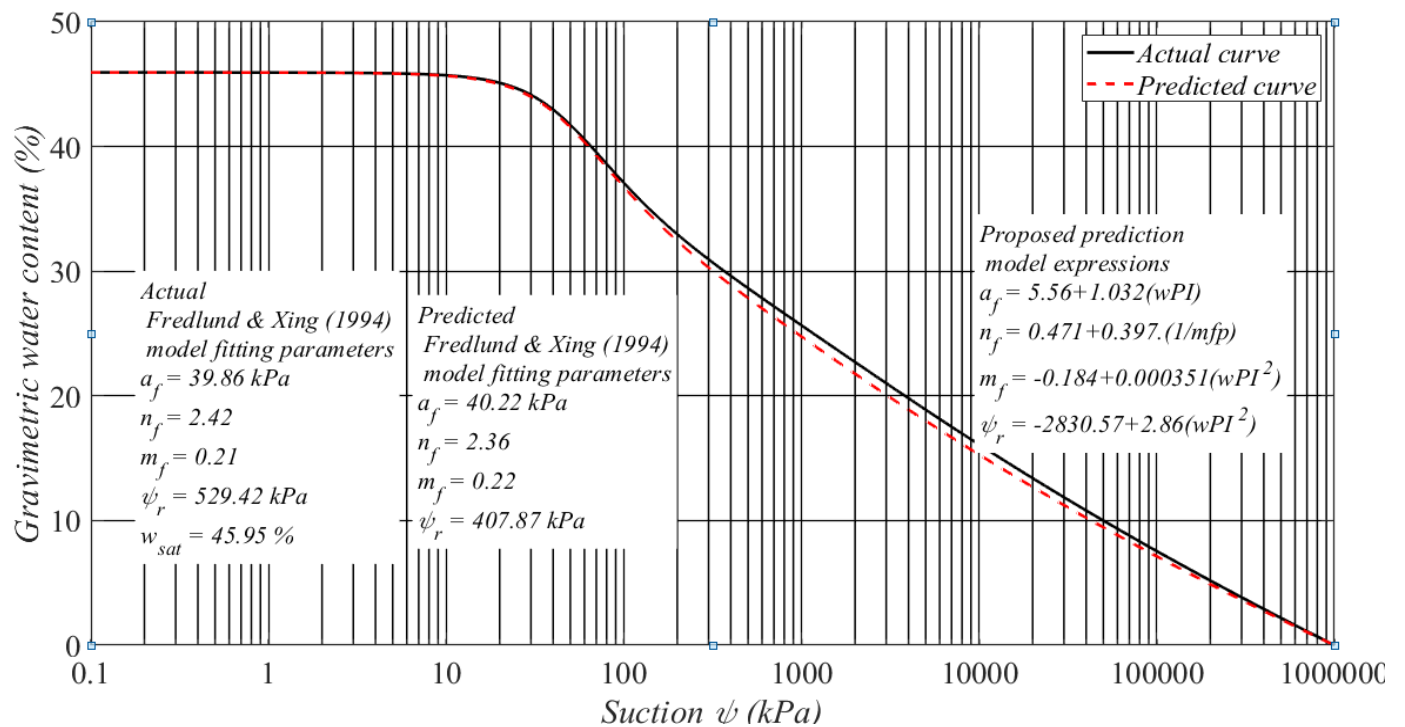


Figure 4.24 Actual vs predicted soil water characteristics curve plot for TP2

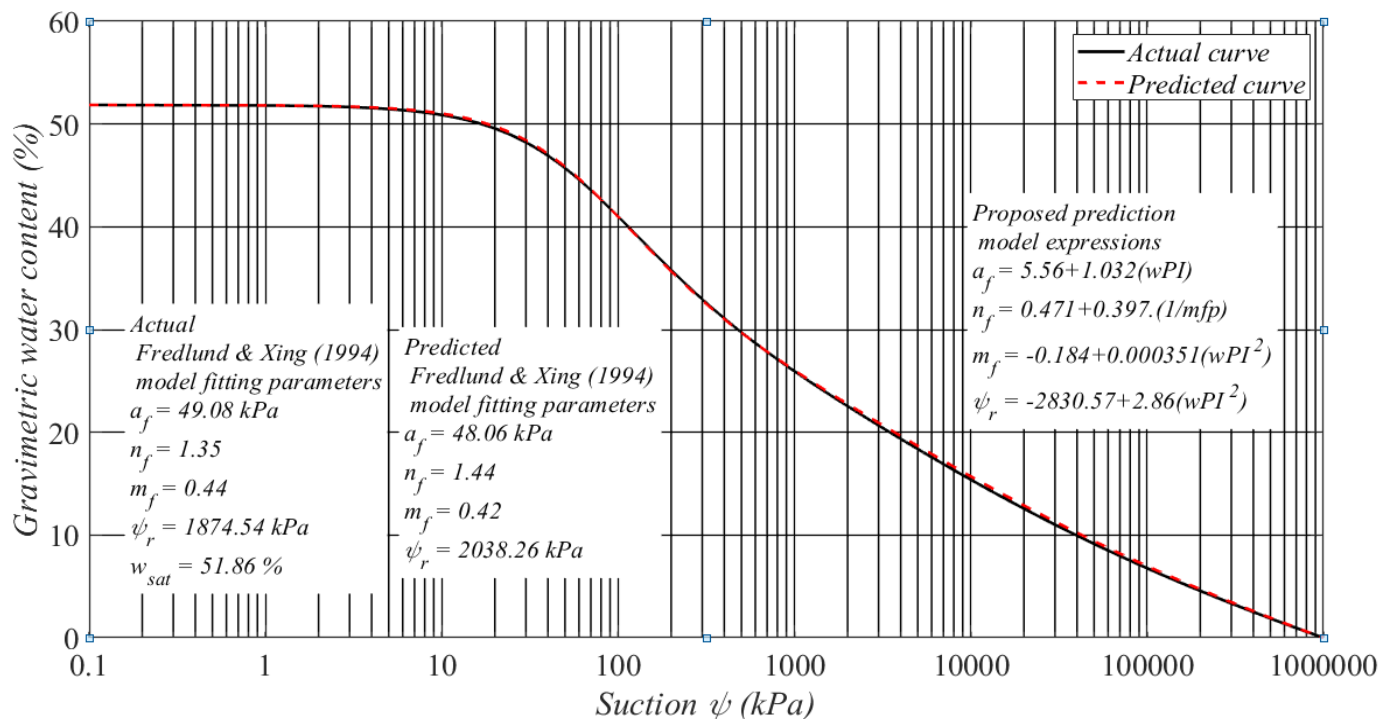


Figure 4.25 Actual vs predicted soil water characteristics curve plot for TP3

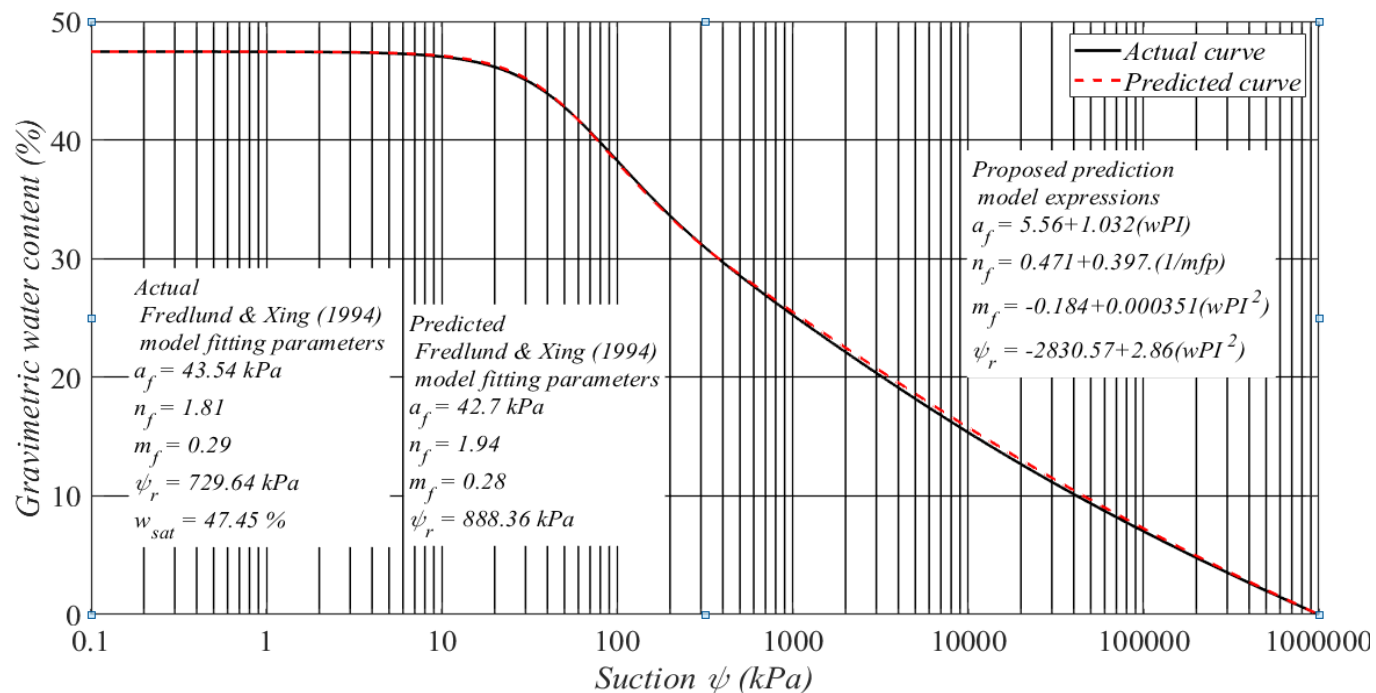


Figure 4.26 Actual vs predicted soil water characteristics curve plot for TP4

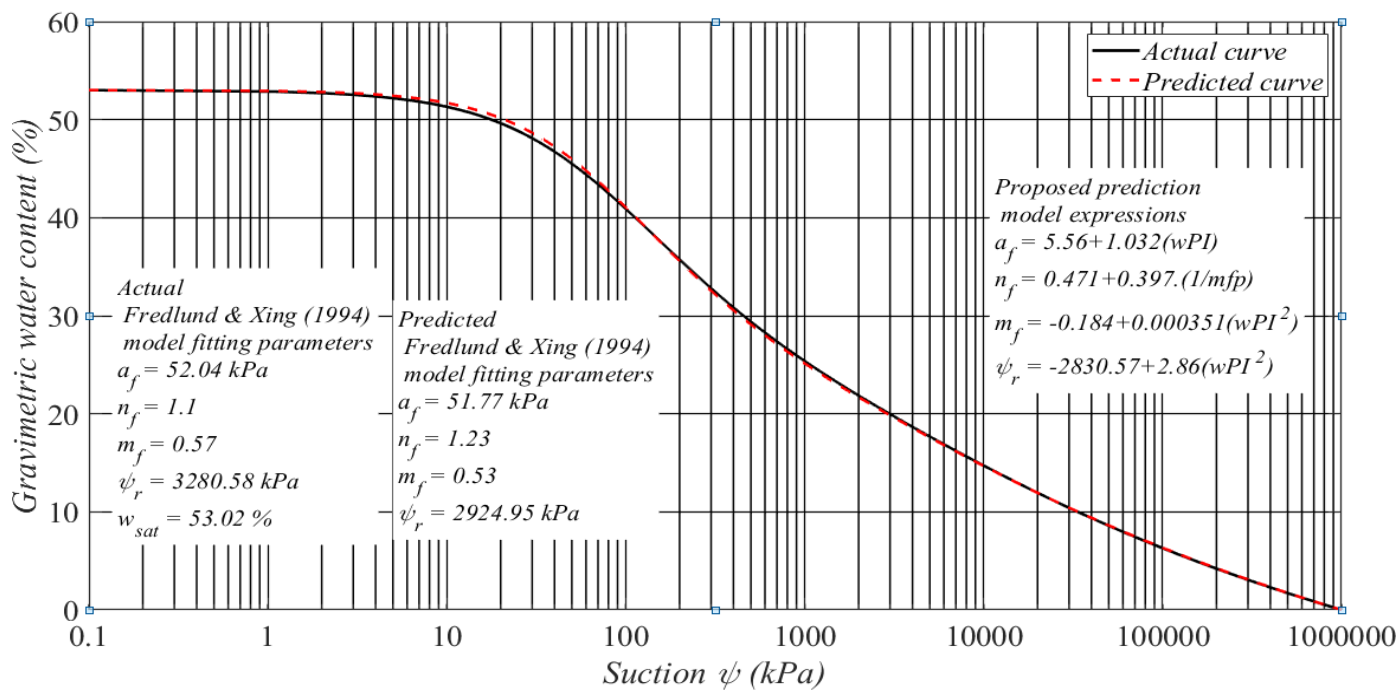


Figure 4.27 Actual vs predicted soil water characteristics curve plot for TP5

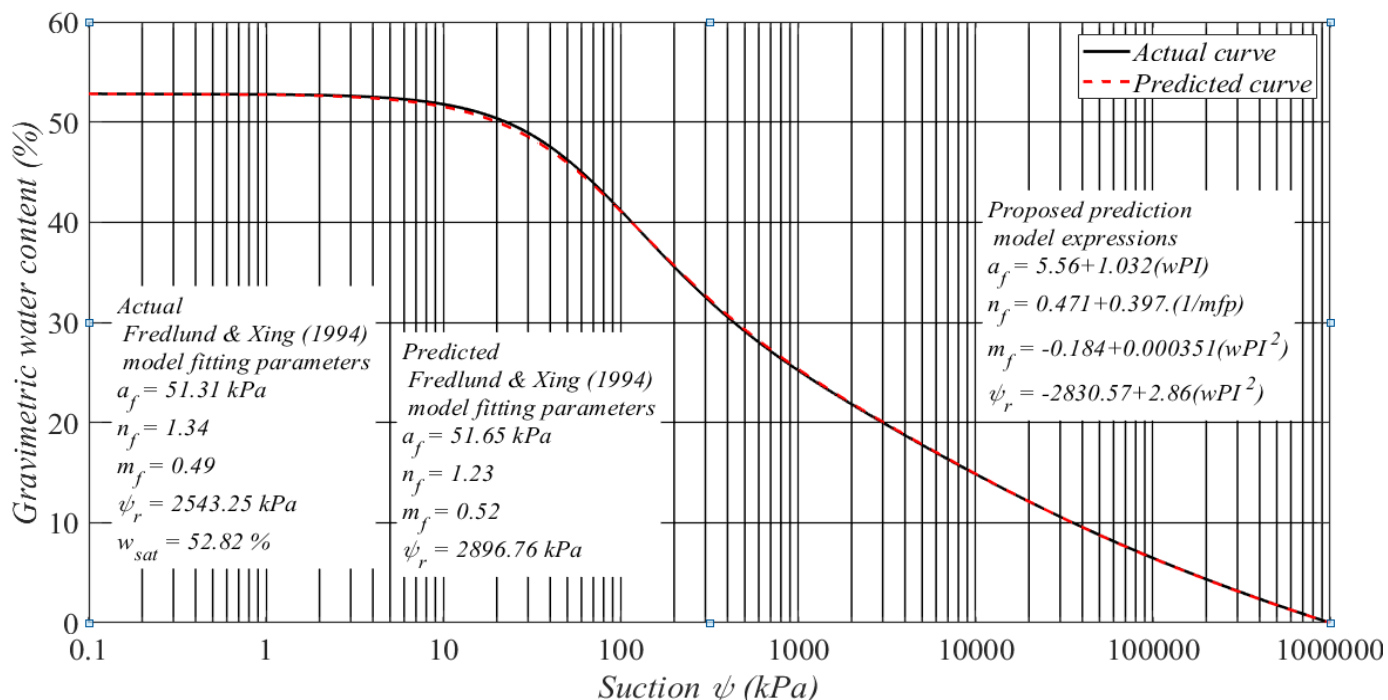


Figure 4.28 Actual vs predicted soil water characteristics curve plot for TP6

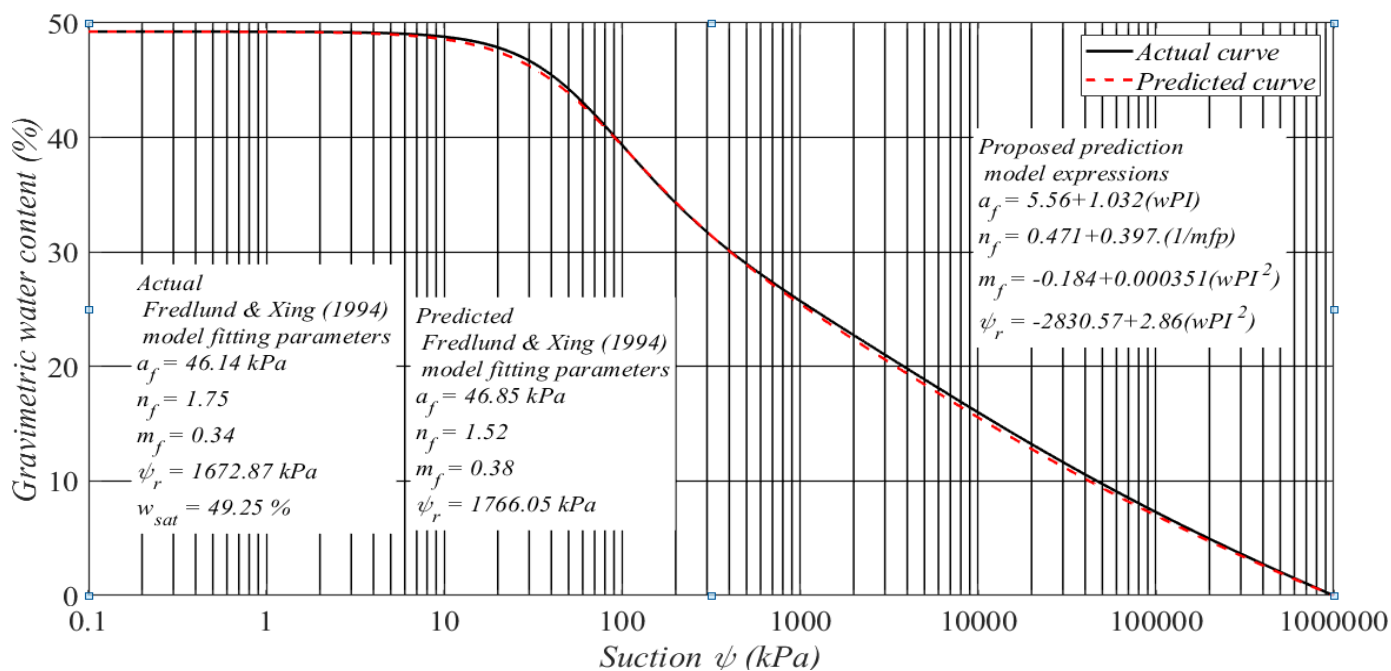


Figure 4.29 Actual vs predicted soil water characteristics curve plot for TP7

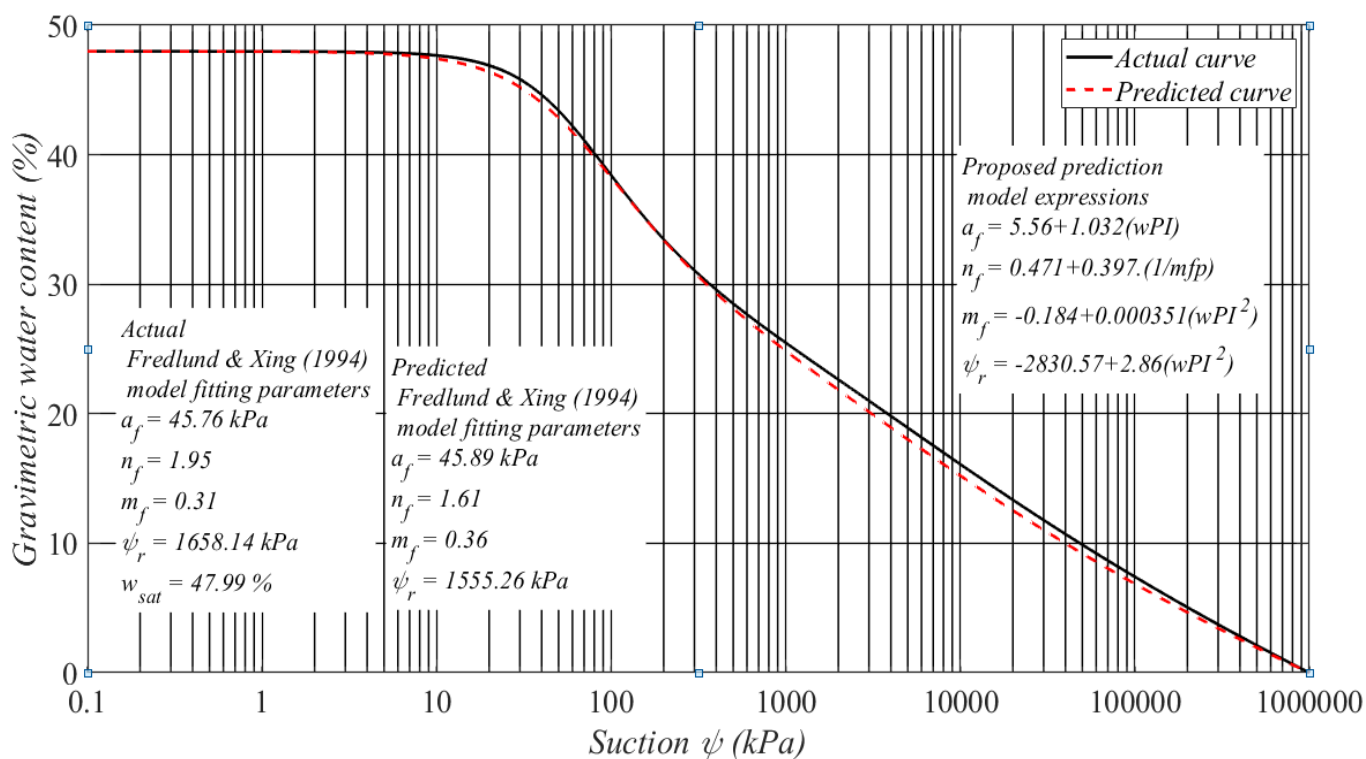


Figure 4.30 Actual vs predicted soil water characteristics curve plot for TP8

Starting from figure 4.23 to figure 4.30 briefly plotted the predicted and actual soil water characteristic curve of each test pit. As shown on the figures the predicted values of each curve fitting parameters were fairly matched with the actual curve fitting parameters. Table 4.12 expressed that the percentage of difference between the actual and predicted value of the whole test pits. From this for all test pits the maximum percentages of difference for af ,nf ,mf .and residual suction were less than 2.12%, 29.55 ,7.69 ,29.8 respectively. This indicated that in the minimum the predicted value was 97.88, 70.45, 92.31, and 70.2% similar with the actual value for each parameter respectively.

Table 4.12 Percentage difference between actual and predicted fitting parameters

Measured curve fitting parameters					Predicted value				difference			
No	af	nf	mf	rsuction	af	nf	mf	rsuction	Difference(%)			
									af	nf	mf	Rs
1	41.94	1.59	0.28	667.83	41.88	2.06	0.26	725.18	0.14	29.55	7.69	8.58
2	39.68	2.42	0.21	529.42	40.22	2.36	0.22	407.87	1.36	2.54	4.76	29.8
3	49.08	1.35	0.44	1874.54	48.06	1.44	0.42	2038.26	2.12	6.66	4.76	8.73
4	43.54	1.81	0.29	729.64	42.7	1.94	0.28	888.36	1.96	7.18	3.57	21.75
5	52.04	1.1	0.57	3280.58	51.77	1.23	0.53	2924.95	0.52	11.81	7.54	12.15
6	51.31	1.34	0.49	2543.25	51.65	1.23	0.52	2896.76	0.66	8.94	6.12	13.89
7	46.14	1.75	0.34	1672.87	46.85	1.52	0.38	1766.05	1.53	15.13	11.76	0.55
8	45.76	1.95	0.31	1658.14	45.89	1.61	0.36	1555.26	0.28	21.11	16.12	6.61

4.6 Validation with related works

Different researchers try to put unsaturated soil mechanics in to real applications by proposing a model with different physical properties of soils that are easily measurable in laboratory test with simple device. Thus, for this study the SWCC was related to index properties of soil. Researchers like (Zapata, 1999; Perera *et al.*, 2005; Hernandez, 2011) were developed a physical model that determine the fitting parameters of Fredlund and Xing with index properties of soil to simplify unsaturated properties of soil into real world. A comparative analysis was developed between the actual SWCC and the SWCC obtained from the proposed model, and with the

related / available model. In comparison with previous models; the proposed model was close to the actual SWCC curve and SWCC data points for each suction level. as shown the figure below the proposed model was fairly related with the three researchers. but it can be seen that in the graph Hernandez(2011) swcc model some what vary compared to the other this due to different factors like method of data analysis, type of data used, type of laboratory testing procedures, case study area, and composition / characteristics of the selected samples. Further more the proposed model was manipulated by using filter paper method of suction measurement while others use direct measurement techniques like pressure plate apparatus. To develop this model all soil parameters used on the model were the result of soil investigation around Jimma towns. As explanation based on this area the town is under different environmental condition i.e high rainfall and high preceptations existing on the town. The investigation on xrd analysis represent that the red soils was dominantly covered with clay minerals koalinite . such soils have different properties with different environmental condition, due this and other factors the developed model was some what difference compared with the model of (Zapata, 1999, Perera *et al.*, 2005, and Hernandez, 2011). Detailed observation value for all curve fitting parameters was shown on figure 4.31 to figure 4.38.

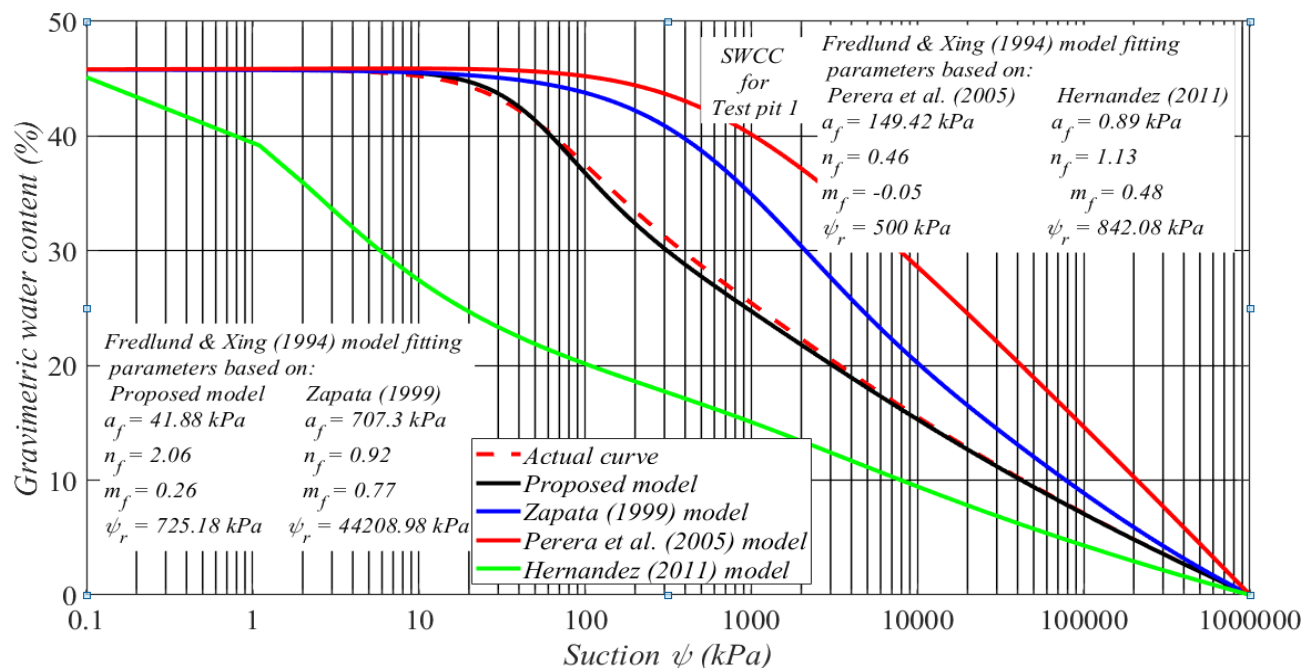


Figure 4.31 Validation between the the proposed model with Zapata, Perera et al., and Hernandez for test pit 1

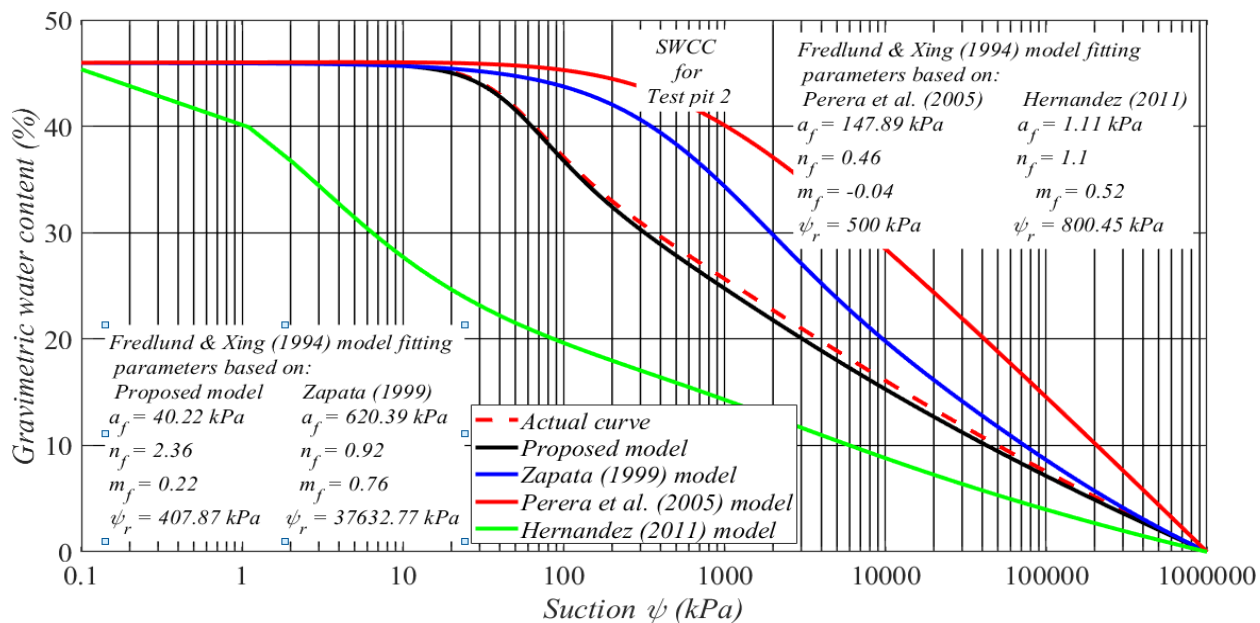


Figure 4.32 Validation between the the proposed model with Zapata,Perera et al,andHernandez for test pit 2

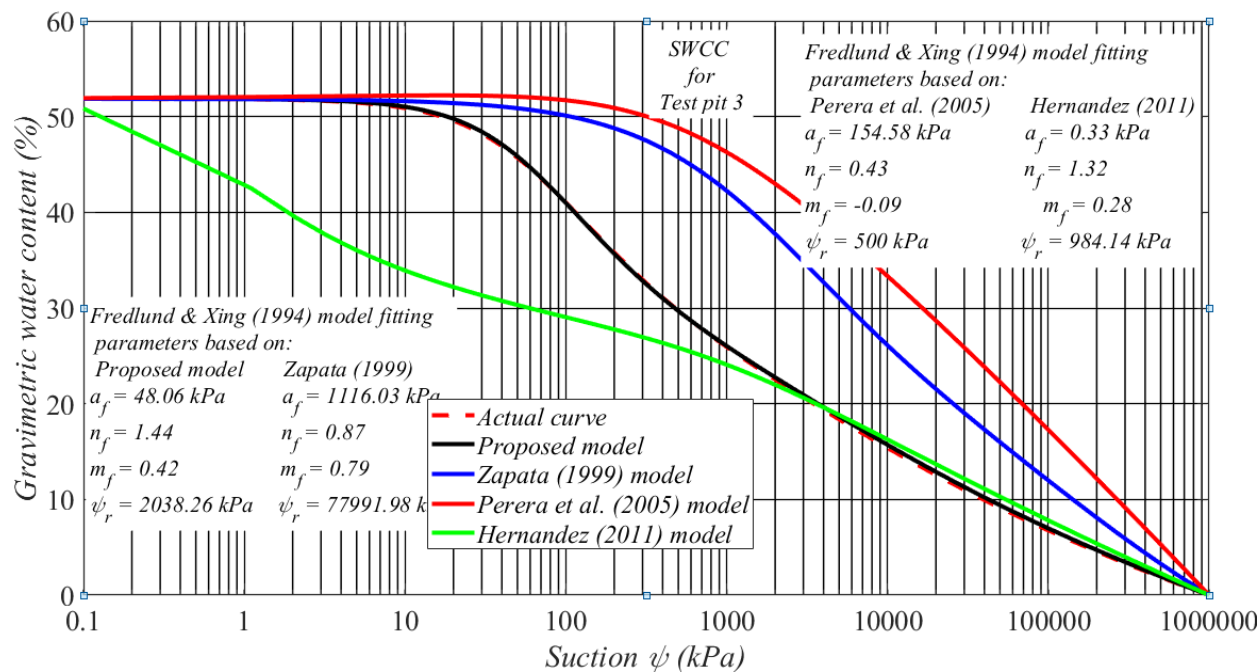


Figure 4.33 Validation between the the proposed model with Zapata,Perera et al,andHernandez for test pit3

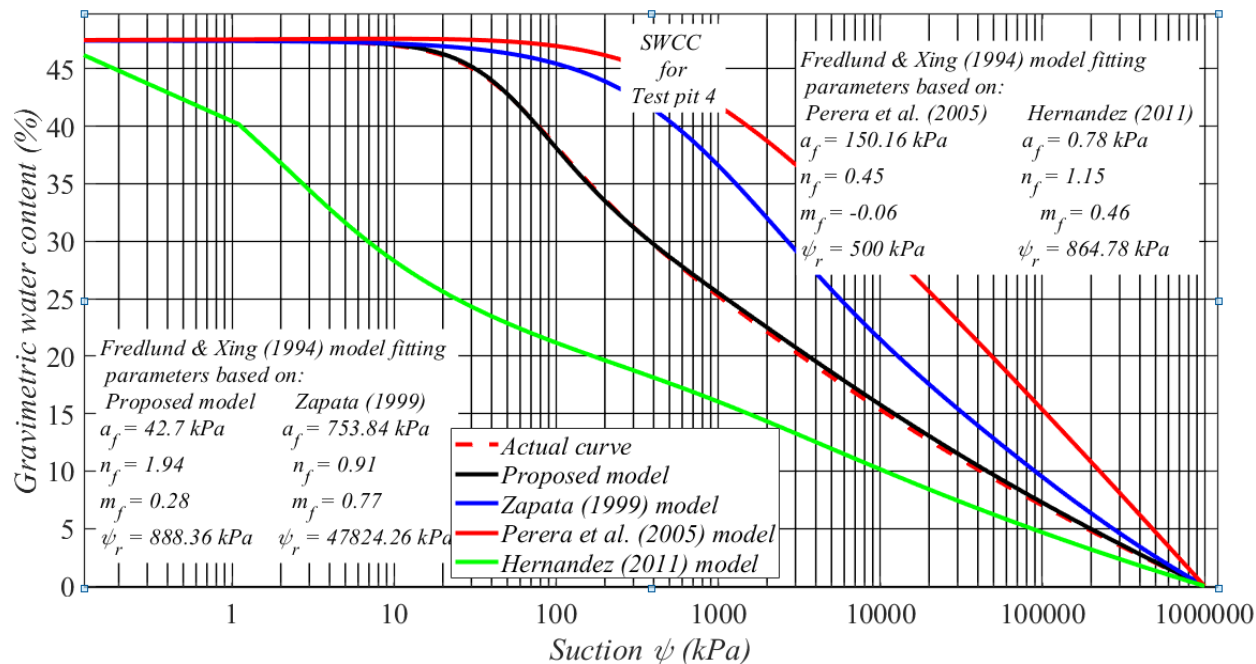


Figure 4.34 Validation between the the proposed model with Zapata,Perera et al,andHernandez for test pit4

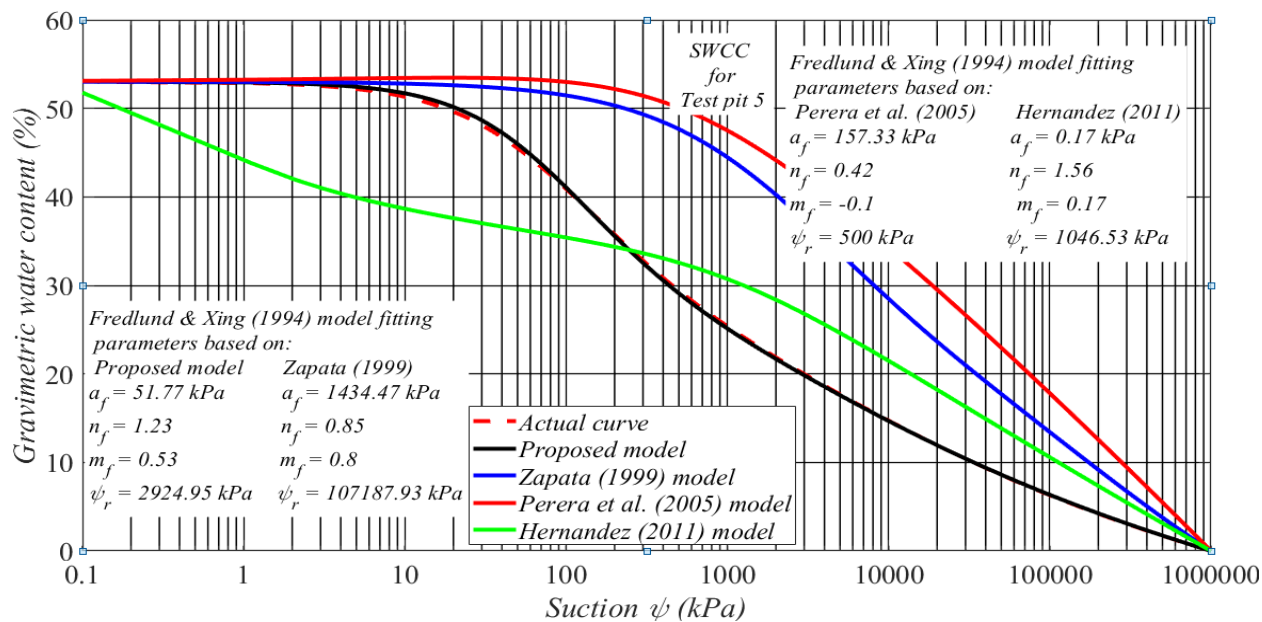


Figure 14.35 Validation between the the proposed model with Zapata,Perera et al, and Hernandez for test pit 5

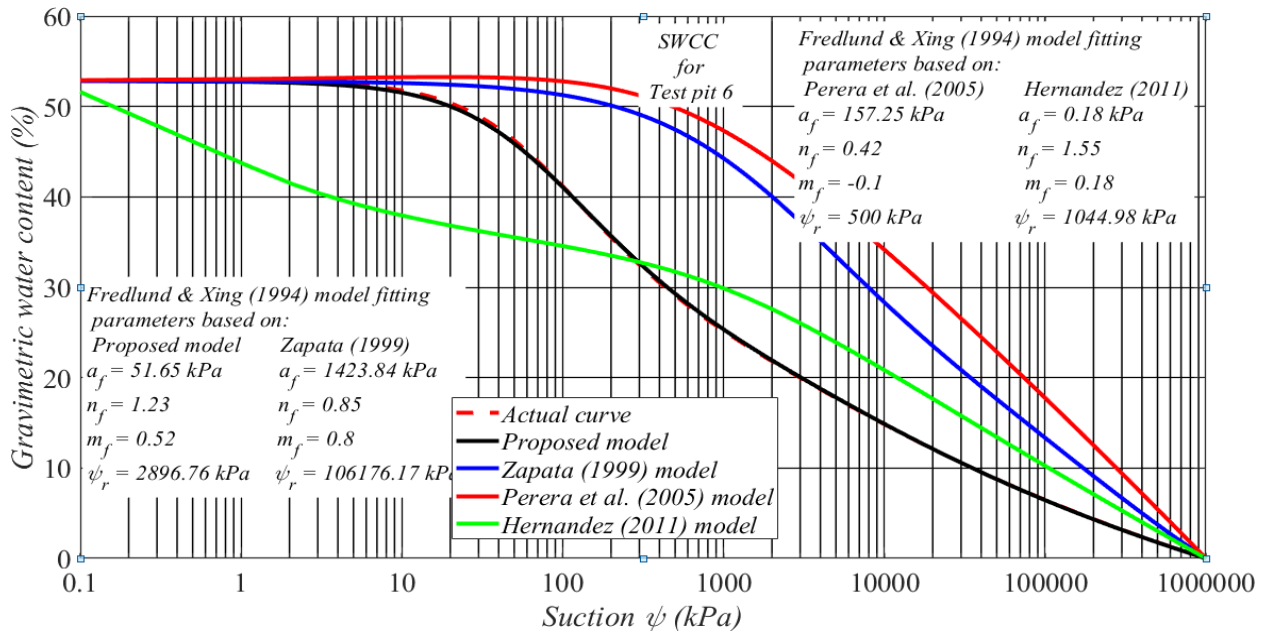


Figure 4.36 Validation between the the proposed model with Zapata,Perera et al, and Hernandez for test pit 6

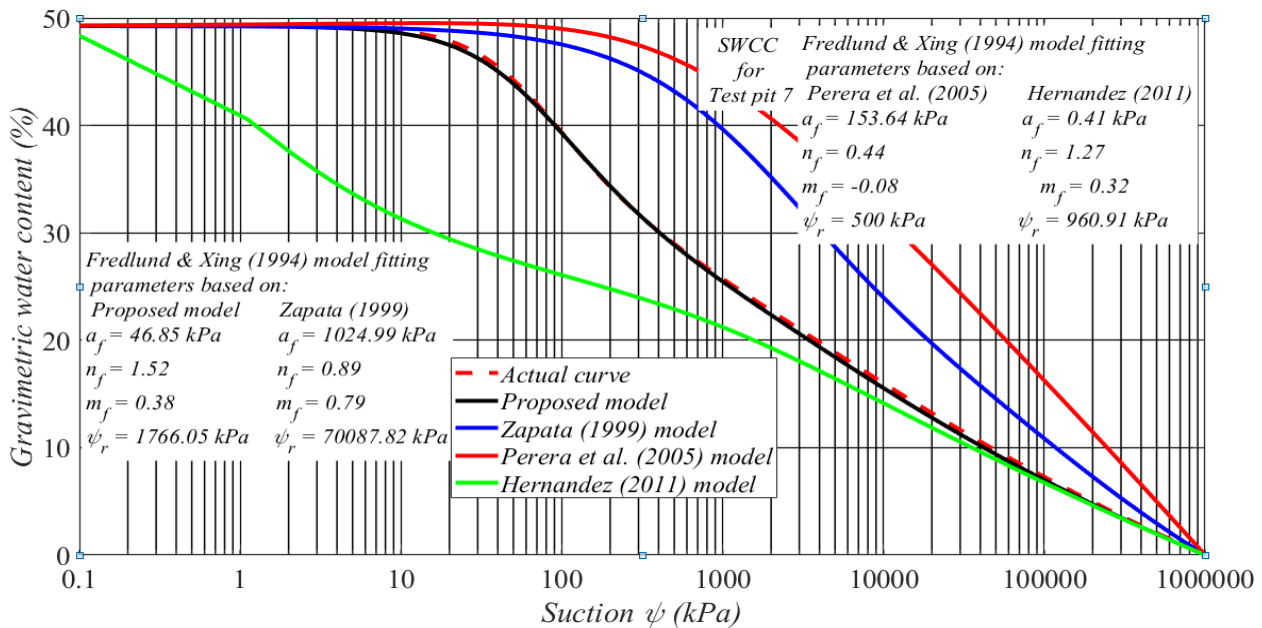


Figure 4.37 Validation between the the proposed model with Zapata,Perera et al,andHernandez for test pit 7

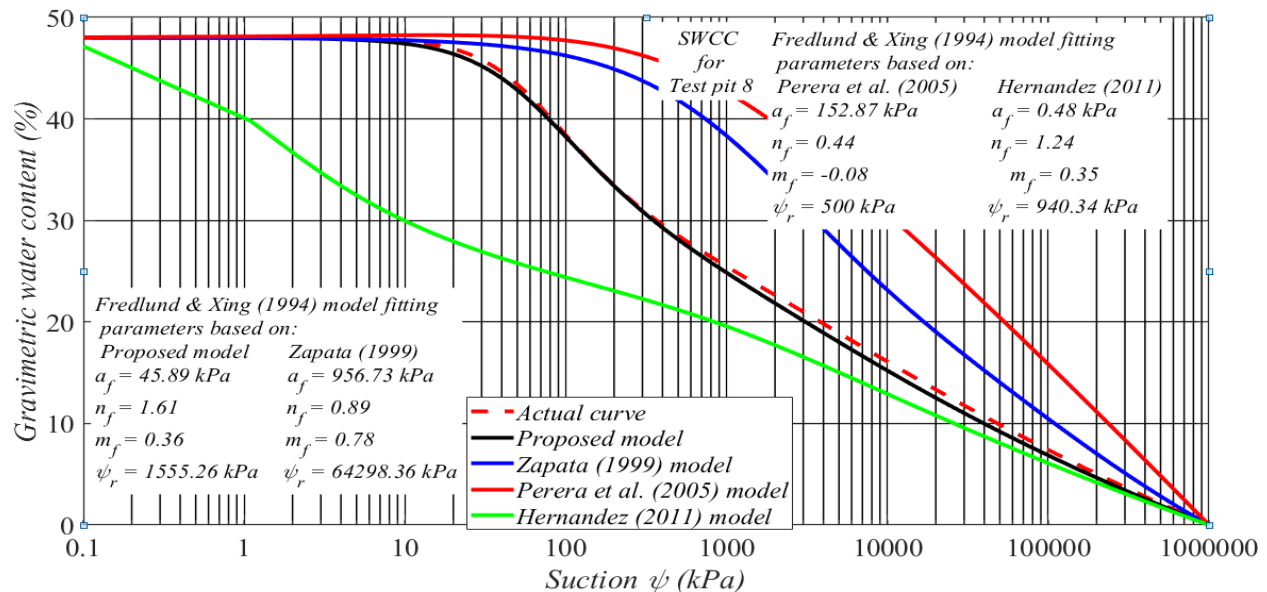


Figure 4.38 Validation between the proposed model with Zapata, Perera et al., and Hernandez for test pit 8

The database available with this study was analyzed to compare the proposed model and the existing models. To show the best model among the models; different statistical analyses were made such as mean algebraic error, mean absolute error, sum of square error, root mean square error (RMSE), adjusted r square, and Akaike information criteria (AIC). To quantify / estimate the error, the actual gravimetric water content was compared with the predicted gravimetric water content. Figure below shows that the error analysis of the actual and predicted gravimetric water content with corresponding suction values 0.1 and 10kpa respectively. For each model type the Fredlund & Xing (1994) model fitting parameters were calculated based on the actual weighted plasticity index and group index. Thereafter, the Fredlund & Xing (1994) model fitting parameters were incorporated into the Fredlund & Xing (1994) model to estimate the predicted gravimetric water content. Several suction values that cover a wide range of suctions were chosen for the comparison between the predicted gravimetric water content and the actual gravimetric water content.

According to the result shown on the chart the percent mean algebraic error, the percent mean absolute error, SSE, RMSE, and AIC associated with the proposed model were found fairly good. In low suction range the Zapata's (1999) model and the proposed model were found close

to the actual SWCC rather than the available models, while the Hernandez (2011) model shows weak performance. In higher suction range the Hernandez (2011) model is better than Zapata (1999) model refer . In general, the Hernandez (2011) model was predicting a far SWCC relative to the actual SWCC. In comparison with previous models; the proposed model was close to the actual SWCC curve and SWCC data points for each suction level, this is due to small number of data points and limited test pits and also on this study only focus in the same type of soil in all test pits (i.e. red clay soil).

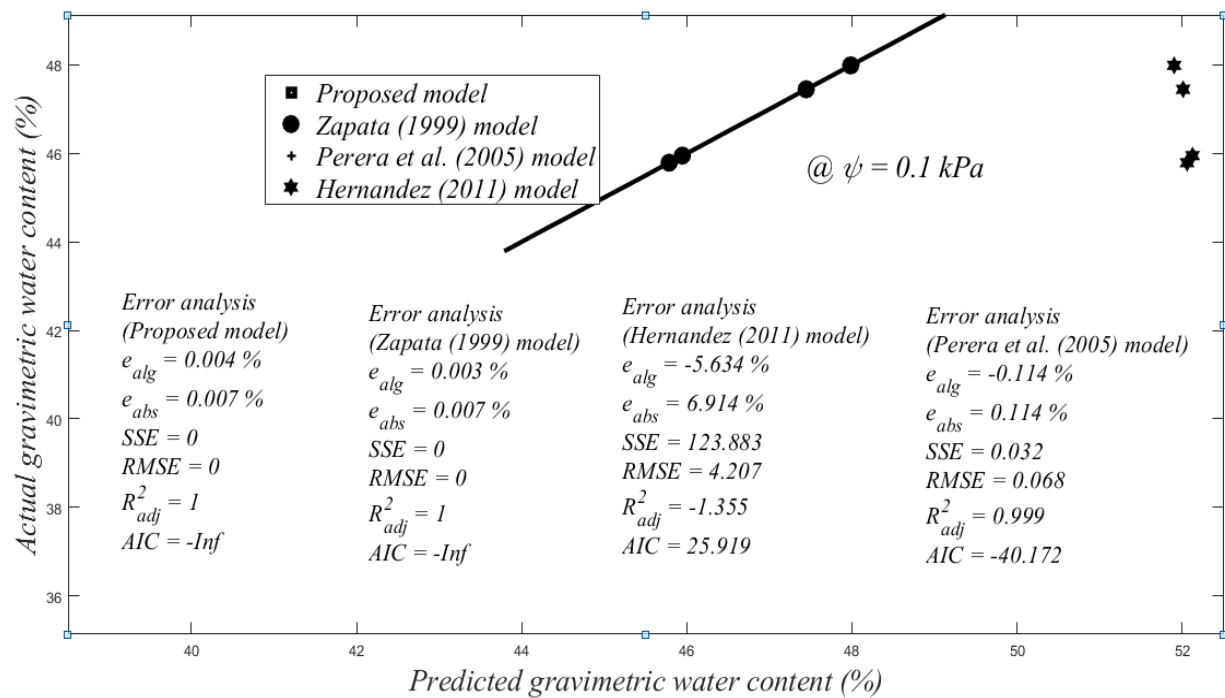


Figure 4.39 Error analysis based on the plot of actual and predicted gravimetric water content

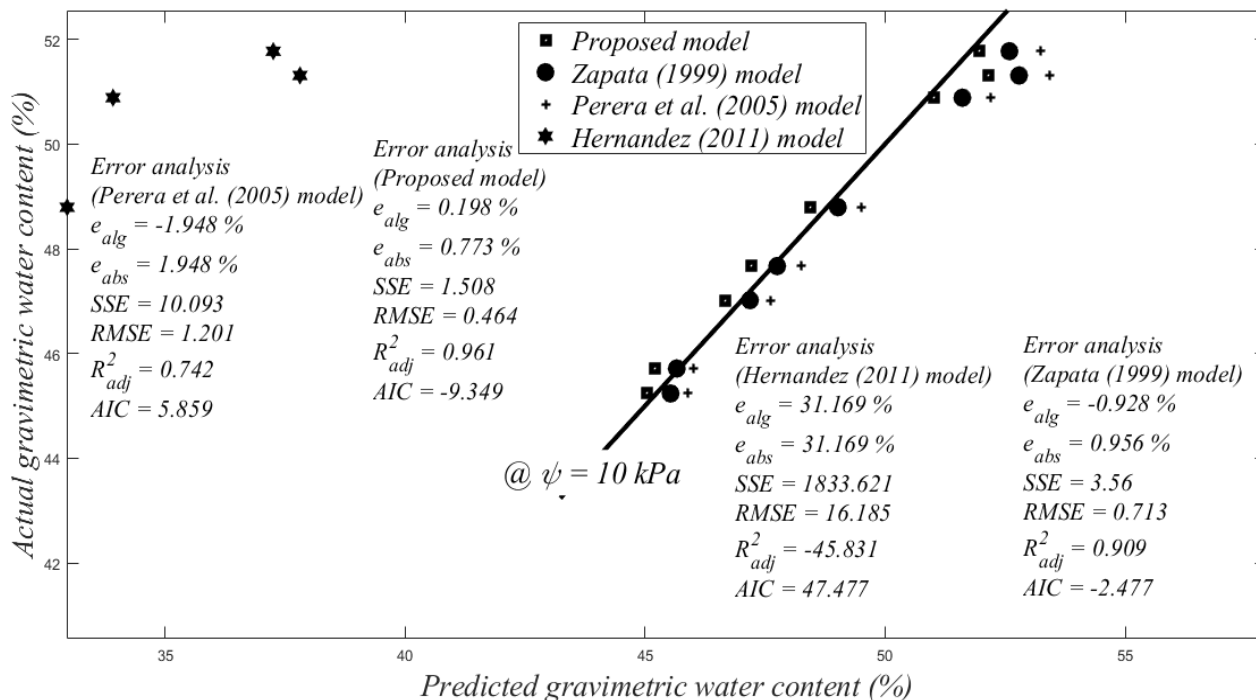


Figure 4.40 Error analysis based on the plot of actual and predicted gravimetric water content

Table 4.13 Analysis of Error for predicted versus actual gravimetric water content at different suction value for different models.

Suction (kPa)	Error Analysis	Model			
		Proposed	Zapata (1999)	Perera et al. (2005)	Hernandez (2011)
0.1	$e_{alg} (\%)$	0.004	0.003	-0.114	-5.634
	$e_{abs} (\%)$	0.007	0.007	0.114	6.914
	SSE	0	0	0.032	123.883
	$RMSE$	0	0	0.068	4.207
	R^2_{adj}	1	1	0.999	-1.355
	AIC	-Inf	-Inf	-40.172	25.919
10	$e_{alg} (\%)$	-0.189	-0.928	-1.948	31.169
	$e_{abs} (\%)$	0.773	0.956	1.948	31.169
	SSE	1.508	3.56	10.093	1833.621
	$RMSE$	0.464	0.713	1.201	16.185
	R^2_{adj}	0.961	0.909	0.742	-45.831
	AIC	-9.349	-2.477	5.859	47.477

33	$e_{alg}(\%)$	0.708	-5.694	-7.626	35.011
	$e_{abs}(\%)$	1.763	5.694	7.626	35.011
	<i>SSE</i>	6.379	65.334	111.238	2083.829
	<i>RMSE</i>	0.955	3.055	3.986	17.254
	R_{adj}^2	0.736	-1.699	-3.596	-85.099
	<i>AIC</i>	-2.189	20.801	25.058	48.5
100	$e_{alg}(\%)$	0.808	-20.887	-24.758	30.328
	$e_{abs}(\%)$	1.75	20.887	24.758	30.328
	<i>SSE</i>	4.752	559.367	777.869	1188.77
	<i>RMSE</i>	0.824	8.939	10.542	13.032
	R_{adj}^2	0.705	-33.699	-47.253	-72.742
	<i>AIC</i>	-0.167	37.979	40.617	44.01
200	$e_{alg}(\%)$	1.467	-33.92	-40.058	24.618
	$e_{abs}(\%)$	2.523	33.92	40.058	24.618
	<i>SSE</i>	8.314	1131.55	1555.501	678.384
	<i>RMSE</i>	1.09	12.714	14.907	9.844
	R_{adj}^2	-0.028	-138.979	-191.424	-82.92
	<i>AIC</i>	4.308	43.615	46.161	39.522

CHAPTER FIVE

CONCLUSION AND RECOMMENDATION

5.1 Conclusion

This study was conducted in Jimma town, south-western Ethiopia. In most part of the area unsaturated soil is prevalent. To study unsaturated soil properties SWCC is a crucial tool. In this study, a prediction model, which predicts the soil-water characteristics curve using simple geotechnical index properties, has been developed. The SWCC prediction model was developed based on index properties data from eight test pits. This study illustrates that the index properties can be used to develop a prediction model for the (Fredlund&Xing,1994) model curve fitting parameters .A prediction model, based on readily simple laboratory tests, provides a useful tool to predict the(Fredlund&Xing,1994) model fitting parameters with a high degree of accuracy.

The combination of Atterberg limit and weighted plastic index properties of soil (WPI) and the model fitting parameters a_f , n_f , m_f and ψ_r of the SWCCs were calculated. Based on the laboratory test result all test pits coincides under the fine grained soil properties and the soil was classified as high plastic red clay soil with plasticity index range from 35.14 to 45.41. According to filter paper measurement test result, the soils of Jimma exist under the fitting parameters of a_f ranges from 39.86 to 52.04 kpa and the residual suction ranges from 529.31 to 3280.49 kpa. From the XRD analysis the red clay soil of Jimma town was dominated by Kaolinite type of clay minerals A MATLAB[®] R2019a which uses a constrained nonlinear optimization method was used along with the measured soil-water characteristics curve data using a filter paper method of suction measurement with wetting curve procedure. To estimate the fitting parameters of model fitting parameters for eight soil samples collected from different test pits. A mathematical equation was proposed to estimate the model fitting parameters. The comparison between the measured and the predicted data gives a higher R square. This indicates that the proposed model is acceptable.

5.2 Recommendation

On the basis of the findings and conclusion of the research, the researcher would like to forward the following recommendations:

- Each type soil show different soil water characteristics curve .This study focused only the red clay soil found in Jimma town. Hence, further studies are needed to develop SWCC for other types of soil in the town.
- Most part of Jimma town is covered by black, red, and grey color types of soil. Due to time constraints and economic limitations in this study eight test pits with red color were used. . A future researcher can develop a prediction model by using many test pits with different soil type.
- In this study, the suction was measured using a filter paper technique method using whatman 42 type of paper. A future researcher can develop a prediction model by measuring the suction range using a pressure plate apparatus to account for suction variations and by using different brand of filter paper.
- The proposed model doesn't account for pore size distribution. Try to develop a prediction model using an undisturbed and disturbed condition. The proposed prediction model was developed on the basis of an undisturbed sample. A future researcher can develop a prediction model on disturbed soil and can investigate the effect of pore size distribution.

References

- A.M. RIDLEY, K. DINEEN, J. B. B. and P. R. V. (2003) 'Soil matrix suction : some examples of its measurement and application in geotechnical engineering', (2), pp. 241–253.
- Al-hashemi, H. M. B. (2018) 'Estimation of SWCC for Unsaturated Soils and Its Application to Design of Shallow Foundations', pp. 1–16. doi: 10.11159/icgre18.131.
- ASTM D5298-16 (2016) 'Standard Test Method for Measurement of Soil Potential (Suction) Using Filter Paper', *Astm International*, 04.08, pp. 1–6. doi: 10.1520/D5298-16.2.
- Bicalho, K., Correia, A. and Ferreira, S. (2007) 'Filter paper method of soil suction measurement', *XIII Panamerican Conference on Soil Mechanics and Geotechnical Engineering*, (July), pp. 4–7. Available at: <http://repositorium.sdum.uminho.pt/handle/1822/12305>.
- Bicalho, K. V, Cupertino, K. F. and Bertolde, A. I. (2011) 'Evaluation of suction-water content calibrations of filter paper', *14th Pan-American Conference on Soil Mechanics and Geotechnical Engineering*.
- Bittelli, M. and Flury, M. (2009) 'Errors in Water Retention Curves Determined with Pressure Plates', *Soil Science Society of America Journal*, 73(5), pp. 1453–1460. doi: 10.2136/sssaj2008.0082.
- Bulut, R. (2001) 'total and matric suction measurements with the filter paper method'.
- Bulut, R. and Leong, E. C. (2008) 'Indirect measurement of suction', *Geotechnical and Geological Engineering*, 26(6), pp. 633–644. doi: 10.1007/s10706-008-9197-0.
- Chiu, C. F., Yan, W. M. and Yuen, K. (2012) 'Reliability analysis of soil – water characteristics curve and its application to slope stability analysis', *Engineering Geology*, 135–136, pp. 83–91. doi: 10.1016/j.enggeo.2012.03.004.
- Choudhury, C. and Tadikonda, B. V. (2015) 'soil-water characteristic curve models for clays soil-water characteristic curve models for clays', (January).
- Clay, R. E. D., In, S. and Dar, B. (2003) 'investigation into some of the engineering properties of

red clay soils IN BAHIR DAR.’, (November).

Dafalla, M. A. *et al.* (2020) ‘Predicting Soil-Water Characteristic Curves of Clayey Sand Soils Using Area Computation’, *Mathematical Problems in Engineering*, 2020. doi: 10.1155/2020/4548912.

Fredlund, D. D. (2020) ‘Interpretation of Soil-Water Characteristic Curves when Volume Change Occurs as Soil Suction is Changed’, c(January 2013). doi: 10.1201/b14393-4.

Fredlund, D. G. (2006) ‘2 . Components of a " boundary value problem "', (Figure 1), pp. 27–45.

Fredlund, D G, Rahardjo, H. and Fredlund, M. D. (2012) *Unsaturated Soil Mechanics in Engineering Practice*.

Fredlund, Delwyn G., Rahardjo, H. and Fredlund, M. D. (2012) ‘Unsaturated Soil Mechanics in Engineering Practice’, *Unsaturated Soil Mechanics in Engineering Practice*, (March), pp. 286–321. doi: 10.1002/9781118280492.

Fredlund, D. G., Sheng, D. and Zhao, J. (2011) ‘Estimation of soil suction from the soil-water characteristic curve’, 198, pp. 186–198. doi: 10.1139/T10-060.

Fredlund, X. and (1994) ‘Equations for the soil-water characteristic ’ curve ’’.

Ganjian, N. *et al.* (2007) ‘Prediction of Soil – Water Characteristic Curve Based on Soil Index Properties Prediction of Soil – Water Characteristic Curve Based on Soil Index Properties’, (January). doi: 10.1007/3-540-69873-6.

George, F. O. (2020) ‘measurement and estimation of soil water characteristic’, (April).

Greene, H. (2012) ‘Tropical soils’, *Journal of the Science of Food and Agriculture*, 5(2), pp. 65–69. doi: 10.1002/jsfa.2740050201.

Hernandez, T. (2011) ‘Estimating the Soil–Water Characteristic Curve Using Grain Size Analysis and Plasticity Index’, *Angewandte Chemie International Edition*, 6(11), 951–952., (May).

Huat, B. B. K. and Toll, D. G. (2012) *Introduction, Handbook of Tropical Residual Soils*

Engineering. doi: 10.1201/b12302-1.

Jemal J, M. (2017) ‘In-depth Investigation into Engineering Characteristics of Jimma Soils In-depth Investigation into Engineering Characteristics of Jimma Soils By’, (October 2014).

Kim, H., Prezzi, M. and Salgado, R. (2017) ‘Calibration of Whatman Grade 42 filter paper for soil suction measurement’, *Canadian Journal of Soil Science*, 97(2), pp. 93–98. doi: 10.1139/cjss-2016-0064.

Leong, E. C., He, L. and Rahardjo, H. (2002) ‘Factors affecting the filter paper method for total and matric suction measurements’, *Geotechnical Testing Journal*, 25(3), pp. 322–333. doi: 10.1520/gtj11094j.

Lu, N. (2020) ‘Unsaturated Soil Mechanics: Fundamental Challenges, Breakthroughs, and Opportunities’, *Journal of Geotechnical and Geoenvironmental Engineering*, 146(5), p. 02520001. doi: 10.1061/(asce)gt.1943-5606.0002233.

Lu, N., Godt, J. W. and Wu, D. T. (2010) ‘A closed-form equation for effective stress in unsaturated soil’, *Water Resources Research*, 46(5), pp. 1–14. doi: 10.1029/2009wr008646.

Matlan, S. J., Mukhlisin, M. and Taha, M. R. (2014) ‘Performance evaluation of four-parameter models of the soil-water characteristic curve’, *Scientific World Journal*, 2014. doi: 10.1155/2014/569851.

Mukherjee, S. (2013) ‘physical properties of clay’, pp. 54–68.

Nam, S. *et al.* (2010) ‘Comparison of testing techniques and models for establishing the SWCC of riverbank soils’, *Engineering Geology*, 110(1–2), pp. 1–10. doi: 10.1016/j.enggeo.2009.09.003.

Oluyemi-ayibiowu, B. D., Akinleye, T. O. and Fadugba, O. G. (2020) ‘Soil-Water Characteristics of Tropical Clay Soil under High and Low Suction Conditions’, pp. 162–175. doi: 10.4236/gep.2020.811010.

Pan, H., Qing, Y. and Pei-yong, L. (no date) ‘Direct and Indirect Measurement of Soil Suction in the Laboratory’.

- Paper, C., Perera, Y. and Zapata, C. (2005) 'Prediction of the Soil-Water Characteristic Curve Based on Grain-Size- Distribution and Index Properties', 40776(August 2016). doi: 10.1061/40776(155)4.
- Pereira, J. M., Delage, P. and Cui, Y. J. (2010) 'measurements on a natural unsaturated soil : a reappraisal of the', (June 2014). doi: 10.1201/b10526-110.
- Perera, Y. Y. *et al.* (2005) 'Prediction of the Soil-Water Characteristic Curve Based on Grain-Size-Distribution and Index Properties', 40776(October), pp. 1–12. doi: 10.1061/40776(155)4.
- Power, K. C. and Vanapalli, S. K. (2008) 'A Revised Contact Filter Paper Method', (November). doi: 10.1520/GTJ101099.
- Strength, S. *et al.* (2021) 'Matric Suction Soil-Water Interaction The Role of Native Vegetation in Sta- bilizing Formation Soil for Transport Corridors Pile behavior modeling in unsaturated expansive soils Assessment of the Postcompaction Fill Characteristics at the Penrith Lakes De'.
- Town, J. *et al.* (2020) 'Engineering Characterization of Subgrade Soils of', pp. 1–17.
- V.Bund (no date) 'Characteristic Curve by Osmotic Method and Filter Paper Method', (1994), pp. 5421–5434.
- Zapata, C. (1999) 'Uncertainty in soil-water-characteristic curve and impacts on unsaturated shear strength predictions /', (March).
- Zhai, Q. and Rahardjo, H. (2013) 'Quanti fi cation of uncertainties in soil – water characteristic curve associated with fi tting parameters', 163, pp. 144–152. doi: 10.1016/j.enggeo.2013.05.014.
- Zhang, J. *et al.* (2018) 'Estimation of Soil-Water Characteristic Curve for Cohesive Soils with Methylene Blue Value', 2018.
- Zhang, Y. *et al.* (2019) 'Research Article A New Soil-Water Characteristic Curve Model for Unsaturated Loess Based on Wetting-Induced Pore Deformation', 2019.

Appendix

Appendix A. Natural moisture content

Formula used

$$w = \frac{M_1 - M_2}{M_2 - M_c} \times 100\%$$

Where M_c : Mass of container

M_1 : Mass of moist soil + container

M_2 : Mass of dry soil + container

w : Moisture content

Table A.1. Natural moisture content for test pit.1

Depth at 2m	Trial1	Trial2	Trial 3
Can code	A1-3	A	A-7
Mass of can	16.13	18.49	19.917
Mass of can +wet soil	60.89	67.08	50.43
Mass of can +dry soil	47.76	53.14	41.699
Mass of dry soil	31.63	34.66	21.78
Mass of water	13.09	13.87	8.731
Water content (%)	41.39	40.01	40.08
Average (%)	40.5		

Table A.2. Natural moisture content for test pit 2

SAMPLE Depth	2m		
	Trial1	Trial2	Trial 3
Can code	B	D1	J41
Mass of can	38.71	31.28	20.22

Mass of can +wet soil	93.32	95.17	113.79
Mass of can +dry soil	78.32	77.32	88.34
Mass of dry soil	39.61	46.04	68.12
Mass of water	15	17.85	25.45
Water content	0.3786	0.3877	0.3736
Average(%)	38.33		

Table A.3. Natural moisture content for test pit.3.

Depth at 2m	Trial1	Trial2	Trial 3
Can code	W11	15 ₁	03-2
Mass of can	41.78	36.64	43.32
Mass of can +wet soil	131.63	116.84	119.29
Mass of can +dry soil	107.82	95.73	99.05
Mass of dry soil	66.03	59.09	55.73
Mass of water	23.82	21.11	20.24
Water content	36.08	35.73	36.32
Average W%	36.04		

Table A.4. Natural moisture content for test pit.4.

Depth at 2m	Trial1	Trial2	Trial 3
Can code	B	A ₁₄	J41
Mass of can	31.4	29.78	32.78
Mass of can +wet soil	140.4	123.22	148.28
	5		
Mass of can +dry soil	109.2	96.81	115.79
	2		
Mass of dry soil	77.82	67.03	83.01
Mass of water	31.23	26.41	32.49
Water content	40.13	39.4	39.14

Average (%)	39.56
-------------	-------

Table A.5. Natural moisture content for test pit.5.

Depth at 2m	Trial1	Trial2	Trial 3
Can code	W11	15 ₁	03-2
Mass of can	40.7	36.63	41.32
Mass of can +wet soil	90.64	70.33	78.89
Mass of can +dry soil	77.63	61.51	69.01
Mass of dry soil	36.93	24.88	27.69
Mass of water	13.00	8.82	9.88
Water content%	35.2	35.43	35.682
Average (%)	35.44		

Table A.6. Natural moisture content for test pit.6.

Depth at 2m	Trial1	Trial2	Trial 3
Can code	J41	02-2	B
Mass of can	35.79	28.773	31.396
	1		
Mass of can +wet soil	77.81	83.773	89.994
Mass of can +dry soil	65.98	68.287	73.268
	2		
Mass of dry soil	30.19	39.51	41.872
	1		
Mass of water	11.28	15.486	16.726
	4		
Water content	39.16	39.19	39.95
Average (%)	39.43		

Table A.7. Natural moisture content for test pit.7.

Depth at 2 m	Trial1	Trial2	Trial 3
Can code	D	P1	B3
Mass of can	29.70	17.92	17.422
Mass of can +wet soil	100.1	67.99	78.05
	4		
Mass of can +dry soil	78.90	52.93	59.79
	8		
Mass of dry soil	49.20	35.02	42.37
	7		
Mass of water	21.23	15.05	18.26
	5		
Water content	43.15	42.99	43.09
Average (%)	43.08		

Table A.8. Natural moisture content for test pit.8.

Depth at 2m	trial1	trial2	trial3
can code	12	P67	B1
mass of can	41.5	35.57	20.22
mass of can +wet soil	124.46	123.96	86.04
mass of can +dry soil	99.97	97.71	66.82
mass of dry soil	58.47	62.14	46.6
mass of water	24.49	26.25	19.22
water content%	41.88	42.24	41.24
Average(%)	41.79		

Apenddix B.Specific gravity

The formula adopted for determination of Specific Gravity of soils.

$$G_s = (M_{ps} - M_p) / [(M_{pw} - M_p) - (M_{pws} - M_{ps})]$$

M_p = mass of pycnometer

M_{ps} = mass of pycnometer + dry soil

M_{pws} = mass of pycnometer + soil + water

M_{pw} = mass of water + pycnometer

Table B.1. Specific gravity for test pit 1

test pit 1	Trial1	Trial2	Trial3
Mass of Pycnometer, M_p	27.004	25.471	27.004
Mass of Pycnometer + Soil, M_{ps}	52.004	50.471	52.004
Mass of Pycnometer + Soil + Water, M_{pws}	137.41	133.655	137.566
Mass of Pycnometer + Water, M_{pw} @ T_i	121.482	117.713	121.692
The water temprature, T_i	26	26	26
Temperature of contents of Pycnometer When M_{pws} was taken, T_x	28	28	28
Mass of Dry Soil, M_s	25	25	25
Density of water at ρ_w @ T_i T_i ,	0.99681	0.99681	0.99681
Density of water at ρ_w @ T_x T_x	0.99626	0.99626	0.99626
M_{pw} (@ T_x) = [ρ_w @ T_x]	121.4299	117.6621	121.6398
Conversion factor, K	0.9986	0.9986	0.9986
Specific Gravity, @ 20°C	2.77	2.77	2.75
Average		2.76	

Table B.2. Specific gravity for test pit 2

Test pit 2			
Mass of Pycnometer, M_p	12.651	12.743	16.176

Mass of Pycnometer + Soil, Mps	18.651	18.743	22.176
Mass of Pycnometer + Soil + Water, Mpws	41.563	41.864	45.851
Mass of Pycnometer + Water, Mpw @ Ti	37.798	38.094	42.089
The water temprature, Ti	25	25	25
Temperature of contents of Pycnometer When Mpws was taken, Tx	27	27	27
Mass of Dry Soil, Ms	6	6	6
Density of water at Ti, $\rho_w @ T_i$	0.99707	0.99707	0.99707
Density of water at Tx $\rho_w @ T_x$	0.99681	0.99681	0.99681
Mpw (@Tx)=[$\rho_w @ T_x$]	37.79144	38.08739	42.08224
Conversion factor, K	0.9988	0.9988	0.9983
Specific Gravity, @ 20°C	2.69	2.70	2.68
		2.69	

Table B.4. Specific gravity for test pit 4

test pit 4			
Mass of Pycnometer, Mp	25.542	27.0701	22.609
Mass of Pycnometer + Soil, Mps	50.542	52.0701	47.609
Mass of Pycnometer + Soil + Water, Mpws	133.623	137.663	134.52
Mass of Pycnometer + Water, Mpw @ Ti	117.813	121.766	118.588
The water temprature, Ti	25	25	25
Temperature of contents of Pycnometer When Mpws was taken, Tx	27	27	27
Mass of Dry Soil, Ms	25	25	25
Density of water at Ti, $\rho_w @ T_i$	0.99707	0.99707	0.99707
Density of water at $\rho_w @ T_x$	0.99654	0.99654	0.99654

T _x			
M _{pw} (@T _x)=[ρ _w @ T _x]	117.764	121.7157	118.537
Conversion factor, K	0.9988	0.9988	0.9983
Specific Gravity, @ 20°C	2.73	2.76	2.77
		2.75	

Table B.5. Specific gravity for test pit 5

Test pit 5			
Mass of Pycnometer, M _p	27.111	27.506	27.15
Mass of Pycnometer + Soil, M _{ps}	52.111	52.506	52.15
Mass of Pycnometer + Soil + Water, M _{pws}	137.507	137.925	140.81
Mass of Pycnometer + Water, M _{pw} @ T _i	121.562	122.128	125.005
The water temperature, T _i	22	22	22
Temperature of contents of Pycnometer When M _{pws} was taken, T _x	24	24	24
Mass of Dry Soil, M _s	25	25	25
Density of water at T _i , ρ _w @ T _i	0.9978	0.9978	0.9978
Density of water at T _x , ρ _w @ T _x	0.99732	0.99732	0.99732
M _{pw} (@T _x)=[ρ _w @ T _x]	121.5166	122.0822	124.9579
Conversion factor, K	0.9996	0.9996	0.9996
Specific Gravity, @ 20°C	2.77	2.73	2.73
Average		2.74	

Table B.6. Specific gravity for test pit 6

test pit 6			
Mass of Pycnometer, M _p	25.542	27.0701	22.609

Mass of Pycnometer + Soil, Mps		50.542	52.0701	45.109
Mass of Pycnometer + Soil + Water, Mpws		133.778	137.857	132.885
Mass of Pycnometer + Water, Mpw @ Ti		117.813	122.066	118.588
The water temperature, Ti		23	23	23
Temperature of contents of Pycnometer When Mpws was taken, Tx		25	25	25
Mass of Dry Soil, Ms		25	25	22.5
Density of water at Ti,	$\rho_w @ T_i$	0.99757	0.99757	0.99757
Density of water at Tx	$\rho_w @ T_x$	0.99707	0.99707	0.99707
Mpw (@Tx)=[$\rho_w @ T_x$]		117.7668	122.0184	118.5399
Conversion factor, K		0.9993	0.9993	0.9993
Specific Gravity, @ 20°C		2.78	2.73	2.76
			2.75	

Table B.7. Specific gravity for test pit 7

test pit 7				
Mass of Pycnometer, Mp		27.506	27.15	27.111
Mass of Pycnometer + Soil, Mps		52.506	52.15	52.111
Mass of Pycnometer + Soil + Water, Mpws		139.536	139.786	137.237
Mass of Pycnometer + Water, Mpw @ Ti		123.837	124.015	121.562
The water temperature, Ti		25	25	25
Temperature of contents of Pycnometer When Mpws was taken, Tx		26	26	26
Mass of Dry Soil, Ms		25	25	25
Density of water at Ti,	$\rho_w @ T_i$	0.99707	0.99707	0.99707
Density of water at Tx	$\rho_w @ T_x$	0.99681	0.99681	0.99681
Mpw (@Tx)=[$\rho_w @ T_x$]		123.8119	123.9897	121.5374
Conversion factor, K		0.9988	0.9988	0.9983
Specific Gravity, @ 20°C		2.69	2.71	2.68

2.70

Table B.8. Specific gravity for test pit 8

Test pit 8			
Mass of Pycnometer, Mp		22.609	27.0701 27.111
Mass of Pycnometer + Soil, Mps		47.609	52.0701 52.111
Mass of Pycnometer + Soil + Water, Mpws		133.873	137.914 136.937
Mass of Pycnometer + Water, Mpw @ Ti		118.288	122.066 121.162
The water temperature, Ti		25	25 25
Temperature of contents of Pycnometer When Mpws was taken, Tx		27	27 27
Mass of Dry Soil, Ms		25	25 25
Density of water at Ti,	$\rho_w @ T_i$	0.99707	0.99707 0.99707
Density of water at Tx	$\rho_w @ T_x$	0.99654	0.99654 0.99654
Mpw (@Tx)=[$\rho_w @ T_x$]		118.2371	122.0155 121.112
Conversion factor, K		0.9988	0.9988 0.9983
Specific Gravity, @ 20°C		2.67	2.74 2.72 2.71

Appendix C: Atterburg limit test result

Table C1:Atterburg

limit result for test
pit 1

Determination	Liquid Limit (D-4318)				Plastic Limit (D-4318)		
Number of blows	31	29	23	16			
can code	F2	k1	P1	P2	2-Mar	1	no

Test No	1	2	2	3	1	2	3
Wt. of Container, (g)	5.87	12.75	5.86	6.53	16.382	6.275	15.351
Wt. of container + wet soil, (g)	28.47	31.65	21.16	28.08	22.981	18.34	21.11
Wt. of container + dry soil, (g)	19.66	24.18	15.01	19.2	21.473	15.53	19.82
Wt. of water, (g)	8.81	7.47	6.15	8.88	1.508	2.81	1.29
Wt. of dry soil, (g)	13.79	11.43	9.15	12.67	5.091	9.255	4.469
Moisture container, (%)	63.89	65.35	67.21	70.09	29.62	30.36	28.87
Average	LL @25 blows =66.54				30		

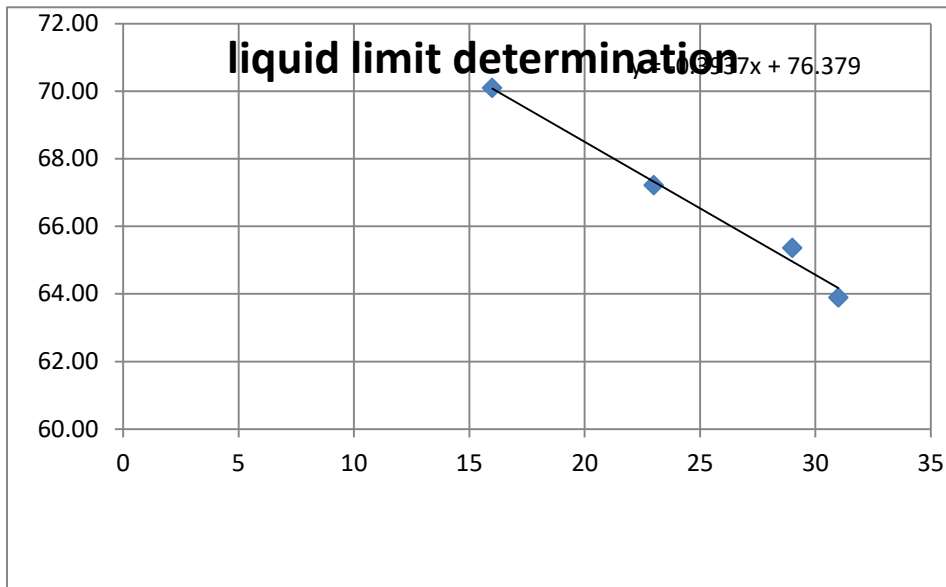


Figure C1 Liquid limit determination graph

Table C2: Atterburg limit result for test pit 2

<i>Determination</i>	<i>Liquid Limit (D-4318)</i>				<i>Plastic Limit (D-4318)</i>		
Number of blows	33	27	21	17			
can code	w12	A31	p9	H2	mn	j2	ss1

Test No	1	2	2	3	1	2	3
Wt. of Container, (g)	21.75	27.53	12.66	18.71	16.382	6.275	15.351
Wt. of container + wet soil, (g)	48.24	56.29	35.58	47.39	22.991	18.427	21.183
Wt. of container + dry soil, (g)	37.71	44.8	26.22	35.41	21.42	15.33	19.743
Wt. of water, (g)	10.53	11.49	9.36	11.98	1.571	3.097	1.44
Wt. of dry soil, (g)	15.96	17.27	13.56	16.7	5.038	9.055	4.392
Moisture container, (%)	65.98	66.53	69.03	71.74	31.18	34.20	32.79
Average	LL @25 blows =68.14				33		

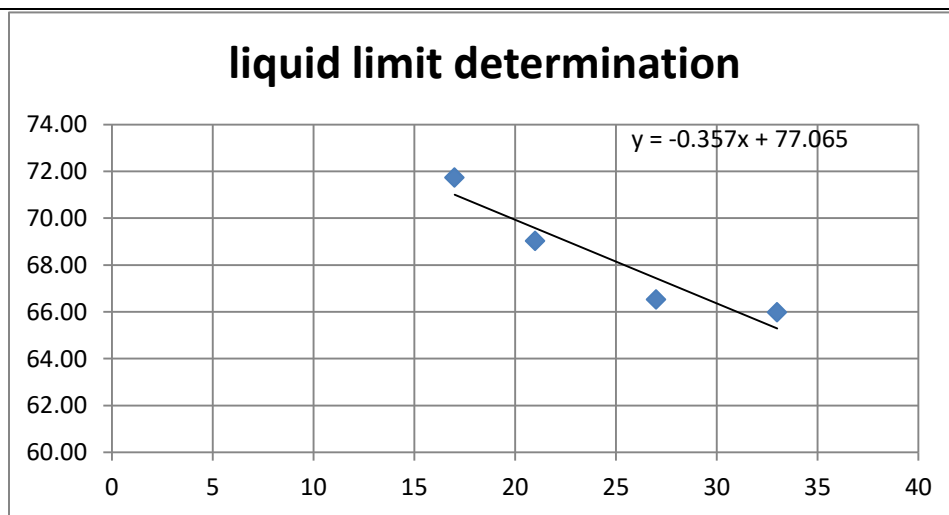


Figure C2: liquid limit determination graph

Table C3: Atterburg limit result of test pit 3

<i>Determination</i>	<i>Liquid Limit (D-4318)</i>				<i>Plastic Limit (D-4318)</i>		
Number of blows	35	28	20	18			
can code	A3	K-4	P2	SB	E-11	F	T-2D
Test No	1	2	3	4	1	2	3
Wt. of Container, (g)	32.7	17.87	17.52	18.49	36.68	36.52	17.661

	9						
Wt. of container + wet soil, (g)	46.8	31.67	32.65	36.36	45.94	43.3	24.3
Wt. of container + dry soil, (g)	41.5	26.26	26.54	29.08	43.83	41.78	22.86
Wt. of water, (g)	5.37	5.41	6.10	7.28	2.11	1.52	1.41
Wt. of dry soil, (g)	8.73	8.40	9.02	10.59	7.15	5.26	5.2
Moisture container, (%)	61.5	64.42	67.63	68.76	29.42	28.89	27.02
Average	LL @25 blows =65.69					28	

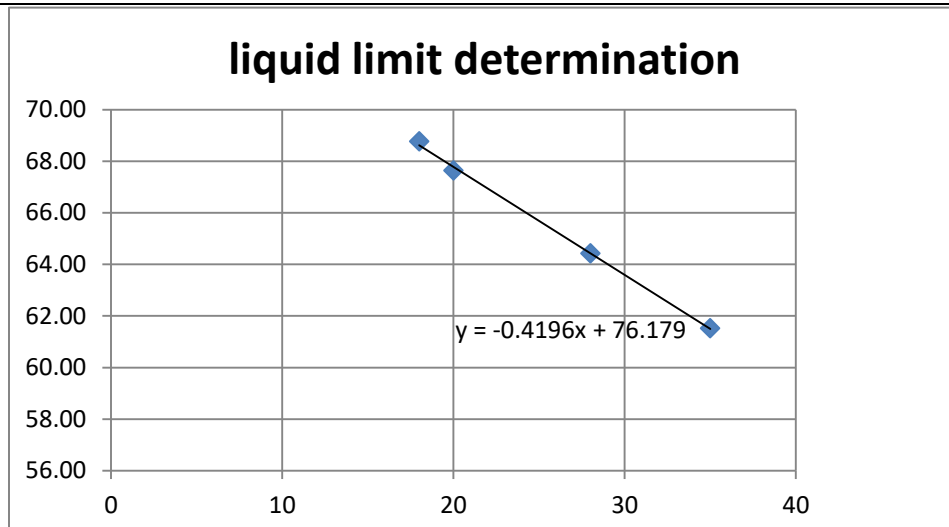


Figure C3: Liquid limit determination graph for test pit 3

Table C4: Atterburg limit result test pit 4

<i>Determination</i>	<i>Liquid Limit (D-4318)</i>				<i>plastic limit</i>		
	31	27	22	15			
Number of blows	31	27	22	15			
can code	P5	P6	LOO	p	2-Jan	B3	J41
Test No	1	2	3	4	1	2	3

Wt. of Container, (g)	17.24	37.72	17.71	17.42	18.39	17.43	32.77
Wt. of container + wet soil, (g)	35.88	54.54	35.57	32.90	26.35	27.54	47.41
Wt. of container + dry soil, (g)	27.93	47.28	27.71	25.95	24.3	24.84	43.60
Wt. of water, (g)	7.95	7.25	7.86	6.95	2.05	2.70	3.81
Wt. of dry soil, (g)	10.69	9.56	10.00	8.53	5.91	7.41	10.83
Moisture container, (%)	74.40	75.84	78.64	81.48	34.60	36.40	35.18
							LL @25 blows =77.02
Average							35

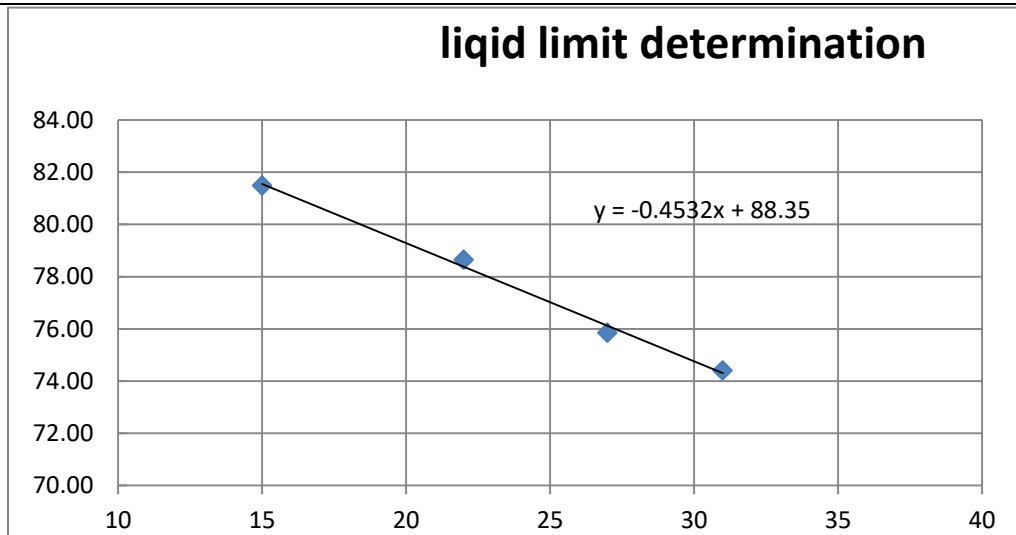


Figure C4: liquid limit determination for test pit 4

Table C5: atterburg limit result for test pit 5

<i>Determination</i>	<i>Liquid Limit (D-4318)</i>				<i>Plastic Limit (D-4318)</i>		
	34	30	23	17	P1	14	P67
Number of blows							
can code	B	w11	A1-C	2-Mar	P1	14	P67
Test No	1	2	3	4	1	2	3

Wt. of Container, (g)	31.41	40.76	49.744	41.338	17.931	17.14	35.57
Wt. of container + wet soil, (g)	45.98	55.39	68.77	56.867	27.84	27.76	46.69
Wt. of container + dry soil, (g)	39.64	48.89	60.142	49.775	25.19	24.88	43.77
Wt. of water, (g)	6.34	6.5	8.628	7.092	2.65	2.88	2.92
Wt. of dry soil, (g)	8.23	8.13	10.398	8.437	7.259	7.74	8.2
Moisture container, (%)	77.04	79.95	82.98	84.06	36.51	37.21	35.61
Average	LL @25 blows =81.41				36		

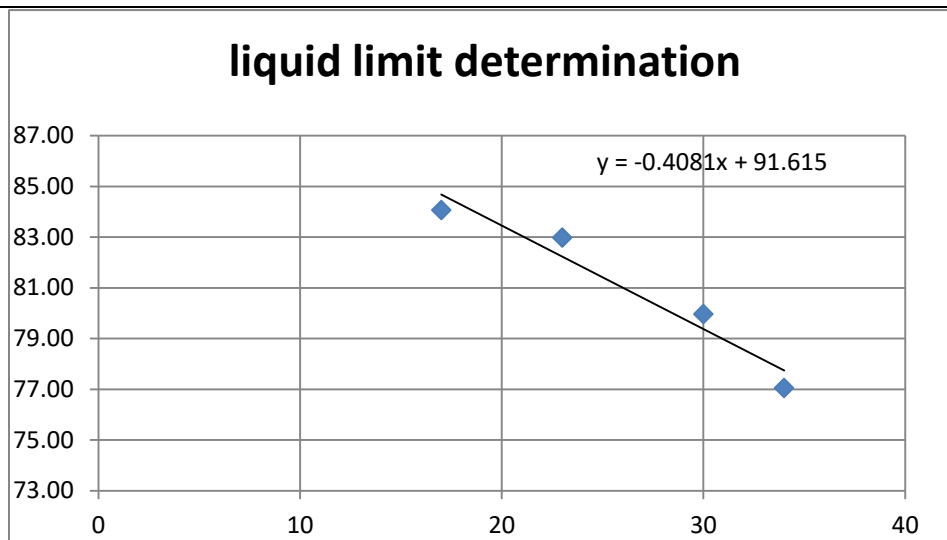


Figure C5: Liquid limit determination graph for test pit 5

Table C6: Atterburg limit result for test pit 6

<i>Determination</i>	<i>Liquid Limit (D-4318)</i>				<i>Plastic Limit (D-4318)</i>		
Number of blows	35	29	23	18	P66	MK3	G10
can code	D	H	G7	A3			
Test No	1	1	2	3	1	2	3
Wt. of Container, (g)	29.7	17.503	17.464	17.605	37.403	17.64	17.20

	2					3	6
Wt. of container + wet soil, (g)	43.5	33.018	36.227	34.951	49.55	34.19	27.08
	9					8	
Wt. of container + dry soil, (g)	37.7	26.303	27.837	27.043	46.39	29.99	24.56
	2						2
Wt. of water, (g)	5.87	6.715	8.39	7.908	3.16	4.208	2.518
						12.34	
Wt. of dry soil, (g)	8	8.8	10.373	9.438	8.987	7	7.356
Moisture container, (%)	73.3	76.31	80.88	83.79	35.16	34.08	34.23
	8						
Average		LL @25 blows =79.37				34	

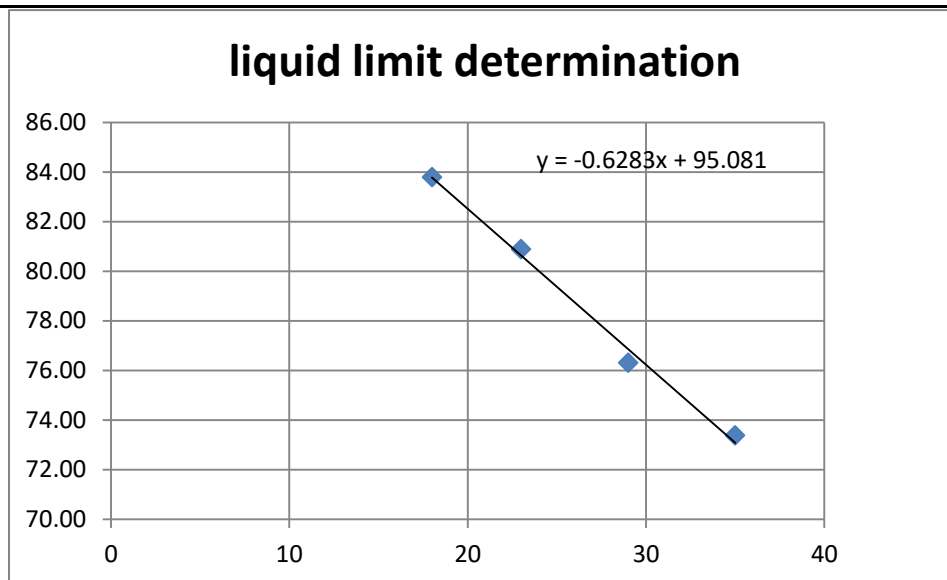


Figure C6: Liquid limit determination graph for test pit 6

Table C7: Atterburg limit result for test pit 7

<i>Determination</i>	<i>Liquid Limit (D-4318)</i>				<i>Plastic Limit (D-4318)</i>		
Number of blows	33	27	23	17	p1	ssb1	HC11
can code	P3	h4	A14	A2			
Test No	1	2	2	3	1	2	3
Wt. of Container, (g)	25.995	31.82	28.8	6.06	17.90	18.044	17.62

					8		6
Wt. of container + wet soil, (g)	50.93	57.06	46.71	33.05	30.72	28.06	26.75
			7	6			4
Wt. of container + dry soil, (g)	40.84	46.59	39.10		21.32	27.73	24.54
			1				5
Wt. of water, (g)	10.09	10.47	7.616	11.73	2.93	2.416	2.209
				6			
Wt. of dry soil, (g)	14.845	14.77	10.30		15.26	9.822	7.6
			1				6.919
Moisture container, (%)	67.97	70.89	73.93	76.91	30.44	31.79	31.93
Average							
						LL @25 blows=72.42	31

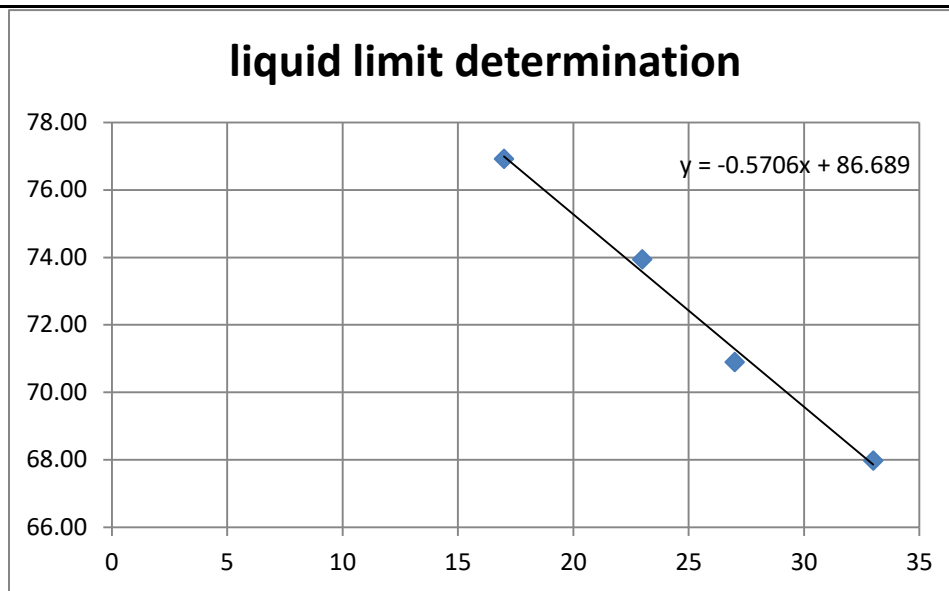


Figure C7: liquid limit determination graph for test pit 7

Table C8: Atterburg limit result for test pit 8

<i>Determination</i>	<i>Liquid Limit (D-4318)</i>				<i>Plastic Limit (D-4318)</i>		
Number of blows	32	26	22	19			
can code	k1	C14	W11	P2	A	B	K
Test No	1	1	2	3	1	2	3

Wt. of Container, (g)	25.4	17.503	25.998	17.462	36.58	17.61	17.61
	1				7	4	4
Wt. of container + wet soil, (g)	44.3	33.018	69.124	41.225	46.12	28.42	28.42
	2				6		4
Wt. of container + dry soil, (g)	36.5	26.463	50.633	30.913	43.68	25.71	25.82
	3				1		
Wt. of water, (g)	7.79	6.555	18.491	10.312	2.445	2.71	2.604
Wt. of dry soil, (g)	11.1	8.96	24.635	13.451	7.094	8.096	8.206
	2						
Moisture container, (%)	70.0	73.16	75.06	76.66	34.47	33.47	31.73
	5						
Average			LL @25 blows=73.66		33		

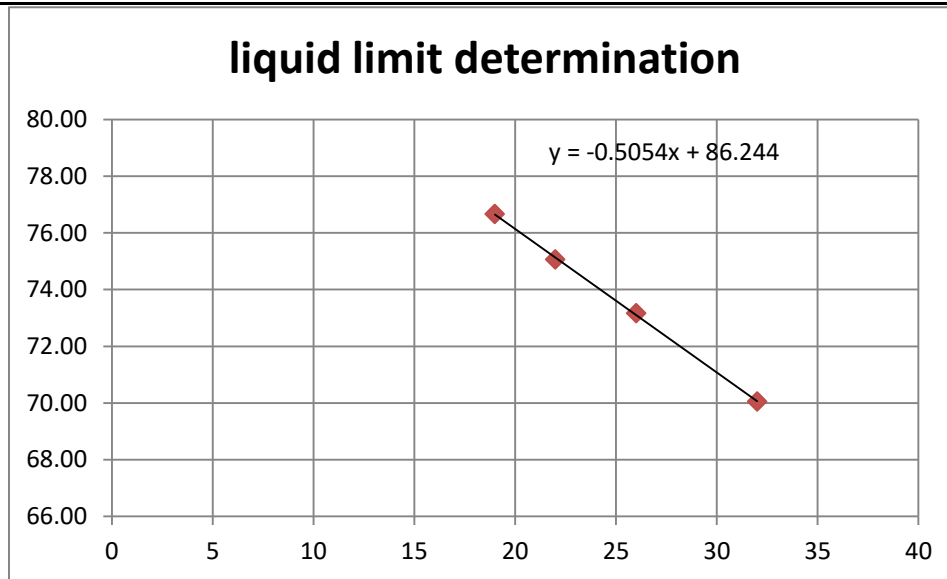


Figure C8: liquid limit determination graph for test pit 8

Appendix D1: Wet Sieve analysis result

Standard Test Method: ASTM D 854-00 Standard Method

Formula used for Wet Sieve analysis

Mass of soil retained = Mass of Sieve and Soil Mass of Empty sieve

$$\text{Soil retained (\%)} = \frac{\text{Mass of soil retained}}{\text{Total Mass of soil}} \times 100$$

$$\text{Soil passing on sieve \#4 (\%)} = 100 - \text{Soil retained on sieve \#4 (\%)}$$

$$\text{Soil passing on remaining } i^{\text{th}} \text{ sieve (\%)} = \text{Soil passing on } (i^{\text{th}} - 1) \text{ sieve (\%)} - \text{Soil retained on } i^{\text{th}} \text{ sieve}$$

$$\text{Soil blocked on } i^{\text{th}} \text{ sieve (\%)} = 100 - \text{Soil passing on } i^{\text{th}} \text{ sieve (\%)}$$

Table D1.1: Wet sieve analysis result of test pit 1 and 2

Test Pit 1	SS, (mm)	MR, (g)	% R	% CR	% P	Test Pit 2	SS, (mm)	MR, (g)	% R	% CR	% P
		9.5	0	0	0		100		9.5	0	0
	4.75	1.5	0.3	0.3	99.7		4.75	0.46	0.092	0.092	99.908
	2	3.3	0.66	0.96	99.04		2	2.7	0.54	0.632	99.368
	0.85	1.2	0.24	1.2	98.80		0.85	1.8	0.36	0.992	99.008
	0.425	2.1	0.42	1.62	98.38		0.425	2.5	0.5	1.492	98.508
	0.25	1.8	0.36	1.98	98.02		0.25	0.78	0.156	1.648	98.352
	0.15	3.9	0.78	2.76	97.24		0.15	3.2	0.64	2.288	97.712
	0.075	7.4	1.48	4.24	95.76		0.075	6	1.2	3.488	96.512
	Pan	478.8	95.76	100	0		Pan	482.56	96.512	100	0

SS= Sieve Size, MR= Mass Retained, %R= Percentage of Retained, %CR= Cumulative Percentage of Retained, %P= Percentage of Pass, g= gram, No. =Number

Table D1.2 Wet sieve analysis result of test pit 3 and 4

Pit	SS,	MR,	%	%	%	Pit	SS,	MR, (g)	% R	%	%
-----	-----	-----	---	---	---	-----	-----	---------	-----	---	---

(mm)	(g)	R	CR	P	(mm)			CR	P
9.5	0	0	0	100	9.5	0	0	0	100
4.75	1.08	0.215	0.215	99.785	4.75	0.476	0.095	0.095	99.905
2	3.34	0.667	0.882	99.118	2	0.618	0.124	0.219	99.781
0.85	3.71	0.741	1.624	98.376	0.85	0.656	0.131	0.350	99.650
0.425	3.5	0.700	2.324	97.676	0.425	1.176	0.235	0.585	99.415
0.25	1.64	0.327	2.651	97.349	0.25	0.918	0.184	0.769	99.231
0.15	2.81	0.562	3.213	96.787	0.15	1.78	0.356	1.125	98.875
0.075	5.14	1.028	4.240	95.760	0.075	3.483	0.697	1.821	98.179
Pan	478.8	95.760	100	0	Pan	490.893	98.179	100	0

Table D1.3 Wet sieve analysis result of test pit 5 and 6

	SS, (mm)	MR, (g)	% R	% CR	% P		SS, (mm)	MR, (g)	% R	% CR	% P
	Test Pit 5	9.5	0	0	0		100	Test Pit 6	9.5	0	0
	4.75	0	0	0	100		4.75	0	0	0	100
	2	0.08	0.016	0.016	99.984		2	0.114	0.023	0.023	99.977
	0.85	0.24	0.049	0.064	99.936		0.85	0.371	0.074	0.097	99.903
	0.425	0.84	0.167	0.231	99.769		0.425	0.759	0.152	0.249	99.751
	0.25	0.76	0.153	0.384	99.616		0.25	0.796	0.159	0.408	99.592
	0.15	1.76	0.352	0.736	99.264		0.15	1.607	0.321	0.729	99.271
	0.075	2.36	0.472	1.208	98.792		0.075	3.185	0.637	1.366	98.634
	Pan	493.96	98.792	100	0		Pan	493.168	98.6336	100	0

Table D1.3 Wet sieve analysis result of test pit 7 and 8

Test Pit 7	SS, (mm)	MR, (g)	% R	% CR	% P	Test Pit 8	SS, (mm)	MR, (g)	% R	% CR	% P
	9.5	0	0	0	100		9.5	0	0	0	100
	4.75	0.172	0.034	0.034	99.966		4.75	0.523	0.105	0.105	99.895
	2	0.14	0.028	0.062	99.938		2	1.233	0.247	0.351	99.649
	0.85	1.094	0.219	0.281	99.719		0.85	1.53	0.306	0.657	99.343
	0.425	1.703	0.341	0.622	99.378		0.425	1.78	0.356	1.013	98.987
	0.25	3.141	0.628	1.250	98.750		0.25	2.819	0.564	1.577	98.423
	0.15	3.291	0.658	1.908	98.092		0.15	3.421	0.684	2.261	97.739
	0.075	6.479	1.296	3.204	96.796		0.075	7.124	1.425	3.686	96.314
	Pan	483.9 8	96.79 6	100	0		Pan	481.57	96.314	100	0

Appendix D2: Hydrometer analysis result

Standard Test Method: ASTM D 854-00 Standard Method

Dispersing Agent: Sodium Metahexaphosphate

Hydrometer Number: 152H

$$R_{CP} = R + F_T - F_Z$$

$$F_T = -4.85 + 0.25 * T(^{\circ}C)$$

$$R_{CL} = R + F_m$$

$$L = 16.3 - 0.163 * R_{CL}$$

$$D (mm) = K \sqrt{\frac{L (cm)}{T (min)}}$$

$$P_F = \frac{R * a}{W_s} * 100$$

$$a = \frac{2.65 - 1}{2.65} * \frac{G_s}{G_s - 1}$$

$$P_{FC} = \frac{PF * \% \text{ Passing \#200}}{100}$$

Where:

R_{CP} : Corrected Hydrometer Reading

R : Actual Hydrometer Reading

F_T : Temperature correction

F_z : Zero correction

R_{CL} : Corrected reading for determination of effective Length (L)

F_m : Meniscus correction

L : Effective Length (cm) (Alternatively Refer Table E1)

D : Grain Size (mm)

K : Constant Coefficient as a function of Temperature, and Specific Gravity (Refer Table E1)

T (*min*) : Elapsed Time in minute

P_F : Percentage Finer (%)

a : Correction for Specific gravity as a function of specific gravity (Alternatively Refer Table E2)

G_s : Specific Gravity of soil

W_s : Mass of Dry Soil passing #200 Sieve (i.e., In This thesis $W_s = 50 \text{ g}$)

P_{FC} : Percentage Finer Combined (%)

$T(^{\circ}C)$: Temperature during the test

Table D2.1: Datasheet for Hydrometer analysis for Test Pit 1

Time,min	Temp. 0c	Rh	R _{cl}	R _{cp}	a	L	K	D(mm)	P _{fc}
0.5	23	55.5	56.5	50.2	0.976	7.0	0.0128	0.048	89.00
1	23	55	56	49.7	0.976	7.1	0.0128	0.034	88.11
2	23	54	55	48.7	0.976	7.3	0.0128	0.024	86.34
4	23	53	54	47.7	0.976	7.4	0.0128	0.017	84.57
8	23	51	52	45.7	0.976	7.8	0.0128	0.013	81.02
15	23	50	51	44.7	0.976	7.9	0.0128	0.009	79.25
30	23	48	49	42.7	0.976	8.3	0.0128	0.007	75.70
60	23	46	47	40.7	0.976	8.6	0.0128	0.005	72.16
120	23	45	46	39.7	0.976	8.8	0.0128	0.003	70.38
240	23	43	44	37.7	0.976	9.1	0.0128	0.002	66.84
480	23	42	43	36.7	0.976	9.2	0.0128	0.002	65.06
1440	23	40	41	34.7	0.976	9.6	0.0128	0.001	61.52

Table D2.2: Datasheet for Hydrometer analysis for Test Pit 2

time,min	temp. 0c	Rh	R _{cl}	R _{cp}	a	L(mm)	K	D(mm)	P _{fc}
0.5	23	56	57	50.7	0.991	6.9	0.0130	0.048	91.23
1	23	55	56	49.7	0.991	7.1	0.0130	0.035	89.43
2	23	54.5	55.5	49.2	0.991	7.2	0.0130	0.025	88.53
4	23	53	54	47.7	0.991	7.4	0.0130	0.018	85.83
8	23	51.5	52.5	46.2	0.991	7.7	0.0130	0.013	83.14
15	23	50	51	44.7	0.991	7.9	0.0130	0.009	80.44

30	23	49	50	43.7	0.991	8.1	0.0130	0.007	78.64
60	23	47	48	41.7	0.991	8.4	0.0130	0.005	75.04
120	23	45	46	39.7	0.991	8.8	0.0130	0.004	71.44
240	23	42.5	43.5	37.2	0.991	9.2	0.0130	0.003	66.94
480	23	41	42	35.7	0.991	9.4	0.0130	0.002	64.24
1440	23	39	40	33.7	0.991	9.7	0.0130	0.001	60.64

Table D2.3: Datasheet for Hydrometer analysis for Test Pit 3

time,min	temp. 0c	Rh	R _{cl}	R _{cp}	a	L(mm)	K	D(mm)	P _{fc}
0.5	23	54	55	48.7	0.982	7.3	0.0129	0.049	86.88
1	23	53.5	54.5	48.2	0.982	7.4	0.0129	0.035	85.99
2	23	52	53	46.7	0.982	7.6	0.0129	0.025	83.31
4	23	51	52	45.7	0.982	7.8	0.0129	0.018	81.53
8	23	49	50	43.7	0.982	8.1	0.0129	0.013	77.96
15	23	48	49	42.7	0.982	8.3	0.0129	0.010	76.18
30	23	47	48	41.7	0.982	8.4	0.0129	0.007	74.39
60	23	46	47	40.7	0.982	8.6	0.0129	0.005	72.61
120	23	44	45	38.7	0.982	8.9	0.0129	0.004	69.04
240	23	42.5	43.5	37.2	0.982	9.2	0.0129	0.003	66.36
480	23	40	41	34.7	0.982	9.6	0.0129	0.002	61.90
1440	23	38	39	32.7	0.982	9.9	0.0129	0.001	58.34

Table D2.4: Datasheet for Hydrometer analysis for Test Pit 4

time,min	temp. 0c	Rh	R _{cl}	R _{cp}	a	L(mm)	K	D(mm)	P _{fc}
1	23	54	55	48.7	0.978	7.3	0.0128	0.034	86.52
2	23	53	54	47.7	0.978	7.4	0.0128	0.025	84.74
4	23	52	53	46.7	0.978	7.6	0.0128	0.018	82.96
8	23	51.5	52.5	46.2	0.978	7.7	0.0128	0.013	82.08

15	23	50.5	51.5	45.2	0.978	7.8	0.0128	0.009	80.30
30	23	49.5	50.5	44.2	0.978	8.0	0.0128	0.007	78.52
60	23	48	49	42.7	0.978	8.3	0.0128	0.005	75.86
120	23	46	47	40.7	0.978	8.6	0.0128	0.003	72.30
240	23	44	45	38.7	0.978	8.9	0.0128	0.002	68.75
480	23	42.5	43.5	37.2	0.978	9.2	0.0128	0.002	66.09
1440	23	40	41	34.7	0.978	9.6	0.0128	0.001	61.65

Table D2.5: Datasheet for Hydrometer analysis for Test Pit 5

Time,min	temp. 0c	Rh	R _{cl}	R _{cp}	a	L(mm)	K	D(mm)	P _{fc}
1	23	56	57	50.7	0.980	6.9	0.0128	0.034	90.26
2	23	55	56	49.7	0.980	7.1	0.0128	0.024	88.48
4	23	54	55	48.7	0.980	7.3	0.0128	0.017	86.70
8	23	53	54	47.7	0.980	7.4	0.0128	0.012	84.92
15	23	52.5	53.5	47.2	0.980	7.5	0.0128	0.009	84.03
30	23	51.5	52.5	46.2	0.980	7.7	0.0128	0.006	82.25
60	23	49	50	43.7	0.980	8.1	0.0128	0.005	77.80
120	23	48	49	42.7	0.980	8.3	0.0128	0.003	76.02
240	23	46	47	40.7	0.980	8.6	0.0128	0.002	72.46
480	23	44	45	38.7	0.980	8.9	0.0128	0.002	68.90
1440	23	43	44	37.7	0.980	9.1	0.0128	0.001	67.12

Table D2.6: Datasheet for Hydrometer analysis for Test Pit 6

Time,min	temp. 0c	Rh	R _{cl}	R _{cp}	a	L(mm)	K	D(mm)	P _{fc}
1	23	57.5	58.5	52.2	0.976	6.7	0.0128	0.033	92.54
2	23	56.5	57.5	51.2	0.976	6.9	0.0128	0.024	90.77
4	23	55.5	56.5	50.2	0.976	7.0	0.0128	0.017	89.00
8	23	54.5	55.5	49.2	0.976	7.2	0.0128	0.012	87.22
15	23	53	54	47.7	0.976	7.4	0.0128	0.009	84.57
30	23	52	53	46.7	0.976	7.6	0.0128	0.006	82.79
60	23	51	52	45.7	0.976	7.8	0.0128	0.005	81.02
120	23	50	51	44.7	0.976	7.9	0.0128	0.003	79.25
240	23	47.5	48.5	42.2	0.976	8.3	0.0128	0.002	74.81
480	23	45	46	39.7	0.976	8.8	0.0128	0.002	70.38
1440	23	43.5	44.5	38.2	0.976	9.0	0.0128	0.001	67.72

Table D2.7: Datasheet for Hydrometer analysis for Test Pit 7

Time,min	temp. 0c	Rh	R _{cl}	R _{cp}	a	L(mm)	K	D(mm)	P _{fc}
1	23	54	55	48.7	0.989	7.3	0.0130	0.035	87.44
2	23	53	54	47.7	0.989	7.4	0.0130	0.025	85.65
4	23	51.5	52.5	46.2	0.989	7.7	0.0130	0.018	82.95
8	23	50.5	51.5	45.2	0.989	7.8	0.0130	0.013	81.16
15	23	49	50	43.7	0.989	8.1	0.0130	0.010	78.46
30	23	47	48	41.7	0.989	8.4	0.0130	0.007	74.87
60	23	45	46	39.7	0.989	8.8	0.0130	0.005	71.28
120	23	44	45	38.7	0.989	8.9	0.0130	0.004	69.49
240	23	43	44	37.7	0.989	9.1	0.0130	0.003	67.69
480	23	41	42	35.7	0.989	9.4	0.0130	0.002	64.10
1440	23	39	40	33.7	0.989	9.7	0.0130	0.001	60.51

Table D2.8: Datasheet for Hydrometer analysis for Test Pit 8

Time,min	temp. 0c	Rh	R _{cl}	R _{cp}	a	L(mm)	K	D(mm)	P _{fc}
1	23	55	56	49.7	0.987	7.1	0.0129	0.034	89.04
2	23	54	55	48.7	0.987	7.3	0.0129	0.025	87.25
4	23	53	54	47.7	0.987	7.4	0.0129	0.018	85.46
8	23	52	53	46.7	0.987	7.6	0.0129	0.013	83.67
15	23	51	52	45.7	0.987	7.8	0.0129	0.009	81.88
30	23	50.5	51.5	45.2	0.987	7.8	0.0129	0.007	80.98
60	23	49.5	50.5	44.2	0.987	8.0	0.0129	0.005	79.19
120	23	47	48	41.7	0.987	8.4	0.0129	0.003	74.71
240	23	44.5	45.5	39.2	0.987	8.8	0.0129	0.002	70.23
480	23	43	44	37.7	0.987	9.1	0.0129	0.002	67.54
1440	23	41	42	35.7	0.987	9.4	0.0129	0.001	63.96

Appendix E: Filter paper method of suction measurement result data

Formula used

For $w_{c_{fp}} > 45.3\%$: $\log_{10}s = 5.336 - 0.0779w_{c_{fp}}$

For $w_{c_{fp}} < 45.3\%$: $\log_{10} s = 2.142 - 0.032w_{c_{fp}}$

$w_{c_{fp}}$ = water content of filter paper in %

S = matric suction in kpa

$$w_{sat} = \frac{M_{sat} (1 + w_n)}{M_m} - 1$$

$$w_i = \frac{M_w}{M_s}$$

Where:

w_{sat} : Saturated gravimetric moisture content

M_{sat} : Mass of saturated soil (i.e., ring + soil after sat - weight of ring)

M_m : Mass of moist soil (i.e., ring + soil before sat - weight of ring)

w_n : Natural moisture content

w_i : Gravimetric moisture content corresponding to i^{th} suction

M_s : Mass of dry soil (Dry weight of soil)

M_w : Mass of water (i.e., soil after equilibrium - M_s)

Table E1: data sheet of filter paper result for test pit 1

matric suction measurement							
Trial sample		T1	T2	T3	T4	T5	T6
moisture tin no		P67	A3	K1-2	A-1C	H2	CK
Percent water added to the sample		8	AD	AD	2	AD	4
cold tare mass	Tc	35.52	17.536	23.514	49.656	25.731	18.176
mass of wet filter paper+ cold tare mass	M1	35.761	17.725	23.718	49.846	25.901	18.398
mass dry filter paper + hot	M2	35.661	17.653	23.67	49.793	25.854	18.283

tar mass							
hot tar mass	Th	35.512	17.508	23.52	49.645	25.72	18.125
mass of dry filter paper	Mf	0.149	0.145	0.15	0.148	0.134	0.158
mass of water in filter paper	Mw	0.092	0.044	0.054	0.042	0.036	0.064
water content of filter paper	Wf	0.6174	0.30344	0.36	0.28378	0.26865	0.40506
suction,pF	h	1.578	2.963	2.523	3.116	3.234	2.172
suction,kpa	h	37.883	918.624	333.11	1307.14	1714.60	148.442
water content of soil sample	wi	43.21	25.91	30.63	24.35	23.45	35.51
Saturated water content	wsatu	45.76					
	Mass of moist soil	Natural moisture content		Mass of saturated soil		Saturated moisture content (Wsat)	
	134.577	40.5		139.61		45.76	

Table E2: data sheet of filter paper result for test pit 2

matric suction measurement							
Trial sample		T1	T2	T3	T4	T5	T6
moisture tin no		4y	A3	F	P4	K1	F4
Percent of water added to the sample (%)		8	AD	4	AD	2	AD
cold tare mass	Tc	9.839	17.541	36.476	23.657	24.155	18.194
mass of wet filter paper+ cold tare mass	M1	10.072	17.719	36.68	23.849	24.356	18.381
mass dry filter paper + hot tar mass	M2	9.975	17.668	36.609	23.797	24.293	18.269
hot tar mass	Th	9.827	17.531	36.463	23.646	24.142	18.12
mass of dry filter paper	Mf	0.148	0.137	0.146	0.151	0.151	0.149

mass of water in filter paper	Mw	0.085	0.041	0.058	0.041	0.05	0.038
water content of filter paper	Wf	0.57432	0.2992	0.3972	0.27152	0.33112	0.25503
suction ,pF	h	1.637	2.996	2.232	3.212	2.748	3.340
suction,kpa	h	43.317	990.11	170.74	1628.67	559.152	2189.21
water content of the sampe	wi	42.56	25.62	33.85	23.62	28.25	22.43
Saturated water content wsatu	45.95						
	Mass of moist soil	Natural moisture content		Mass of saturated soil	Saturated moisture content (Wsat)		
	167.703	38.33		176.94	45.95		

Table E3: data sheet of filter paper result for test pit 3

matric suction measurement							
Trial sample		T1	T2	T3	T4	T5	T6
moisture tin no		P67	4	2	P2	A3	P4
Percent of water added to the sample		8	4	2	AD	AD	AD
cold tare mass	Tc	35.92	36.639	18.38	17.455	17.536	21.236
mass of wet filter paper+ cold tare mass	M1	36.175	37.015	18.565	17.633	17.728	21.427
mass dry filter paper + hot tar mass	M2	35.667	36.9	18.509	17.585	17.676	21.355
hot tar mass	Th	35.515	36.633	18.369	17.447	17.525	21.203
mass of dry filter paper	Mf	0.152	0.267	0.14	0.138	0.151	0.152
mass of water in filter paper	Mw	0.103	0.109	0.045	0.04	0.041	0.039
water content of filter paper	Wf	0.6776	0.4082	0.3214	0.2898	0.2715	0.2565
suction,pF	h	1.497	2.147	2.823	3.069	3.212	3.328
sction,kpa	h	31.419	140.22	665.38	1172.2	1628.6	2129.3

water content of soil sample	wi	48.01	38.44	28.06	25.07	23.68	22.12
Saturated water content	wsat	51.86					
	Mass of moist soil	Natural moisture content		Mass of saturated soil	Saturated moisture content (Wsat)		
	128.79	36.04		143.766	51.86		

Table E4: data sheet of filter paper result for test pit 4

matric suction measurement							
Trial sample		T1	T2	T3	T4	T5	T6
moisture tin no		P1/N2	C14/SSB1	H	F2/N3	P2/N2	A7
Percent of water added to the sample(%)		4	8	2	AD	AD	AD
cold tare mass	Tc	23.54	24.008	17.5	23.557	25.155	24.537
mass of wet filter paper+ cold tare mass	M1	23.756	24.241	17.699	23.737	25.342	24.732
mass dry filter paper + hot tar mass	M2	23.678	24.142	17.644	23.693	25.289	24.622
hot tar mass	Th	23.523	23.998	17.494	23.55	25.142	24.471
mass of dry filter paper	Mf	0.155	0.144	0.15	0.143	0.147	0.151
mass of water in filter paper	Mw	0.061	0.089	0.049	0.037	0.04	0.044
water content of filter paper	Wf	0.3935	0.61805	0.3267	0.2587	0.2721	0.29139
suction,pF	h	2.261	1.578	2.782	3.311	3.207	3.057
suction,kpa	h	182.498	37.812	605.71	2048.35	1611.65	1140.42
water content of the sample	wi	34.25	44.17	27.67	22.05	23.19	24.72
Saturated water content	wsatu	47.45					
	Mass of moist soil	Natural moisture content		Mass of	Saturated moisture		

			saturated soil	content (W _{sat})
	137.041	39.56	144.788	47.45

Table E5: data sheet of filter paper result for test pit 5

MATRIC suction measurement							
Trial sample		T1	T2	T3	T4	T5	T6
moisture tin no		A-13	TP3	29	[2]	B2	B1-K
Percent of water added to the sample		8	4	AD	2	AD	AD
cold tare mass	Tc	36.533	17.509	17.431	18.351	24.431	20.724
mass of wet filter paper+ cold tare mass	M1	37.001	17.774	17.609	18.551	24.616	20.913
mass dry filter paper + hot tar mass	M2	36.797	17.685	17.566	18.495	24.564	20.852
hot tar mass	Th	36.522	17.499	17.424	18.344	24.42	20.703
mass of dry filter paper	Mf	0.275	0.186	0.142	0.151	0.144	0.149
mass of water in filter paper	Mw	0.193	0.079	0.036	0.049	0.041	0.04
water content of filter paper	Wf	0.70181	0.42473	0.25352	0.32450	0.28472	0.26845
suction, pF	hf	1.465	2.018	3.352	2.799	3.109	3.236
suction, kpa	h	29.144	104.314	2249.41	629.679	1285.32	1720.77
water content of the sample	wi	48.18	40.56	21.17	27.81	24.13	22.46
Saturated water content	wsatu	53.02					
	Mass of moist soil	Natural moisture content		Mass of saturated soil		Saturated moisture content (W _{sat})	
	123.64	35.44		139.688		53.02	

Table E6: data sheet of filter paper result for test pit 6

Matric suction measurement							
Trial sample		T1	T2	T3	T4	T5	T6
moisture tin no		P2	J41	B	2R	W22	CK
Percent of water added to the sample		8	AD	AD	AD	2	4
cold tare mass	Tc	17.455	32.716	31.394	18.375	21.347	33.805
mass of wet filter paper+ cold tare mass	M1	17.711	32.891	31.581	18.553	21.546	34.021
mass dry filter paper + hot tar mass	M2	17.599	32.846	31.533	18.509	21.488	33.939
hot tar mass	Th	17.447	32.71	31.384	18.368	21.338	33.786
mass of dry filter paper	Mf	0.152	0.136	0.149	0.141	0.15	0.153
mass of water in filter paper	Mw	0.104	0.039	0.038	0.037	0.049	0.063
water content of filter paper	Wf	0.6842	0.2867	0.2550	0.26241	0.32666	0.41176
suction,pF	hf	1.488	3.093	3.340	3.283	2.782	2.119
suction,pF	h	30.783	1239.09	2189.21	1917.85	605.713	131.629
water content of soil sample	wi	48.82	24.22	21.54	22.02	28.02	38.97
Saturated water content	wsatu	52.82					
	Mass of moist soil	Natural moisture content		Mass of saturated soil	Saturated moisture content (Wsat)		
	129.57	39.43		142.01	52.82		

Table E7: data sheet of filter paper result for test pit 7

matric suction measurement							
----------------------------	--	--	--	--	--	--	--

Trial sample code		T1	T2	T3	T4	T5	T6
moisture tin no		E-11	SSB1	S2	K24	W80	PP
Percent of water add to the sample		AD	2	4	AD	AD	8
cold tare mass	Tc	36.671	24.009	25.156	22.715	18.284	21.736
mass of wet filter paper+ cold tare mass	M1	36.849	24.213	25.37	22.894	18.476	21.983
mass dry filter paper + hot tar mass	M2	36.782	24.149	25.297	22.845	18.417	21.877
hot tar mass	Th	36.642	23.996	25.144	22.703	18.269	21.726
mass of dry filter paper	Mf	0.14	0.153	0.153	0.142	0.148	0.151
mass of water in filter paper	Mw	0.038	0.051	0.061	0.037	0.044	0.096
water content of filter paper	Wf	0.2714 2	0.3333	0.3986	0.2605 6	0.2972 9	0.6357
suction,pF	h	3.213	2.730	2.221	3.297	3.011	1.554
suction,kpa	h	1631.4 4	537.44 4	166.41 1	1982.4 9	1025.7 8	35.787
water content of soil sample	wi	23.49	28.71	35.59	22.57	25.73	46.01
Saturated water content	wsat	49.25					
	Mass of moist soil	Natural moisture content		Mass of saturated soil		Saturated moisture content (Wsat)	
	141.44	43.08		147.539		49.25	

Table E8: data sheet of filter paper result for test pit 8

matric suction mesearment							
Trial sample code		T1	T2	T3	T4	T5	T6
moisture tin no		12	D	LOO	B	K12	CP2
Percent of water added to the sample		8	AD	4	AD	2	AD

cold tare mass	Tc	41.319	29.718	17.692	31.394	23.578	26.113
mass of wet filter paper+ cold tare mass	M1	41.547	29.901	17.894	31.57	23.769	26.328
mass dry filter paper + hot tar mass	M2	41.443	29.848	17.833	31.522	23.701	26.248
hot tar mass	Th	41.299	29.703	17.683	31.384	23.554	26.096
mass of dry filter paper	Mf	0.144	0.145	0.15	0.138	0.147	0.152
mass of water in filter paper	Mw	0.084	0.038	0.052	0.038	0.044	0.063
water content of filter paper	Wf	0.5833 3	0.26206	0.34666	0.27536	0.2993	0.41447
sucion.pF		1.625	3.285	2.626	3.182	2.995	2.098
suction,kpa	h	42.121	1929.66	423.123	1520.29	989.23	125.386
water content of soil sample	wi	42.03	22.57	29.53	23.44	25.56	36.18
Saturated water content	wsat	47.889					
	Mass of moist soil	Natural moisture content		Mass of saturated soil	Saturated moisture content (Wsat)		
	153.28	41.79		159.87	47.89		

Appendix F: MATLAB[®] 2019a fmincon script for optimization of curve fitting parameters

```

%%%%%%%%%%%%%%%%%%%%%%%%%%%%%%%%%%%%%%%%%%%%%%%%%%%%%%%%%%%%%%%%%%%%%%%%
%%%%%%%%%%%%%%%%%%%%%%%%%%%%%%%%%%%%%%%%%%%%%%%%%%%%%%%%%%%%%%%%%%%%%%%%
%
% Author: Tenaye Zeberga
% Script: fmincon
% Use: Optimize the Model fitting parameters
%%%%%%%%%%%%%%%%%%%%%%%%%%%%%%%%%%%%%%%%%%%%%%%%%%%%%%%%%%%%%%%%%%%%%%%%
%%%%%%%%%%%%%%%%%%%%%%%%%%%%%%%%%%%%%%%%%%%%%%%%%%%%%%%%%%%%%%%%%%%%%%%%
    
```

```

% clear session, close plots, clear screen
close all; clc
% Data for regression. psi represent the measured suction, and
% Gravimetric_WC_M is the Measured gravimetric water content
psi = [
43.32
170.74
559.15
990.12
1628.68
2189
];
Gravimetric_WC_M = [
42.56
33.85
28.25
25.62
23.62
22.43
];
W_sat=45.95; % Saturated gravimetric water content
% Set initial guess value for the Freduland & Xing (1994) model parameters
dimension, and Load guess values into array
% xo = [Psi_r a n m ws]= [x(1) x(2) x(3) x(4) x(5)]
xo = [1.5e3 1 1 1 W_sat];
% Define prediction function [i.e Freduland & Xing (1994) Model]
% Gravimetric_WC_P is the predicted Gravimetric water content using fmincon
Gravimetric_WC_P = @(x) (1-
((log(1+(psi./x(1)))) ./ (log(1+(1000000./x(1)))))) .* ((x(5) ./ (((log(exp(1)+(ps
i./x(2)).^x(3))).^x(4))))));

% Define Objective function for optimization. [Root Mean Square Error (RMSE)
is selected as
% objective function]. fmincon attempt to minimize the RMSE, and gives the
% optimized parameter which gives lower RMSE
objective = @(x) sqrt(sum((((Gravimetric_WC_P(x)-
Gravimetric_WC_M)).^2) ./ (length(Gravimetric_WC_M)-length(xo)+2))));
disp(['Initial Objective: ' num2str(objective(xo))])

% optimize with fmincon
% [X, FVAL, EXITFLAG, OUTPUT, LAMBDA, GRAD, HESSIAN]
% = fmincon(FUN, X0, A, B, Aeq, Beq, LB, UB, NONLCON, OPTIONS)
A = [];
b = [];
Aeq = [];
beq = [];
% Bounds. fmincon try an iteration within lower bound (lb), and upper bound
(ub)
lb = [1e0 1 0.1 0.1 W_sat];
ub = [1e6 1e4 20 20 W_sat];
% Define optimization options
options = optimset('TolX',1e-12, 'TolCon',1e-12, 'TolFun',1e-
12, 'Algorithm', 'interior-point');
% options = optimset('TolX',1e-12, 'TolCon',1e-12, 'TolFun',1e-
12, 'MaxFun',3e5, 'MaxIte',1e6, 'Algorithm', 'interior-point', 'Display', 'iter');

```

```
%options = optimset('Display','off'); % Turn off Display

% Load solver (i.e. fmincon) to minimize the objective function given the
constraint
xopt = round(fmincon(objective,xo,A,b,Aeq,beq,lb,ub,[],options),2);
%SSE Sum of Square Error
SSE=sum(((Gravimetric_WC_P(xopt)-Gravimetric_WC_M).^2);
%for FX (1994) model the no. of parameters are 4

%Compute Akaike information criteria (AIC)
N=length(Gravimetric_WC_M);
AIC=(N.*log10(SSE./N))+(2.*(length(xopt)-1));% saturated water content is not
fitting parameter (-1)

% SST Total Sum of Square
SST=sum((Gravimetric_WC_M-
((sum(Gravimetric_WC_M))./length(Gravimetric_WC_M)).^2);
% R Squared =1-(SSE/SST)
R_Squared=(1-(SSE./SST));
% print results
disp(['R Squared: ' num2str(R_Squared)])
disp(['Final Objective: ' num2str(objective(xopt))])
disp(['AIC: ' num2str(AIC)])
disp(['Optimal parameters: ' num2str(xopt)])

psi_Extendend=0.1:1:1e6; % Start:Increment:End;
Gravimetric_WC_Extended = (1-
((log(1+(psi_Extendend./xopt(1)))) ./ (log(1+(1000000./xopt(1)))))).*(xopt(5)./
(log(exp(1)+((psi_Extendend./xopt(2)).^xopt(3)).^xopt(4))));
% plot results
semilogx(psi,Gravimetric_WC_M,'ks','linewidth',5) % black(k) Square(s) marker
hold on
%semilogx(psi,Gravimetric_WC_P(xopt),'k-','linewidth',2) % This will give
the same effect as psi_Extended vs Gravimetric_WC_Extended
semilogx(psi_Extendend,Gravimetric_WC_Extended,'k-','linewidth',2)
legend('Measured data point','Best fitt line (Optimal
predicted)','Location','northeast','FontSize',16,'FontName','times new
roman','lineWidth',0.1,'Color','[1 1 1]')
ylabel('Gravimetric water content (%)','FontSize',20,'FontName','times new
roman')
xlabel('Suction \psi (kPa)','FontSize',20,'FontName','times new roman')
grid on
% Add text in to matlab plot (Optimized Parameters for The Freduland & Xing
(1994) Model parameters)
messageBLine = sprintf(['\psi_{r} = ' num2str(xopt(1)) ' kPa' '\n' 'a_{f} = '
' num2str(xopt(2)) ' kPa' '\n' 'n_{f} = ' num2str(xopt(3)) ' '\n' 'm_{f} = '
num2str(xopt(4)) ' '\n' 'w_{s} = ' num2str(xopt(5)) ' %' '\n' 'RMSE = '
num2str(objective(xopt)) ' '\n' 'R^{2} = ' num2str(R_Squared) ']);
text(1,(max(Gravimetric_WC_M)-15),messageBLine,'BackgroundColor','[1 1
1]','FontSize',16,'FontName','times new roman','FontAngle','italic')

ax = gca;
ax.GridColor = [0 0 0];
ax.GridLineStyle = '-';
```

```

ax.GridAlpha = 1;
ax.Layer = 'bottom';
ax.LineWidth=1;
%%%%
ax.MinorGridColor = [0 0 0];
ax.MinorGridLineStyle = '-';
ax.MinorGridAlpha = 1;
% Increase the size of x & y axis
ax.XAxis.FontSize = 20;
ax.XAxis.FontName = 'times new roman';
ax.YAxis.FontSize = 20;
ax.XAxis.FontWeight = 'normal'; % normal or bold
ax.YAxis.FontName = 'times new roman';
% to change the exponential
xticks([0.1 1 10 100 1000 10000 100000 1000000])
xticklabels({'0.1', '1', '10', '100', '1000', '10000', '100000', '1000000'})
    
```

Appendix G. JMP® Pro 14 outputs

Appendix G1. Multivariate Analysis

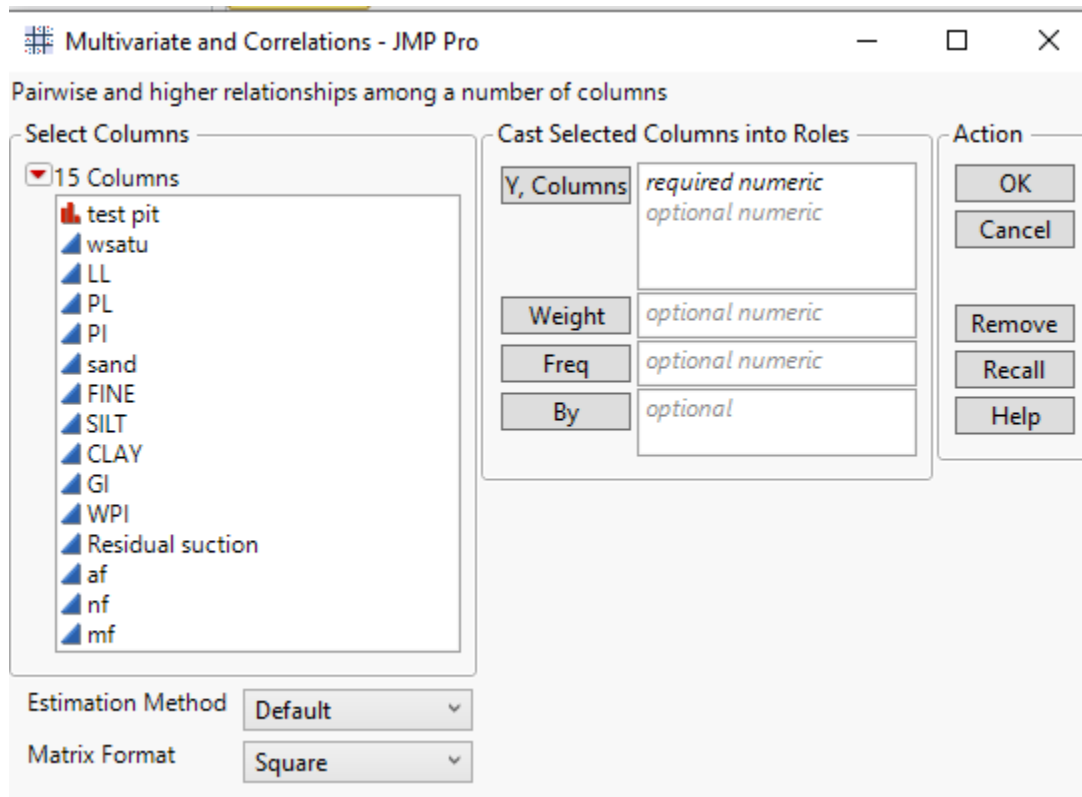


Figure G1.1. Multivariate analysis

Table G1.1: Correlation matrix of af with the predictor variables

	af	LL	PL	PI	sand	FINE	SILT	CLAY	GI	WPI
af	1.0000	0.9381	0.6670	0.9866	-0.9206	0.9297	-0.4918	0.7425	0.9903	0.9906
LL	0.9381	1.0000	0.8715	0.9400	-0.9201	0.9216	-0.6333	0.8542	0.9483	0.9490
PL	0.6670	0.8715	1.0000	0.6519	-0.7752	0.7584	-0.6224	0.7931	0.6724	0.6742
PI	0.9866	0.9400	0.6519	1.0000	-0.8835	0.8974	-0.5464	0.7692	0.9986	0.9983
sand	-0.9206	-0.9201	-0.7752	-0.8835	1.0000	-0.9985	0.4874	-0.7841	-0.9068	-0.9089
FINE	0.9297	0.9216	0.7584	0.8974	-0.9985	1.0000	-0.4936	0.7894	0.9191	0.9211
SILT	-0.4918	-0.6333	-0.6224	-0.5464	0.4874	-0.4936	1.0000	-0.9202	-0.5480	-0.5475
CLAY	0.7425	0.8542	0.7931	0.7692	-0.7841	0.7894	-0.9202	1.0000	0.7810	0.7816
GI	0.9903	0.9483	0.6724	0.9986	-0.9068	0.9191	-0.5480	0.7810	1.0000	1.0000
WPI	0.9906	0.9490	0.6742	0.9983	-0.9089	0.9211	-0.5475	0.7816	1.0000	1.0000

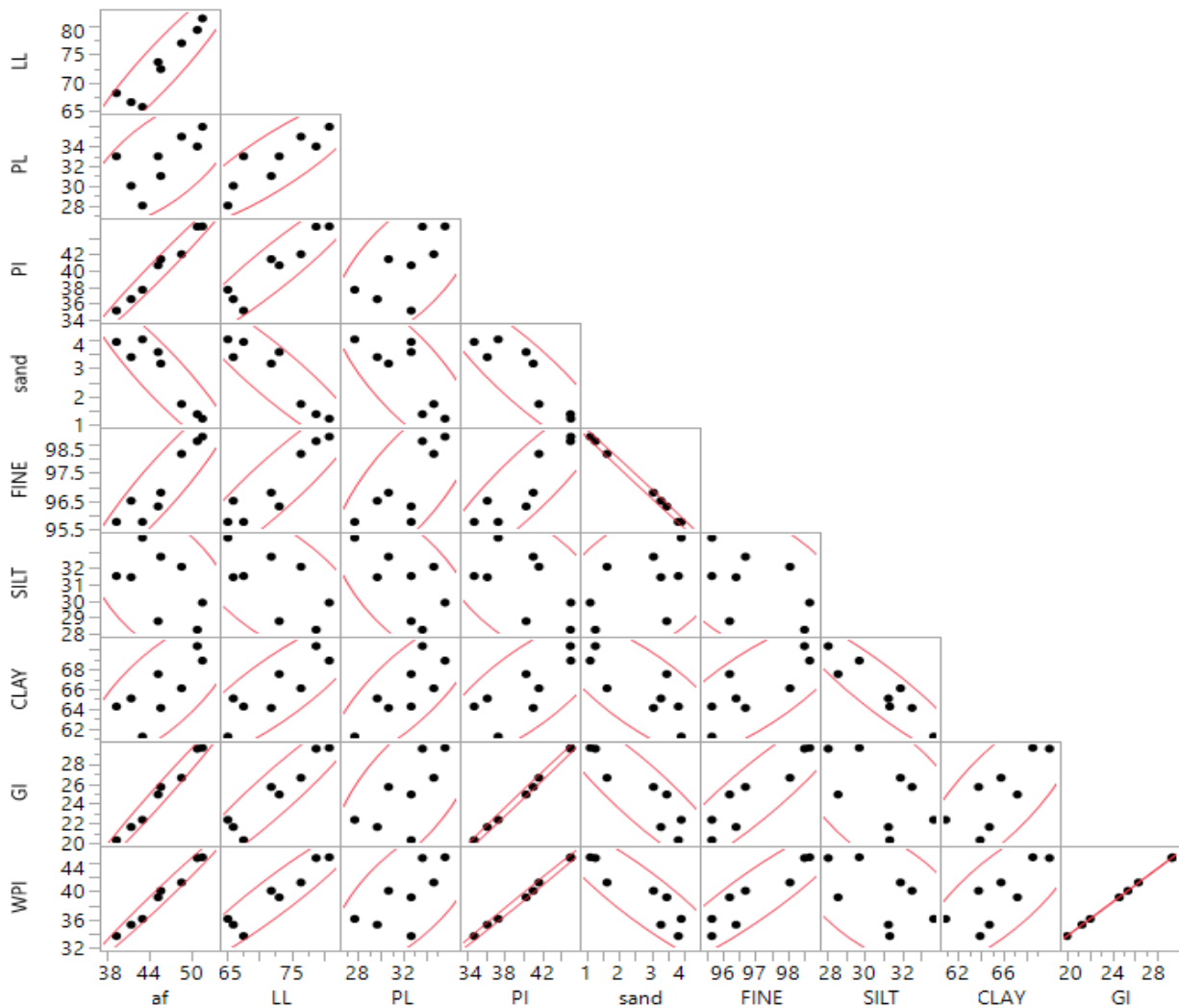


Figure G1.2: Scatter plot of af with predictor variables

Table G1.3 Correlation matrix of residual suction with predictor variables

	Residual suction	LL	PL	PI	sand	FINE	SILT	CLAY	GI	WPI
Residual suction	1.0000	0.9639	0.7513	0.9678	-0.8917	0.9010	-0.5786	0.7984	0.9712	0.9711
LL	0.9639	1.0000	0.8715	0.9400	-0.9201	0.9216	-0.6333	0.8542	0.9483	0.9490
PL	0.7513	0.8715	1.0000	0.6519	-0.7752	0.7584	-0.6224	0.7931	0.6724	0.6742
PI	0.9678	0.9400	0.6519	1.0000	-0.8835	0.8974	-0.5464	0.7692	0.9986	0.9983
sand	-0.8917	-0.9201	-0.7752	-0.8835	1.0000	-0.9985	0.4874	-0.7841	-0.9068	-0.9089
FINE	0.9010	0.9216	0.7584	0.8974	-0.9985	1.0000	-0.4936	0.7894	0.9191	0.9211
SILT	-0.5786	-0.6333	-0.6224	-0.5464	0.4874	-0.4936	1.0000	-0.9202	-0.5480	-0.5475
CLAY	0.7984	0.8542	0.7931	0.7692	-0.7841	0.7894	-0.9202	1.0000	0.7810	0.7816
GI	0.9712	0.9483	0.6724	0.9986	-0.9068	0.9191	-0.5480	0.7810	1.0000	1.0000
WPI	0.9711	0.9490	0.6742	0.9983	-0.9089	0.9211	-0.5475	0.7816	1.0000	1.0000

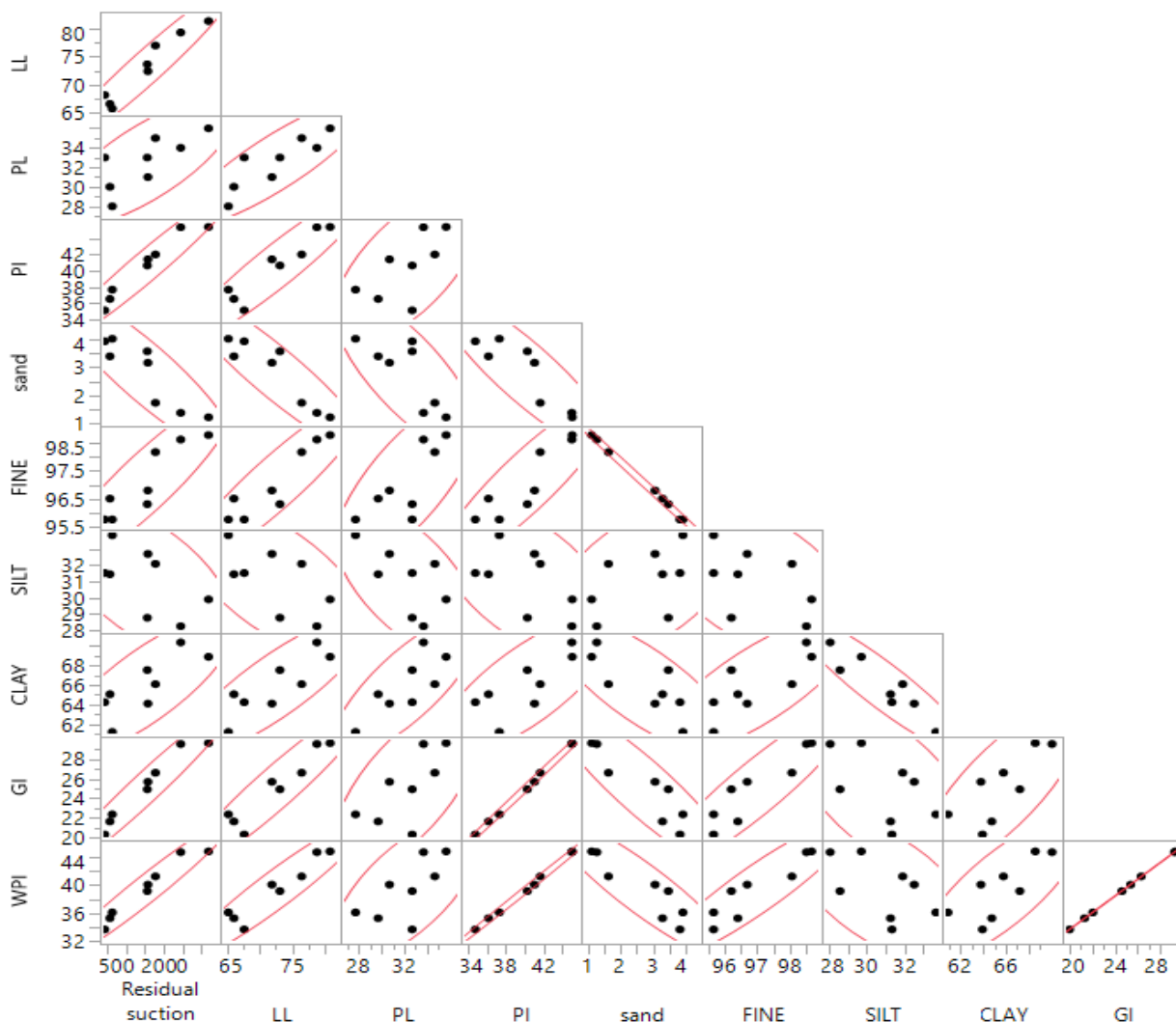


Figure G1.3 scatter plot for residual suction

Table G1.4: Correlation matrix for nf

	nf	LL	PL	PI	sand	FINE	SILT	CLAY	GI	WPI
nf	1.0000	-0.7056	-0.4276	-0.7935	0.8637	-0.8781	0.2574	-0.5568	-0.8105	-0.8123
LL	-0.7056	1.0000	0.8715	0.9400	-0.9201	0.9216	-0.6333	0.8542	0.9483	0.9490
PL	-0.4276	0.8715	1.0000	0.6519	-0.7752	0.7584	-0.6224	0.7931	0.6724	0.6742
PI	-0.7935	0.9400	0.6519	1.0000	-0.8835	0.8974	-0.5464	0.7692	0.9986	0.9983
sand	0.8637	-0.9201	-0.7752	-0.8835	1.0000	-0.9985	0.4874	-0.7841	-0.9068	-0.9089
FINE	-0.8781	0.9216	0.7584	0.8974	-0.9985	1.0000	-0.4936	0.7894	0.9191	0.9211
SILT	0.2574	-0.6333	-0.6224	-0.5464	0.4874	-0.4936	1.0000	-0.9202	-0.5480	-0.5475
CLAY	-0.5568	0.8542	0.7931	0.7692	-0.7841	0.7894	-0.9202	1.0000	0.7810	0.7816
GI	-0.8105	0.9483	0.6724	0.9986	-0.9068	0.9191	-0.5480	0.7810	1.0000	1.0000
WPI	-0.8123	0.9490	0.6742	0.9983	-0.9089	0.9211	-0.5475	0.7816	1.0000	1.0000

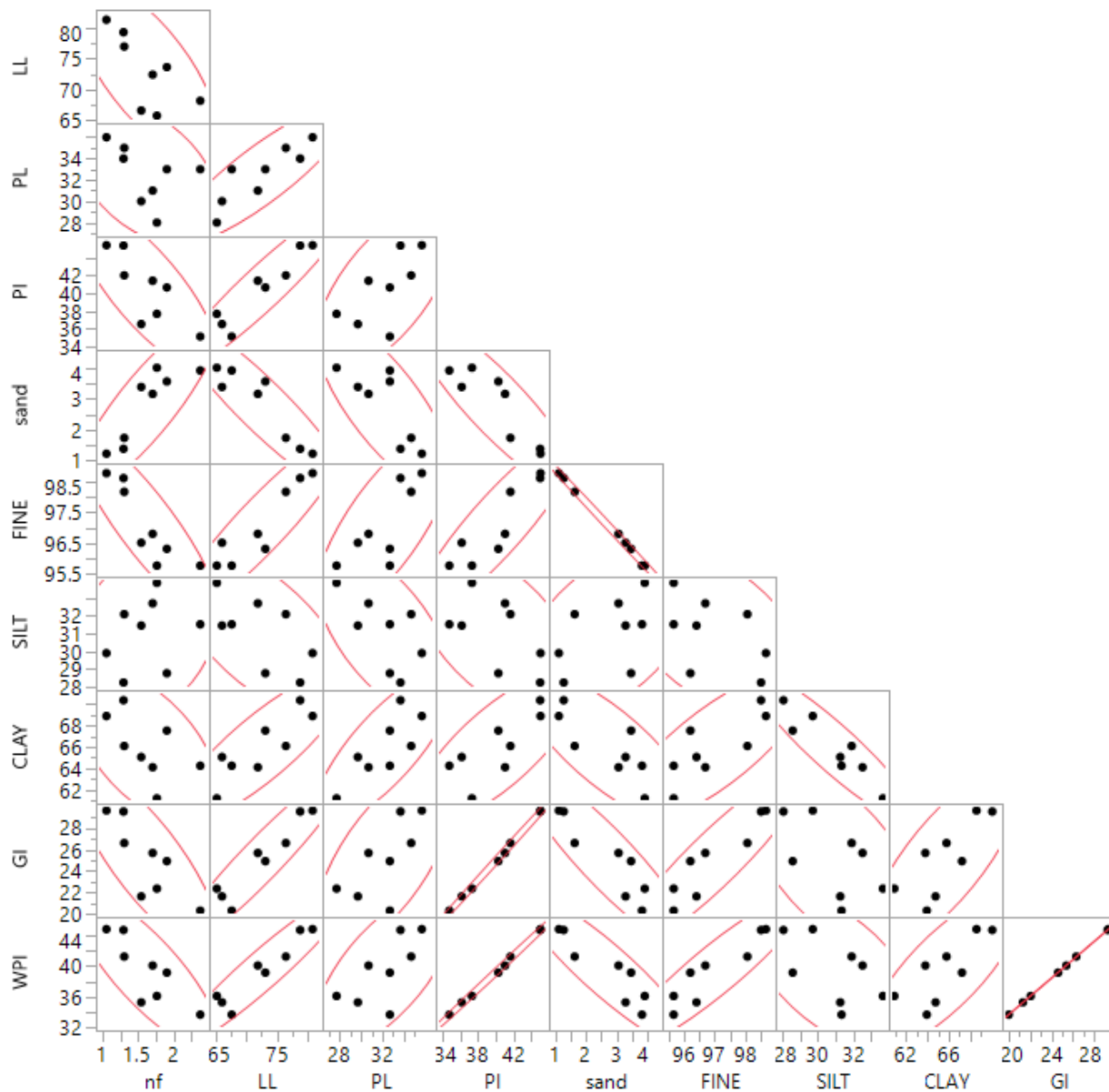


Figure G1.4 Scatter plot for nf

Table G1.5: Correlation matrix of mf

	mf	LL	PL	PI	sand	FINE	SILT	CLAY	GI	WPI
mf	1.0000	0.9184	0.6914	0.9392	-0.9571	0.9615	-0.4476	0.7275	0.9526	0.9535
LL	0.9184	1.0000	0.8715	0.9400	-0.9201	0.9216	-0.6333	0.8542	0.9483	0.9490
PL	0.6914	0.8715	1.0000	0.6519	-0.7752	0.7584	-0.6224	0.7931	0.6724	0.6742
PI	0.9392	0.9400	0.6519	1.0000	-0.8835	0.8974	-0.5464	0.7692	0.9986	0.9983
sand	-0.9571	-0.9201	-0.7752	-0.8835	1.0000	-0.9985	0.4874	-0.7841	-0.9068	-0.9089
FINE	0.9615	0.9216	0.7584	0.8974	-0.9985	1.0000	-0.4936	0.7894	0.9191	0.9211

	mf	LL	PL	PI	sand	FINE	SILT	CLAY	GI	WPI
SILT	-0.4476	-0.6333	-0.6224	-0.5464	0.4874	-0.4936	1.0000	-0.9202	-0.5480	-0.5475
CLAY	0.7275	0.8542	0.7931	0.7692	-0.7841	0.7894	-0.9202	1.0000	0.7810	0.7816
Y										
GI	0.9526	0.9483	0.6724	0.9986	-0.9068	0.9191	-0.5480	0.7810	1.0000	1.0000
WPI	0.9535	0.9490	0.6742	0.9983	-0.9089	0.9211	-0.5475	0.7816	1.0000	1.0000

Scatter plot of mf

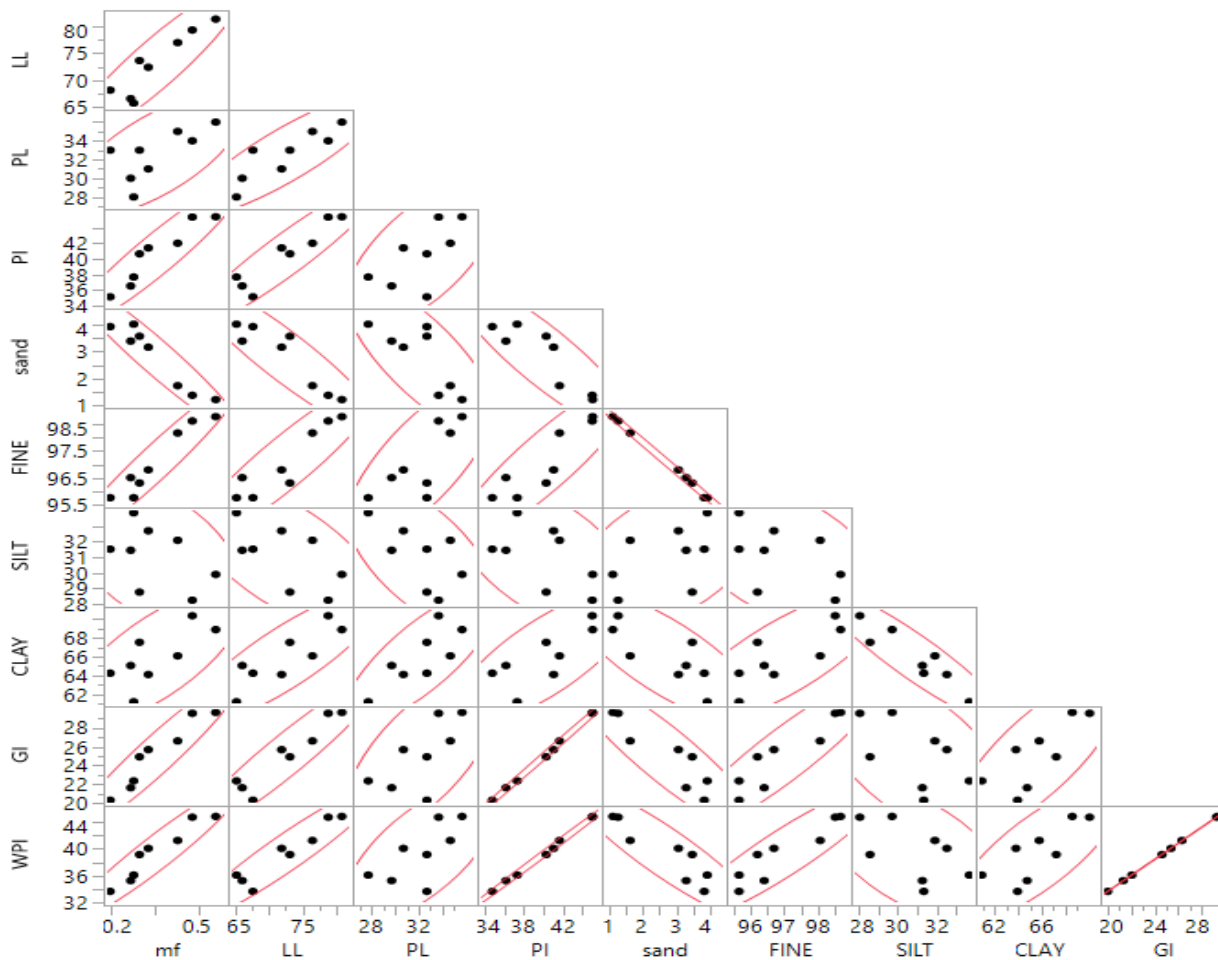


Figure G1:5 scatter plot for mf

Appendix G2: Fit model analysis result

To get to JMP® Pro 14's Fit Model platform, go to Analyze and select Fit Model from the drop-down menu. The Fit model (i.e., Personality: Standard Least Squares, and Emphasis: Effect Leverage) platform of JMP® Pro 14 was used to check for multicollinearity in the predictor. Multicollinearity is not taken into consideration in a stepwise regression.

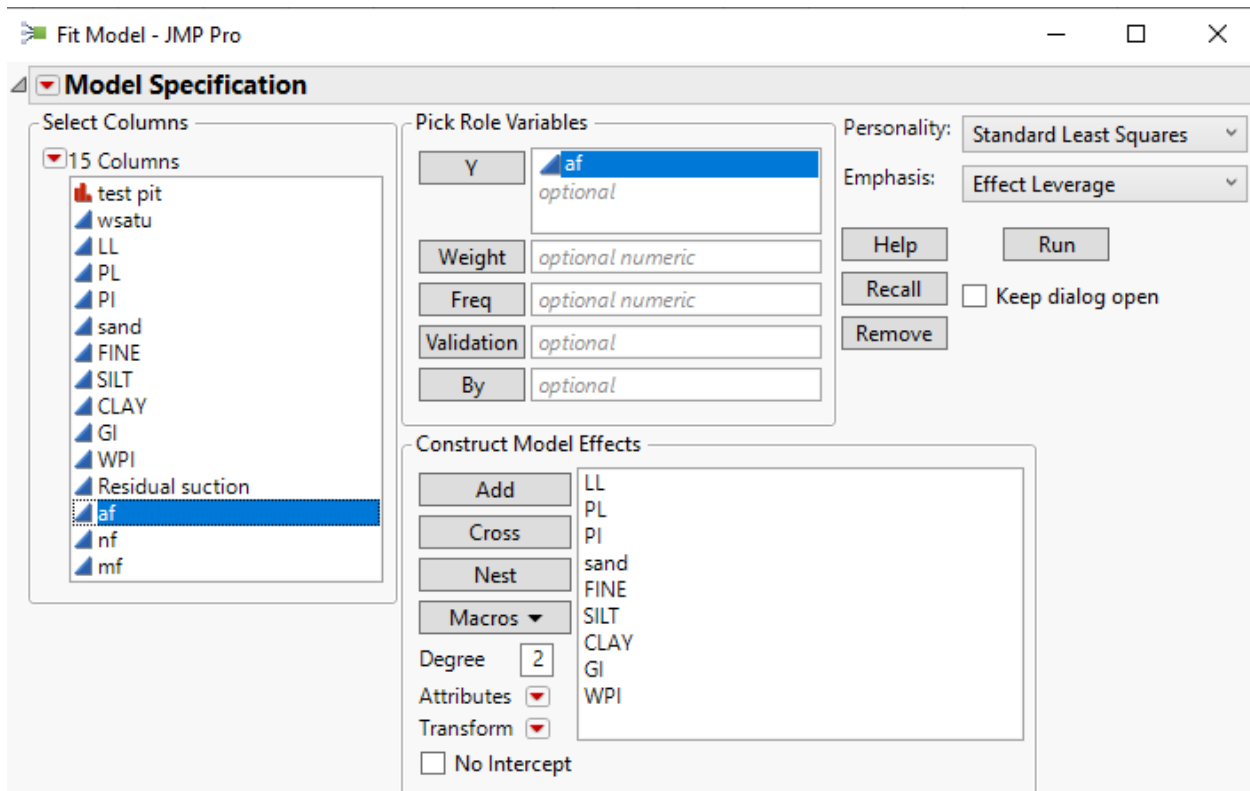


Figure G2.1: Fit model analysis for af

Trial 1

Singularity Details

Term Details

LL = PL + PI

Whole model

Summary of fit

RSquare	1
RSquare Adj	.
Root Mean Square Error	.
Mean of Response	46.20875
Observations (or Sum Wgts)	8

Parameter estimates

Trial 1

Table G2.1: Parameter estimate for all predictors

Term		Estimate	Std Error	t Ratio	Prob> t
Intercept	Biased	-1011.374	.	.	.
LL	Biased	9.2086138	.	.	.
PL	Biased	-8.815339	.	.	.
PI	Zeroed	0	.	.	.
sand	Biased	5.2514213	.	.	.
FINE	Biased	14.221713	.	.	.
SILT	Biased	-4.80262	.	.	.
CLAY	Biased	-4.733751	.	.	.
GI	Biased	-10.4641	.	.	.
WPI	Zeroed	0	.	.	.

Trial 2

Table G2.3: Parameter estimate for all predictors after eliminating PL\$LL

Term		Estimate	Std Error	t Ratio	Prob> t
Intercept		327.77091	.	.	.
PI		121.46299	.	.	.
sand		-37.57274	.	.	.
FINE		37.23982	.	.	.
SILT		-4.162732	.	.	.
CLAY		-3.856863	.	.	.
GI		418.3554	.	.	.
WPI		-478.0924	.	.	.

Trial 3

Table G2.4: Parameter estimate for all predictors after eliminating PI

Term		Estimate	Std Error	t Ratio	Prob> t
Intercept		-190.3947	509.1256	-0.37	0.7722
sand		-1.325166	4.590688	-0.29	0.8211
FINE		-0.29285	5.509267	-0.05	0.9662
SILT		-2.289021	1.595151	-1.43	0.3875
CLAY		-2.22102	1.45794	-1.52	0.3698
GI		-55.13425	44.68343	-1.23	0.4336
WPI		47.478597	37.74321	1.26	0.4276

Trial 4

Table G2.5: Parameter estimate for all predictors after eliminating PI

Term		Estimate	Std Error	t Ratio	Prob> t
------	--	----------	-----------	---------	---------

Term	Estimate	Std Error	t Ratio	Prob> t
Intercept	-211.6139	223.7636	-0.95	0.4441
sand	-1.096342	1.129252	-0.97	0.4340
SILT	-2.330669	0.983884	-2.37	0.1414
CLAY	-2.259852	0.893425	-2.53	0.1272
GI	-54.6811	31.05937	-1.76	0.2204
WPI	47.088251	26.21543	1.80	0.2143

Trial 5

Table G2.6: Parameter estimate for all predictors after eliminating clay

Term	Estimate	Std Error	t Ratio	Prob> t
Intercept	-119.8517	369.4304	-0.32	0.7669
sand	0.1230206	1.708564	0.07	0.9471
SILT	0.1431978	0.179235	0.80	0.4827
GI	-15.10232	44.88972	-0.34	0.7587
WPI	13.717573	37.9025	0.36	0.7414

Trial 6

Table G2.7 Parameter estimate after eliminating GI

Term	Estimate	Std Error	t Ratio	Prob> t
Intercept	4.3843425	9.43423	0.46	0.6663
sand	-0.418384	0.506398	-0.83	0.4551
SILT	0.1591091	0.152519	1.04	0.3557
WPI	0.9660962	0.147549	6.55	0.0028*

Trial 7

Table G2.8 Parameter estimates after eliminating sand

Term	Estimate	Std Error	t Ratio	Prob> t
Intercept	-1.122817	6.460947	-0.17	0.8689
SILT	0.1628062	0.147535	1.10	0.3201
WPI	1.0732112	0.068168	15.74	<.0001*

Trial 8

Table G2.9 Parameter estimates after eliminating silt

Term	Estimate	Std Error	t Ratio	Prob> t
Intercept	5.5572863	2.29868	2.42	0.0520
WPI	1.032025	0.058069	17.77	<.0001*

Appendix G3. model development using fit model

In JMP® Pro 14, the Analyze option has many platforms for developing a prediction model (i.e., Fit Y by X, Fit Model, and Specialized Modeling). Because of its capacity to modify the predictor variable with less effort, the Fit Model platform was employed in this work to create the prediction model.

Appendix G31. Model Development for af

Due to the model's ability to fit the data point, a linear model without modification can be used to suggest a pre-diction model. For the Fredlund & Xing (1994) model fitting parameters, five sets of models were generated (i.e., No Transform, Square transform, reciprocal transform, log transform, and exponential transform).

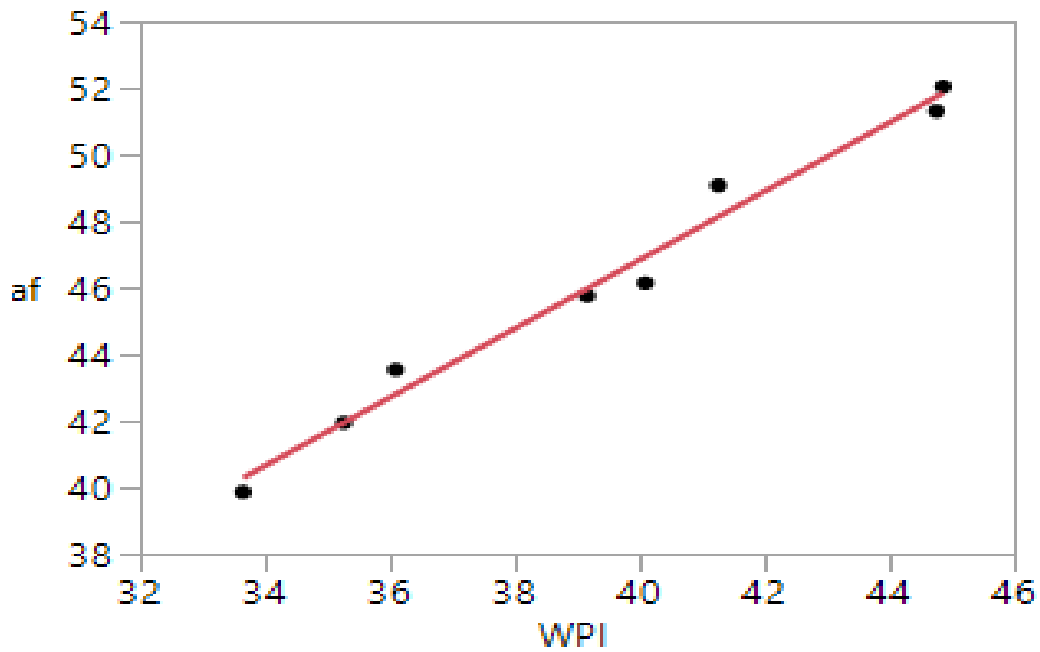
A) No Transform

Response a_f

Whole Model

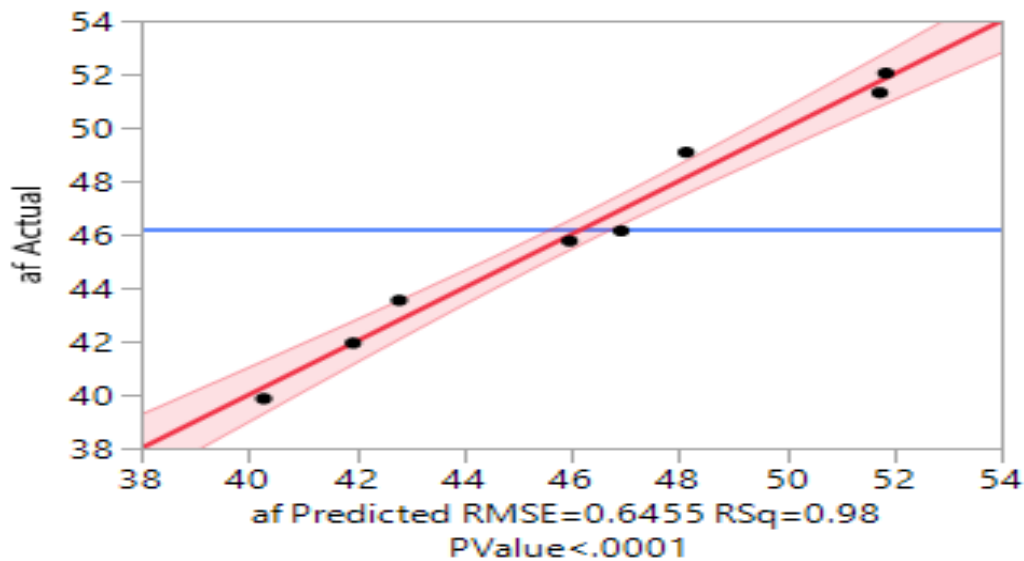
i) Regression Plot

The regression plot shows a basic linear fitting between the dependent variable and the independent variable wPI .



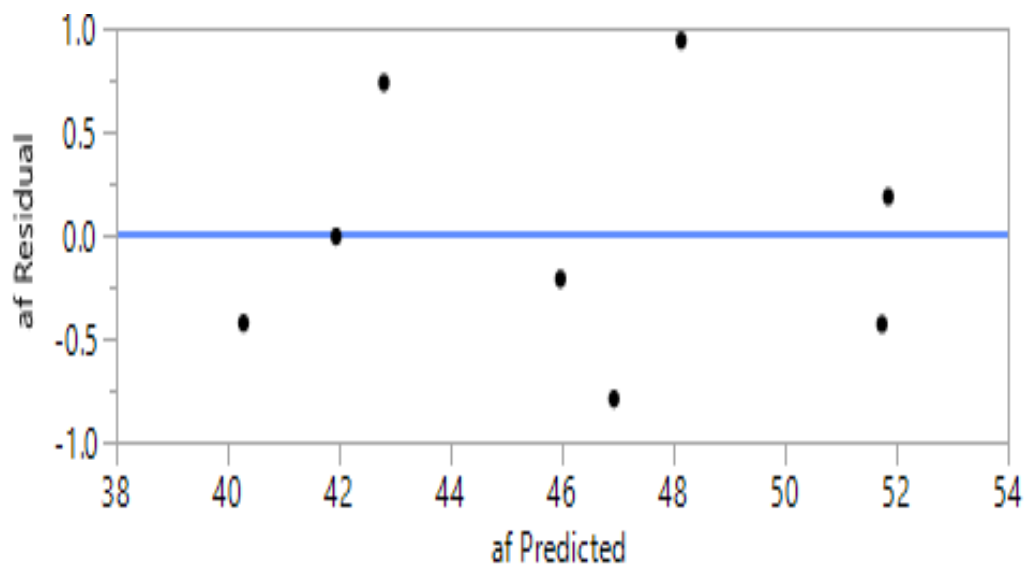
ii) Actual by Predicted Plot

By inserting the predictor variable into the proposed prediction model, the Actual by Predicted plot displays the plot of the actual measured dependent variable and the predicted dependent variable.



iii) Residual by Predicted Plot

The residual by predicted plot can explain heteroscedasticity (i.e., close data point) and homoscedasticity (i.e., far data point) from the reference line. Homoscedasticity and heteroscedasticity are both problematic. There is neither heteroscedasticity or homoscedasticity in the residual by anticipated plot. The data points were evenly distributed.



iv) Summary of Fit

R-squared (R^2) is a statistical measure that represents the proportion of the variance for a dependent variable that's explained by an independent variable. The R^2 of the proposed prediction model is 0.98 which indicates that the proposed prediction model is greatly accepted.

RSquare	0.981358
RSquare Adj	0.978252
Root Mean Square Error	0.645541
Mean of Response	46.20875
Observations (or Sum Wgts)	8

Analysis of Variance

Source	DF	Sum of Squares	Mean Square	F Ratio
Model	1	131.62715	131.627	315.8623
Error	6	2.50034	0.417	Prob > F
C. Total	7	134.12749		<.0001*

v) Parameter Estimates

The parameter estimates section deals with the coefficient of the prediction model and the significance level of the predictor variable. WPI has a significance level of <0.0001. This means that the inclusion of WPI in the prediction model results only a 0.01 % error.

Term	Estimate	Std Error	t Ratio	Prob> t
Intercept	5.5572863	2.29868	2.42	0.0520
WPI	1.032025	0.058069	17.77	<.0001*

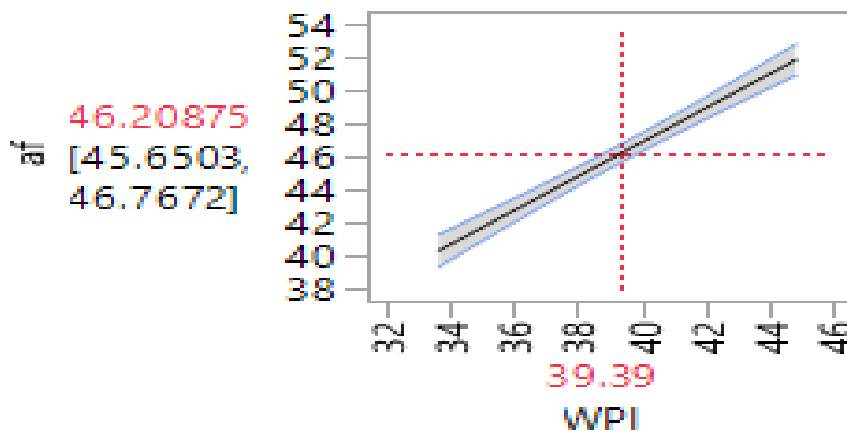
vi) Prediction Expression

The proposed prediction model for a_f

$$af=5.558+1.032WPI \tag{G3.1}$$

Predictor profile

Predictor profiler basically hints whether the proposed prediction model expressions are correct or not. Furthermore, the predictor profiler illustrates the monotonicity of the proposed prediction model. From the prediction profiler it can be seen that the proposed prediction model is physical (i.e., as wPI increases).



B) Square Transform

Response a_f

i) Parameter Estimates

Term	Estimate	Std Error	t Ratio	Prob> t
Intercept	25.796672	1.281545	20.13	<.0001*
Square(WPI	0.013026	0.000802	16.24	<.0001*

Prediction Expression

$$a_f = 25.797 + 0.013WPI^2 \quad (G3.2)$$

C Reciprocal Transform

Summary of fit

RSquare	0.978828
RSquare Adj	0.9753
Root Mean Square Error	0.687957
Mean of Response	46.20875
Observations (or Sum Wgts)	8

Parameter estimates

Term	Estimate	Std Error	t Ratio	Prob> t
Intercept	86.631017	2.439157	35.52	<.0001*
Reciprocal(WPI)	-1576.366	94.6468	-16.66	<.0001*

Prediction expression

$$a_f = 86.63 - 1576.36(1/WPI) \quad (G3.3)$$

D) Log Transform

Response a_f

Summary of fit

RSquare	0.981728
RSquare Adj	0.978682
Root Mean Square Error	0.639117
Mean of Response	46.20875
Observations (or Sum Wgts)	8

Parameters estimates

Term	Estimate	Std Error	t Ratio	Prob> t
Intercept	-102.4282	8.281607	-12.37	<.0001*

Term	Estimate	Std Error	t Ratio	Prob> t
Log(WPI)	40.516969	2.256644	17.95	<.0001*

Prediction expression

$$af = -102.42 + 40.52 \log(WPI)$$

E) Exponential Transform

Summary of fit

RSquare	0.612887
RSquare Adj	0.548369
Root Mean Square Error	2.941724
Mean of Response	46.20875
Observations (or Sum Wgts)	8

Parameter estimates

Term	Estimate	Std Error	t Ratio	Prob> t
Intercept	44.31067	1.208708	36.66	<.0001*
Exp(WPI)	2.584e-19	8.38e-20	3.08	0.0216*

Prediction expression

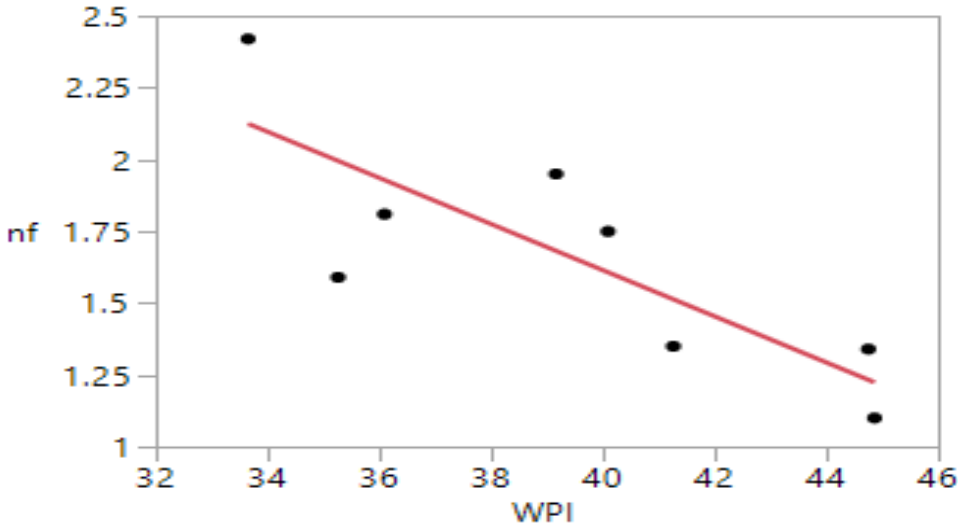
$$af = 44.31 + 2.584e^{-19} \text{Exp}(WPI)$$

Appendix G32. Model Development for n_f

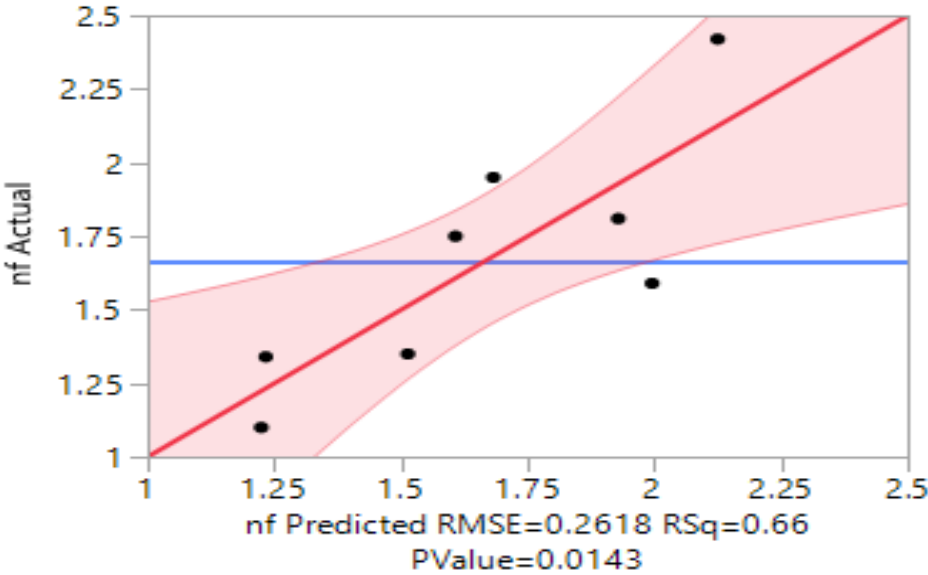
A) No Transform

Whole Model

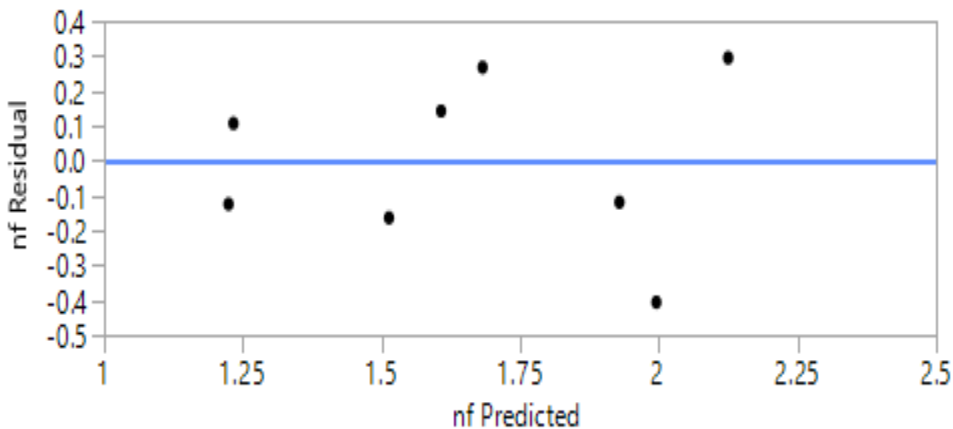
i) Regression Plot



ii) Actual by Predicted Plot



iii) Residual by Predicted Plot



iv) Summary of Fit

RSquare 0.659855
 RSquare Adj 0.603164
 Root Mean Square Error 0.26182
 Mean of Response 1.66375
 Observations (or Sum Wgts) 8

Parameter estimates

Term	Estimate	Std Error	t Ratio	Prob> t
Intercept	4.828756	0.932305	5.18	0.0021*
WPI	-0.08035	0.023552	-3.41	0.0143*

V) Prediction expression

$$n_f = 4.829 - 0.081WPI \quad (G32.1)$$

B) Square Transform

Summary of fit

RSquare 0.658106
 RSquare Adj 0.601123
 Root Mean Square Error 0.262493
 Mean of Response 1.66375
 Observations (or Sum Wgts) 8

Parameter estimates

Term	Estimate	Std Error	t Ratio	Prob> t
Intercept	3.2537929	0.476992	6.82	0.0005*
Square(WPI)	-0.001015	0.000299	-3.40	0.0145*

Prediction expression

$$nf=3.253-0.001WPI^2 \quad (G32.2)$$

C Reciprocal transform

Summary of fit

Square	0.659343
RSquare Adj	0.602567
Root Mean Square Error	0.262017
Mean of Response	1.66375
Observations (or Sum Wgts)	8

Parameter estimates

Term	Estimate	Std Error	t Ratio	Prob> t
Intercept	-1.486255	0.928984	-1.60	0.1607
Reciprocal(WPI)	122.84218	36.04744	3.41	0.0144*

Prediction expression

$$nf=-1.486+122.84(1/WPI) \quad (G32.3)$$

D Log transform

Summary of fit

RSquare	0.660245
RSquare Adj	0.60362

Root Mean Square Error 0.26167
 Mean of Response 1.66375
 Observations (or Sum Wgts) 8

Parameter estimates

Term	Estimate	Std Error	t Ratio	Prob> t
Intercept	13.237442	3.39069	3.90	0.0079*
Log(WPI)	-3.154874	0.923924	-3.41	0.0142*

Prediction expression

$$13.237 - 3.155 \text{ Log (WPI)} \quad (\text{G32.4})$$

E Exponential transform

Summary of fit

RSquare 0.458765
 RSquare Adj 0.368559
 Root Mean Square Error 0.330266
 Mean of Response 1.66375
 Observations (or Sum Wgts) 8

Parameter estimates

Term	Estimate	Std Error	t Ratio	Prob> t
Intercept	1.8196719	0.135701	13.41	<.0001*
Exp(WPI)	-2.12e-20	9.41e-21	-2.26	0.0650

Prediction expression

Prediction expression

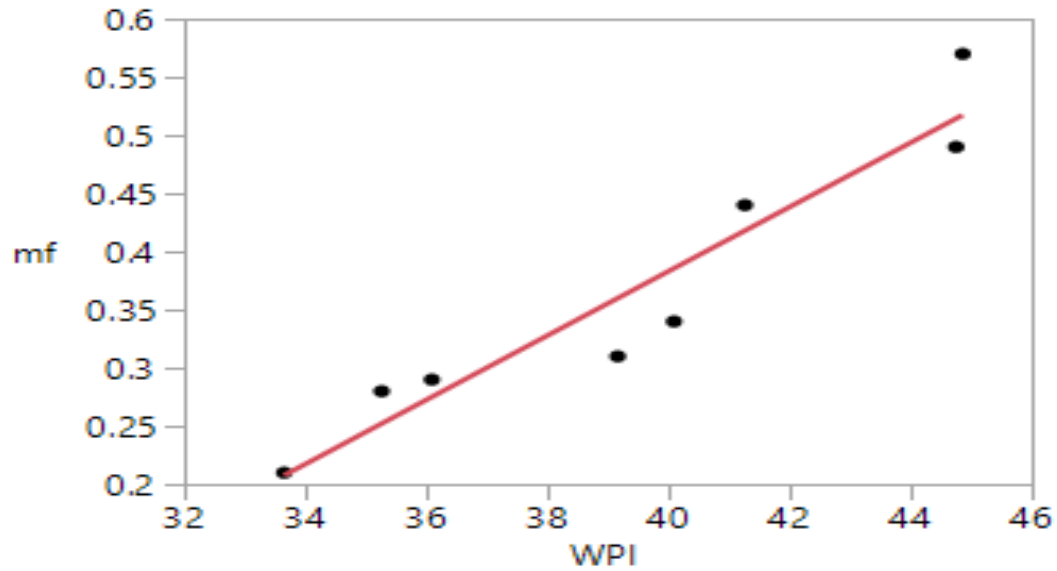
$$nf = 1.82 \text{ Exp(WPI)} - 2.12e-20 \quad (\text{G32.5})$$

Appendix G33. Model Development for m_f

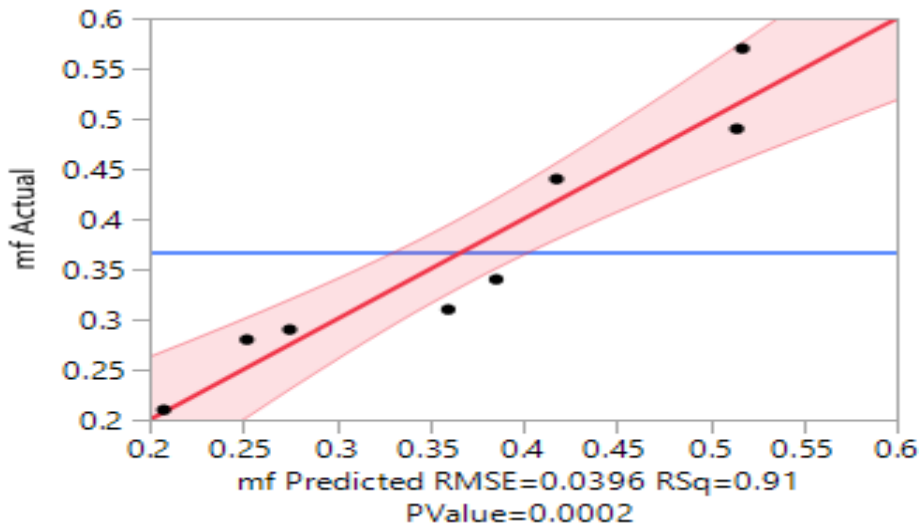
A) No Transform

Whole Model

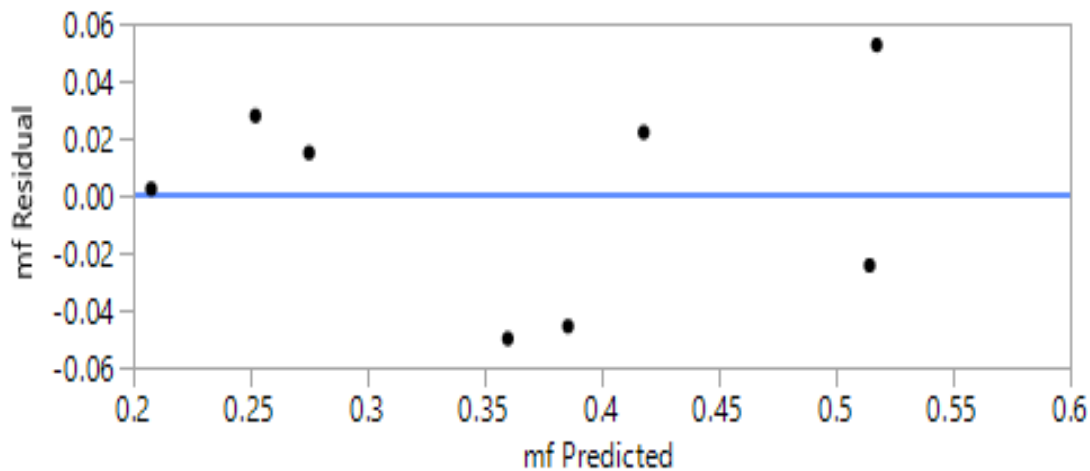
i) Regression Plot



ii) Actual by predicted plot



iii) Residual by predicted



iv) Summary of fit

RSquare	0.909225
RSquare Adj	0.894096
Root Mean Square Error	0.039626
Mean of Response	0.36625
Observations (or Sum Wgts)	8

Variance analysis

Source	DF	Sum of Squares	Mean Square	F Ratio
Model	1	0.09436618	0.094366	60.0974
Error	6	0.00942132	0.001570	Prob > F
C. Total	7	0.10378750		0.0002*

v) Prediction expression

$$m_f = -0.722 + 0.028WPI \quad (G33.1)$$

B Square transform

Summary of fit

RSquare	0.918762
RSquare Adj	0.905222
Root Mean Square Error	0.037487
Mean of Response	0.36625
Observations (or Sum Wgts)	8

Parameter estimates

Term	Estimate	Std Error	t Ratio	Prob> t
Intercept	-0.184162	0.068119	-2.70	0.0354*
Square(WPI)	0.0003512	4.264e-5	8.24	0.0002*

Prediction expression

$$mf = -0.184 + 0.0004WPI^2 \quad (G33.2)$$

C Reciprocal transform

Summary of fit

RSquare	0.881651
RSquare Adj	0.861926
Root Mean Square Error	0.045246
Mean of Response	0.36625
Observations (or Sum Wgts)	8

Parameter estimates

Term	Estimate	Std Error	t Ratio	Prob> t
Intercept	1.4334095	0.16042	8.94	0.0001*
Reciprocal(WPI)	-41.61651	6.224786	-6.69	0.0005*

Prediction expression

$$mf = 1.4334(1/WPI) - 41.6165 \quad (G33.3)$$

D Log transform

Summary of fit

RSquare	0.896789
RSquare Adj	0.879587
Root Mean Square Error	0.042253
Mean of Response	0.36625

Observations (or Sum Wgts) 8

Parameter Estimate

Term	Estimate	Std Error	t Ratio	Prob> t
Intercept	-3.585505	0.547514	-6.55	0.0006*
Log(WPI)	1.0772093	0.149191	7.22	0.0004*

Prediction expression

$$mf = -3.5855 \text{ Log}(WPI) + 1.0772 \quad (G33.4)$$

D Exponential transform

Summary of fit

RSquare	0.721459
RSquare Adj	0.675035
Root Mean Square Error	0.069413
Mean of Response	0.36625
Observations (or Sum Wgts)	8

Parameter Estimates

Term	Estimate	Std Error	t Ratio	Prob> t
Intercept	0.3089647	0.028521	10.83	<.0001*
Exp(WPI)	7.797e-21	1.98e-21	3.94	0.0076*

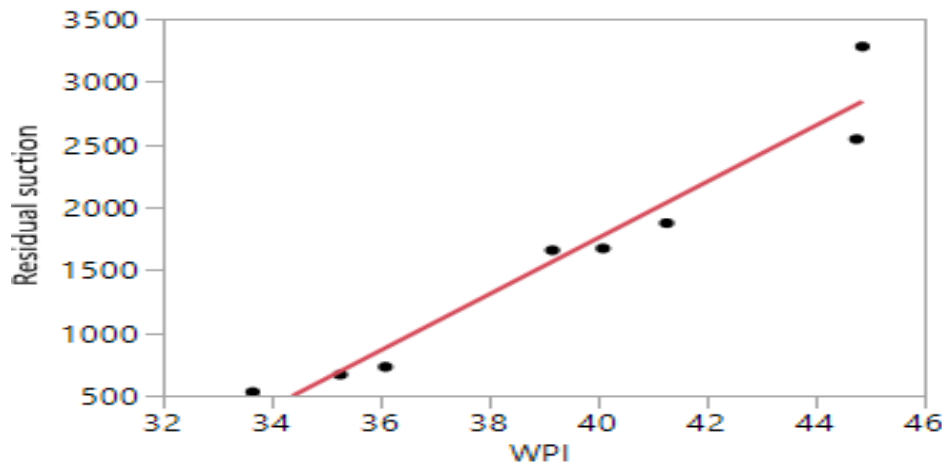
Prediction Expression

$$mf = 0.3089 \text{ Exp}(WPI) + 7.797e-21 \quad (G33.5)$$

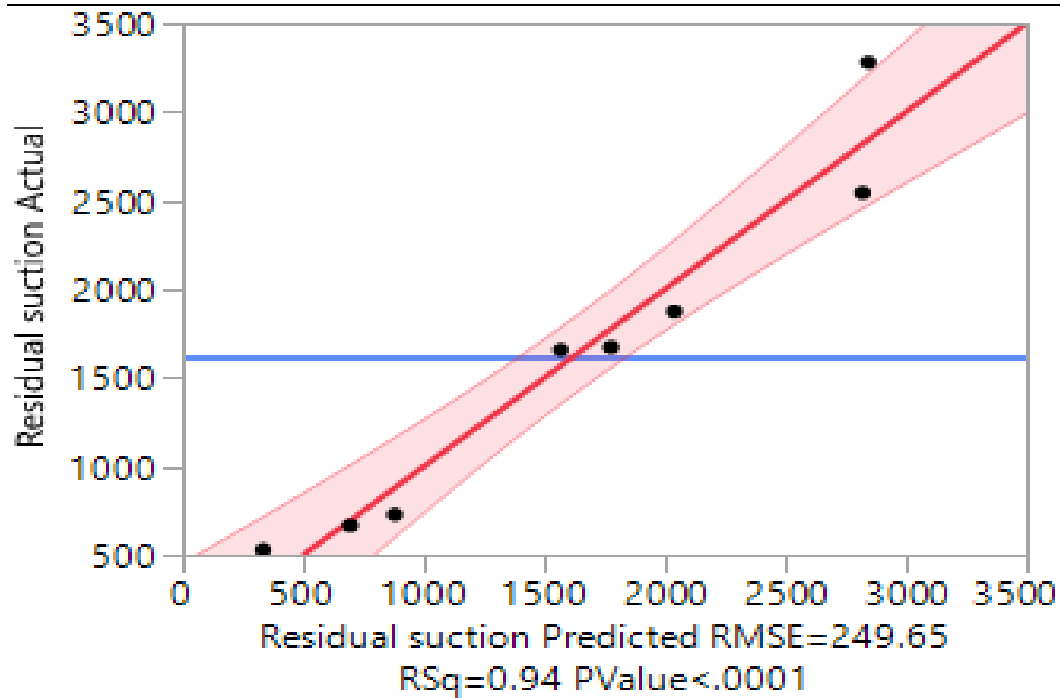
Appendix G34: Model development for residual suction

Whole model

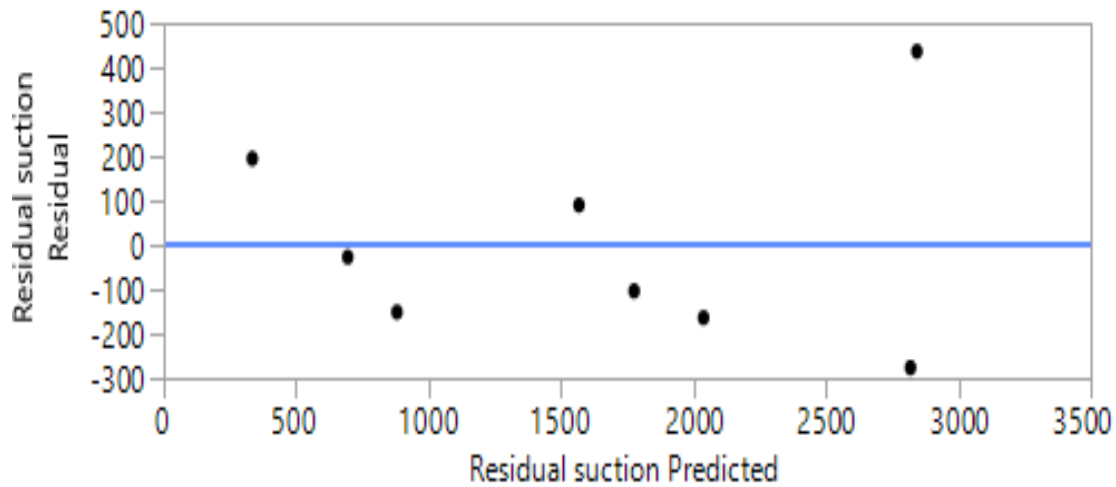
i) Regression plot



ii) Actual by predicted plot



iii) Residual by predicted plot



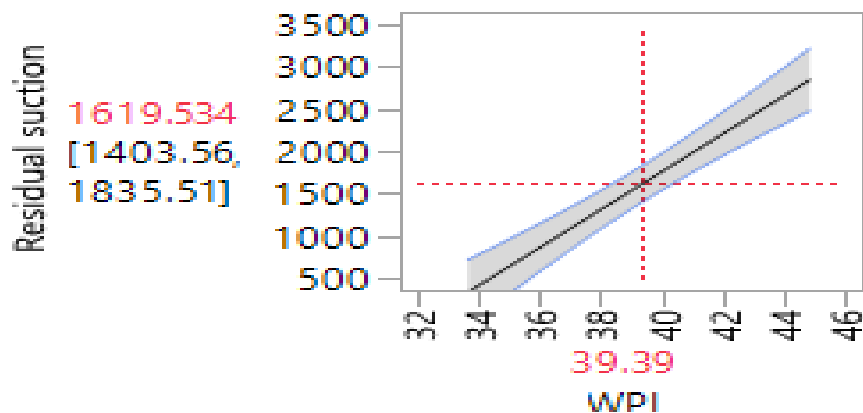
Summary fit

RSquare	0.943062
RSquare Adj	0.933572
Root Mean Square Error	249.6503
Mean of Response	1619.534
Observations (or Sum Wgts)	8

Parameter estimates

Term	Estimate	Std Error	t Ratio	Prob> t
Intercept	-7198.664	888.9696	-8.10	0.0002*
WPI	223.86894	22.45689	9.97	<.0001*

Prediction profile



Prediction expression

$$mf = -7198.664 + 223.87WPI \quad (G34.1)$$

B Square transform

Summary fit

RSquare	0.949072
RSquare Adj	0.940584
Root Mean Square Error	236.1069
Mean of Response	1619.534
Observations (or Sum Wgts)	8

Parameter estimate

Term	Estimate	Std Error	t Ratio	Prob> t
Intercept	-2830.57	429.0447	-6.60	0.0006*
Square(WPI)	2.8398507	0.268564	10.57	<.0001*

Prediction expression

$$Rsuction = -2830.57 + 2.84(WPI)^2 \quad (G34.2)$$

C Reciprocal transform

summary of fit

RSquare	0.921172
RSquare Adj	0.908034
Root Mean Square Error	293.7455
Mean of Response	1619.534
Observations (or Sum Wgts)	8

Parameter estimates

Term	Estimate	Std Error	t Ratio	Prob> t
Intercept	10296.844	1041.477	9.89	<.0001*
Reciprocal(WPI)	-338393.1	40412.53	-8.37	0.0002*

Prediction expression

$$R_{\text{suction}} = 10296.84 - 338393.1(1/WPI) \quad (G34.3)$$

D Log transform

Summary of fit

RSquare	0.933729
RSquare Adj	0.922684
Root Mean Square Error	269.3344
Mean of Response	1619.534
Observations (or Sum Wgts)	8

Parameter estimate

Term	Estimate	Std Error	t Ratio	Prob> t
Intercept	-30457.13	3490.004	-8.73	0.0001*
Log(WPI)	8743.7813	950.9865	9.19	<.0001*

Prediction expression

$$R_{\text{suction}} = -30457.13 + 8743.78 \text{ Log (WPI)} \quad (G34.4)$$

E) Exponential transform

Summary of fit

RSquare	0.710366
RSquare Adj	0.662094
Root Mean Square Error	563.0609
Mean of Response	1619.534
Observations (or Sum Wgts)	8

Parameter estimate

Term	Estimate	Std Error	t Ratio	Prob> t
Intercept	1167.3525	231.3528	5.05	0.0023*
Exp(WPI)	6.155e-17	1.6e-17	3.84	0.0086*

Prediction expression

$$R_{\text{suction}} = 1167.35 + 6.155e-17 \quad (G34.5)$$

Appendix H: Images taken during laboratory testing program





